Astronomy & Astrophysics manuscript no. SStarsRevised
June 27, 2008

© ESO 2008

arXiv:0806.4591v1 [astro-ph] 27 Jun 2008

Infrared Photometry and Evolution of Mass-Losing AGB Stars.

II. Luminosity and Colors of MS and S Stars

R. Guandalini[1] and M. Busso[1]

Department of Physics, University of Perugia, and INFN, Sezione di Perugia, Via A. Pascoli 1, 06123 Perugia, Italy
e-mail: `guandalini@fisica.unipg.it;busso@fisica.unipg.it`

Received / Accepted

ABSTRACT

Context. Asymptotic Giant Branch (AGB) phases mark the end of the evolution for Low- and Intermediate-Mass Stars. Our understanding of the mechanisms through which they eject the envelope and our assessment of their contribution to the mass return to the Interstellar Medium and to the chemical evolution of Galaxies are hampered by poor knowledge of their Luminosities and mass loss rates, both for C-rich and for O-rich sources.

Aims. We plan to establish criteria permitting a more quantitative determination of luminosities (and subsequently of mass loss rates) for the various types of AGB stars on the basis of infrared fluxes. In this paper, in particular, we concentrate on O-rich and s-element-rich MS, S stars and include a small sample of SC stars.

Methods. We reanalyze the absolute bolometric magnitudes and colors of MS, S, SC stars on the basis of a sample of intrinsic (single) and extrinsic (binary) long period variables. We derive bolometric corrections as a function of near- and mid-infrared colors, adopting as references a group of stars for which the Spectral Energy Distribution could be reconstructed in detail over a large wavelength range. We determine the absolute HR diagrams, and compare luminosities and colors of S-type giants with those, previously derived, of C-rich AGB stars. Luminosity estimates are also verified on the basis of existing Period-Luminosity relations valid for O-rich Miras.

Results. S star bolometric luminosities are almost indistinguishable from those of C-rich AGB stars. On the contrary, their circumstellar envelopes are thinner and less opaque. Despite this last property the IR wavelengths remain dominant, with the bluest stars having their maximum emission in the H or K(short) bands. Near-to-Mid infrared color differences are in any case smaller than for C stars. Based on Period-Luminosity relations for O-rich Miras and on Magnitude-color relations for the same variables we show how approximate distances (hence intrinsic parameters) for sources of so far unknown parallax can be inferred. We argue that most of the sources have a rather small mass ($< 2\ M_\odot$); dredge-up might then be not effective enough to let the C/O ratio exceed unity.

Key words. Stars: fundamental parameters (classification, colors,luminosities, masses, radii, temperatures, etc.) – Stars: AGB and post-AGB – Stars: evolution – Infrared: stars – Stars: variables: general

1. Introduction

The Asymptotic Giant Branch phases (hereafter AGB) represent the second ascent along the Red Giant Branch, occurring after the exhaustion of core He burning for all stars between ~ 0.8 and 8.0 $M_\odot$. In these evolutionary stages, stars are powered by two nuclear shells, burning H and He alternatively. In particular, in the final 1-2 Myr of the AGB, the He-burning shell remains mainly quiescent, if not for recurrent explosive ignitions during which a lot of C (from 20 to 25% by mass) is produced and spread over the whole He-rich layer, in short phases of convective mixing (the so-called *thermal pulses*). Convective penetration of the envelope follows, in repeated episodes collectively called ”the third dredge-up”, and carries the new carbon to the surface, together with other nucleosynthesis products, in particular s-elements generated by efficient neutron captures (Busso et al., 1999).

Due to the above phenomena, the atmospheres of AGB stars are characterized by an increasing enrichment of ^{12}C (up to C/O > 1 by number, in which case we speak of C stars) and of s-process nuclei, in particular revealing the recent nucleosynthesis through the short-lived ^{99}Tc (Merrill, 1952). Sometimes Tc itself offers actually the only real evidence of ongoing s-processing in stars that do not show other remarkable chemical anomalies (Uttenthaler et al., 2007). When instead the third dredge-up process is efficient enough, changes in the photospheric abundances of other s-elements begin to occur, first of all for Zr, which has various isotopes on the main s-process path. In such cases the appearance of ZrO bands in the spectra (at wavelengths 464.1, 462.0, 530.4, 537.9, and 555.1 nm) tells us that the star, although still richer in O than in C, is mixing to the surface the products of shell-He burning. The cool giants presenting these signatures are called MS and S stars (the second group showing more prominent features). They also have a C/O abundance ratio by number higher than in the Sun, but lower than unity. There is still some confusion about the exact values of the C/O ratios in MS and S stars, which is mainly induced by the remaining uncertainty in the calibrating solar oxygen abundance. If one excludes for this calibration the recent, still debated suggestion (Allende Prieto et al., 2002) and adopts instead the previous more traditional reference (Anders & Grevesse, 1989), then MS stars are found typically at C/O = 0.5 to 0.7, and S stars are found above this range and up to more that 0.95. Around the border between O-rich and C-rich giants, the so-called SC stars represent a rare, but important, transition group.

Send offprint requests to: R. Guandalini, guandalini@fisica.unipg.it

Table 1. Sample A − First part. Spectral Type is from the GCVS catalogue whenever possible, otherwise it is obtained from the SIMBAD Astronomical Database.

IRAS name	Other name	Stephenson name	Coordinates ICRS	Spectral Type	Var. Type (GCVS)
01159+7220	S Cas	CSS 28	01 19 41.97 +72 36 39.3	S3,4e−S5,8e	M
19126−0708	W Aql	CSS 1115	19 15 23.44 −07 02 49.9	S3,9e−S6,9e	M
19354+5005	R Cyg	CSS 1150	19 36 49.381 +50 11 59.46	S2.5,9e−S6,9e(Tc)	M
19486+3247	chi Cyg	CSS 1165	19 50 33.9220 +32 54 50.610	S6,2e−S10,4e/MSe	M
23595−1457	W Cet	CSS 1346	00 02 07.3891 −14 40 33.065	S6,3e−S9,2e	M
22196−4612	pi1 Gru	CSS 1294	22 22 44.2053 −45 56 52.598	S5,7e	SRB
20026+3640	AA Cyg	CSS 1188	20 04 27.6055 +36 49 00.465	S7,5−S7.5,6(MpTc)	SRB
20120−4433	RZ Sgr	CSS 1196	20 15 28.4049 −44 24 37.480	S4,4ep	SRB
03452+5301	WX Cam	CSS 82	03 49 03.77 +53 10 59.2	S5,8	LB
23070+0824	GZ Peg	CSS 1322	23 09 31.4570 +08 40 37.778	M4SIII	SRA
15492+4837	ST Her	CSS 903	15 50 46.6248 +48 28 58.856	M6−7IIIaS	SRB
00192−2020	T Cet	CSS 8	00 21 46.2737 −20 03 28.885	M5−6SIIe	SRC
05374+3153	NO Aur	CSS 149	05 40 42.0504 +31 55 14.187	M2SIab	LC
22476+4047	RX Lac	CSS 1308	22 49 56.8992 +41 03 04.312	M7.5Se	SRB
00213+3817	R And	CSS 9	00 24 01.9469 +38 34 37.328	S3,5e−S8,8e/M7e	M
22521+1640	HR Peg	CSS 1315	22 54 35.6272 +16 56 30.601	S5,1/M4	SRB
17553+4521	OP Her	–	17 56 48.5274 +45 21 03.063	M5IIb−IIIa/S	SRB
13372−7136	LY Mus	CSS 826	13 41 13.5883 −71 52 05.767	M4III	LB
18058−3658	–	CSS 1023	18 09 17.1853 −36 57 57.614	M2II−III	–
19111+2555	S Lyr	CSS 1112	19 13 11.79 +26 00 28.3	SCe	M
15194−5115	II Lup	CSS 886	15 23 04.91 −51 25 59.0	C	M

Table 2. Sample A − Second part.

Source name	J [Jy]	H [Jy]	K [Jy]	[8.8] [Jy]	[9.8] [Jy]	[11.7] [Jy]	[12.5] [Jy]	D [Jy]	E [Jy]	Mid−IR Data Origin	ISO TDT Number
S Cas	56.6	168	244	232	316	304	281	235	185	ISO−SWS1	41602133
W Aql	388	822	1113	969	1099	1043	789	625	488	ISO−SWS1	16402335
R Cyg	200	288	302	77.3	87.8	79.3	69.2	52.8	29.7	ISO−SWS1	42201625
chi Cyg	1365	2823	3176	1408	1655	1579	1095	736	487	ISO−SWS1	15900437
W Cet	74.1	113	101	12.7	12.4	10.5	10.9	8.3	4.5	ISO−SWS1	37802225
pi1 Gru	3080	–	5812	544	632	679	683	505	365	ISO−SWS1	34402039
AA Cyg	238	389	375	42.6	42.5	42.9	36.8	27.5	16.9	ISO−SWS1	36401817
RZ Sgr	139	206	190	25.0	26.2	25.7	24.5	21.8	21.0	ISO−SWS1	14100818
WX Cam	43.5	79.3	87.6	8.1	7.9	8.4	16.6	9.3	4.0	ISO−SWS1	81002721
GZ Peg	735	1100	965	88.6	78.9	62.4	56.8	40.9	21.0	ISO−SWS1	37600306
ST Her	804	1162	1098	166	186	200	187	149	104	ISO−SWS1	41901305
T Cet	1009	1596	1403	172	163	172	171	134	83.0	ISO−SWS1	55502308 − 37801819
NO Aur	226	362	273	33.2	41.6	46.3	36.1	23.3	17.2	ISO−SWS1	86603434
RX Lac	465	737	681	91.0	85.4	81.9	68.6	50.3	28.8	ISO−SWS1	78200427
R And	247	506	596	193	264	248	210	176	135	ISO−SWS1	40201723
HR Peg	191	327	256	27.0	24.4	20.9	20.0	12.6	7.8	ISO−SWS1	37401910
OP Her	416	731	556	63.5	58.1	46.4	37.8	30.9	16.0	ISO−SWS1	77800625
LY Mus	221	334	300	28.4	24.7	19.7	16.4	12.9	7.6	ISO−SWS1	13201304
CSS 1023	33.2	51.7	39.9	2.3	2.2	1.5	1.4	0.83	0.46	ISO−SWS1	14100603
S Lyr	8.2	13.2	17.9	20.0	23.2	25.5	24.4	22.1	15.7	ISO−SWS1	52000546
II Lup	3.7	25.5	99.0	860	852	860	681	506	391	ISO−SWS6	29700401

In some cases, red giants showing s-element enhancement are Tc-poor. This is a clear indication that a sufficiently long time interval has passed since the production of neutron capture nuclei, so that Tc has decayed. In general, this is the case when the nucleosynthesis phenomena occurred not in the same star we see today, but in a more massive companion, which is now evolved to the white dwarf stage, and whose mass loss enriched in the past the photosphere of the observed object (Busso et al., 2001). In these cases we speak more properly of an *extrinsic* AGB star (Smith & Lambert, 1990).

AGB stars lose mass very effectively, and their winds replenish the Interstellar Medium (ISM) guaranteeing up to 70% of the mass return from stars (Sedlmayr, 1994). Before being dispersed over the Galaxy, the material thus lost forms cool envelopes (Winters et al., 2003) where dust grains condense (Carciofi et al., 2004). These solid particles carry the elemental and isotopic composition generated by AGB nucleosynthesis; they have been found in ancient meteorites offering the possibility of high precision isotopic abundance measurements on matter coming from circumstellar environments (e.g. Zinner, 2000).

The cool AGB photospheres radiate most of their flux at red-infrared wavelengths. The infrared component of the Spectral Energy Distribution (SED) grows in importance (and in average wavelength) as far as the evolution proceeds, because

Table 3. Sample A − Third part. The indication I. − E. (Intrinsic − Extrinsic) is given according to the suggestions from Van Eck et al. (2000) and Yang et al. (2006). In discordant cases we prefer the choice by Van Eck et al. (2000) and show the one of Yang et al. (2006) in parenthesis. For few sources, for which neither study offers a suggestion, we infer that they are extrinsic from their low intrinsic Luminosity: in the tables they are underlined.

Source name	Var. Type (GCVS)	Period (GCVS)	Distance (kpc)	Min. − Max. (kpc)	Ref. Distance	Bol. Magnitudes ISO Integration	I. − E.
S Cas	M	612.43	0.85	–	P−L / this paper	−5.71	I
W Aql	M	490.43	0.34	–	P−L / this paper	−5.44	I
R Cyg	M	426.45	0.55	–	P−L / this paper	−5.42	–
chi Cyg	M	408.05	0.18	0.15 − 0.22	Hip. / van Leeuwen (2007a)	−5.39	I
W Cet	M	351.31	0.83	–	P−L / this paper	−5.18	I
pi1 Gru	SRB	150	0.16	0.15 − 0.19	Hip. / van Leeuwen (2007a)	−5.75	I
AA Cyg	SRB	212.7	–	–	–	–	I
RZ Sgr	SRB	223.2	–	–	–	–	I
WX Cam	LB	–	–	–	–	–	I
GZ Peg	SRA	92.66	0.24	0.22 − 0.26	Hip. / van Leeuwen (2007a)	−5.02	E
ST Her	SRB	148	0.30	0.25 − 0.36	Hip. / van Leeuwen (2007a)	−5.64	I
T Cet	SRC	158.9	0.27	0.24 − 0.31	Hip. / van Leeuwen (2007a)	−5.63	I
NO Aur	LC	–	0.60	0.47 − 0.83	Hip. / van Leeuwen (2007a)	−5.73	I
RX Lac	SRB	650	–	–	–	–	I
R And	M	409.33	0.41	–	P−L / this paper	−5.19	I
HR Peg	SRB	50	0.41	0.36 − 0.50	Hip. / van Leeuwen (2007a)	−4.75	I
OP Her	SRB	120.5	0.30	0.27 − 0.32	Hip. / van Leeuwen (2007a)	−4.92	–
LY Mus	LB	–	0.29	0.26 − 0.33	Hip. / van Leeuwen (2007a)	−4.12	E
CSS 1023	–	–	–	–	–	–	E
S Lyr	M	438.4	2.27	–	P−L / this paper	−5.50	I
II Lup	M	–	0.59	–	Groenewegen et al. (2002)	−4.82	–

Table 4. Sample B − First part. Suggestions from Smith & Lambert (1986) for Spectral Type: *1* RS Cnc: M6eIIIaS. *2* V1743 Cyg: M5IIIaS. *3* V1981 Cyg: M4IIIaS.

IRAS name	Other name	Stephenson name	Coordinates ICRS	Spectral Type	Var. Type (GCVS)
05199−0842	V1261 Ori	CSS 133	05 22 18.6453 −08 39 58.034	S	Algol Type
04497+1410	omi Ori	CSS 114	04 52 31.9621 +14 15 02.311	M3.2IIIaS	SRB
10226+0902	DE Leo	–	10 25 15.1951 +08 47 05.441	M2IIIabS	SRB
07245+4605	Y Lyn	CSS 347	07 28 11.6109 +45 59 26.207	M6SIb−II	SRC
07392+1419	NZ Gem	CSS 382	07 42 03.2185 +14 12 30.612	M3II−IIIS	SR
06457+0535	V613 Mon	CSS 260	06 48 22.2963 +05 32 30.050	M2/S5,1	SRB
09076+3110	RS Cnc	CSS 589	09 10 38.7990 +30 57 47.300	M6eIb−II/S [1]	SRC
03377+6303	BD Cam	CSS 79	03 42 09.3250 +63 13 00.501	S5,3/M4III	LB
07095+6853	AA Cam	CSS 312	07 14 52.0703 +68 48 15.380	M5/S	LB
13079−8931	BQ Oct	CSS 804	14 35 29.5001 −89 46 18.182	M4III/S5,1	LB
12272−4127	V928 Cen	CSS 796	12 29 57.8871 −41 44 09.242	M2II−III	SRB
19323+4909	V1743 Cyg	–	19 33 41.6068 +49 15 44.347	M4.5III [2]	SRB
–	V1981 Cyg	–	21 02 24.1993 +44 47 27.528	M4s... [3]	SRB
08214−3807	V436 Pup	CSS 500	08 23 16.9344 −38 17 09.884	M1III	LB
–	V2141 Cyg	CSS 1254	20 57 53.1771 +44 47 17.336	M1	LB
12106−3350	V335 Hya	–	12 13 12.9423 −34 07 30.981	M4III	LB
14510−6052	CR Cir	CSS 867	14 54 56.9389 −61 04 33.027	M2/M3II	LC
16418−1359	–	CSS 937	16 44 42.1936 −14 04 48.553	M1III	–
13136−4426	UY Cen	CSS 816	13 16 31.8300 −44 42 15.741	SC	SR
16425−1902	–	CSS 938	16 45 30.1769 −19 08 12.939	K5II	–
20076+3331	–	CSS 1194	20 09 32.9873 +33 40 53.851	K5III	–

of the increased extinction of the photospheric flux operated by dust, which then re-radiates at long wavelengths (see e.g. Habing, 1996). This correlation between extinction and evolutionary stage is however confused by the stars switching from Semiregular to Mira-type surface variability, which fact modulates the mass loss efficiency and hence the extinction properties. Due to these complicacies, large surveys of infrared (IR) observations play a fundamental role in studying luminosities and mass loss rates of AGB stars and in disentangling the variability and evolution effects (see e.g. Wood & Cohen, 2001; Le Bertre et al., 2001, 2003; Groenewegen et al., 2002; Cioni et al., 2003; Omont et al., 2003; Olofsson et al., 2003).

Longstanding efforts have been devoted to describe the mass loss mechanisms, either with phenomenological models or with sophisticated hydrodynamical approaches (Salpeter, 1974; Knapp & Morris, 1985; Winters et al., 2003; Wachter et al., 2002; Sandin & Höfner, 2003a,b). Despite this, our quantitative knowledge of AGB winds is still poor and forces us to

Table 5. Sample B − Second part.

Source name	J [Jy]	H [Jy]	K [Jy]	[8.8] [Jy]	[9.8] [Jy]	[11.7] [Jy]	[12.5] [Jy]	D [Jy]	E [Jy]	Mid−IR Data Origin
V1261 Ori	73.8	111	93.1	16.4	16.5	19.6	21.3	–	–	IRAS−LRS
omi Ori	1022	1587	1227	103	82.4	64.8	60.9	–	–	IRAS−LRS
DE Leo	178	234	184	34.0	30.7	34.4	36.4	–	–	IRAS−LRS
Y Lyn	876	1448	1256	132	150	121	107	–	–	IRAS−LRS
NZ Gem	369	566	399	38.9	34.5	32.6	32.5	–	–	IRAS−LRS
V613 Mon	49.6	74.3	68.9	5.2	–	–	3.3	2.0	–	MSX
RS Cnc	3065	4324	3742	512	693	493	436	–	–	TIRCAM2
BD Cam	439	630	521	62.3	52.5	43.6	41.2	–	–	IRAS−LRS
AA Cam	146	220	185	–	–	–	–	–	–	–
BQ Oct	139	196	170	24.8	22.5	23.5	23.6	–	–	IRAS−LRS
V928 Cen	196	267	225	25.4	21.9	20.3	20.5	–	–	IRAS−LRS
V1743 Cyg	259	421	335	40.4	36.4	34.5	34.2	–	–	IRAS−LRS
V1981 Cyg	197	279	245	28.9	–	–	16.3	10.8	4.7	MSX
V436 Pup	139	198	165	17.1	–	–	10.3	7.0	2.7	MSX
V2141 Cyg	147	216	195	20.8	–	–	12.2	8.2	3.5	MSX
V335 Hya	611	946	833	88.6	78.7	67.4	63.3	–	–	IRAS−LRS
CR Cir	75.1	117	99.6	9.9	–	–	5.8	3.8	–	MSX
CSS 937	104	169	151	15.7	15.9	20.1	21.6	–	–	IRAS−LRS
UY Cen	184	360	350	66.7	62.9	61.4	55.6	–	–	IRAS−LRS
CSS 938	142	200	175	20.4	19.7	21.4	23.2	–	–	IRAS−LRS
CSS 1194	31.1	41.5	37.0	2.9	–	–	2.4	0.96	–	MSX

Table 6. Sample B − Third part.

Source name	Var. Type (GCVS)	Period (GCVS)	Distance (kpc)	Min. − Max. (kpc)	Ref. Distance	Bol. Magnitudes Bol. Corrections	I. − E.
V1261 Ori	Algol Type	–	0.29	0.23 − 0.38	Hip. / van Leeuwen (2007a)	−2.71	E
omi Ori	SRB	30	0.20	0.17 − 0.23	Hip. / van Leeuwen (2007a)	−4.89	I
DE Leo	SRB	–	0.31	0.27 − 0.37	Hip. / van Leeuwen (2007a)	−3.60	*E*
Y Lyn	SRC	110	0.25	0.20 − 0.33	Hip. / van Leeuwen (2007a)	−5.33	I
NZ Gem	SR	–	0.39	0.32 − 0.51	Hip. / van Leeuwen (2007a)	−5.06	E
V613 Mon	SRB	–	0.50	0.35 − 0.84	Hip. / van Leeuwen (2007a)	−3.76	E
RS Cnc	SRC	120	0.14	0.13 − 0.15	Hip. / van Leeuwen (2007a)	−5.21	I
BD Cam	LB	–	0.16	0.15 − 0.17	Hip. / van Leeuwen (2007a)	−3.40	E
AA Cam	LB	–	0.78	0.50 − 1.82	Hip. / van Leeuwen (2007a)	–	I
BQ Oct	LB	–	0.49	0.41 − 0.60	Hip. / van Leeuwen (2007a)	−4.55	I
V928 Cen	SRB	–	0.23	0.21 − 0.25	Hip. / van Leeuwen (2007a)	−3.27	E
V1743 Cyg	SRB	40	0.41	0.38 − 0.44	Hip. / van Leeuwen (2007a)	−4.94	–
V1981 Cyg	SRB	–	0.30	0.27 − 0.33	Hip. / van Leeuwen (2007a)	−3.96	*E*
V436 Pup	LB	–	0.33	0.30 − 0.38	Hip. / van Leeuwen (2007a)	−3.75	E
V2141 Cyg	LB	–	0.38	0.31 − 0.51	Hip. / van Leeuwen (2007a)	−4.24	*E*
V335 Hya	LB	–	0.36	0.31 − 0.43	Hip. / van Leeuwen (2007a)	−5.68	–
CR Cir	LC	–	0.31	0.25 − 0.42	Hip. / van Leeuwen (2007a)	−3.08	E
CSS 937	–	–	0.42	0.31 − 0.66	Hip. / van Leeuwen (2007a)	−4.11	E
UY Cen	SR	114.6	0.69	0.47 − 1.33	Hip. / van Leeuwen (2007a)	−6.05	I
CSS 938	–	–	0.25	0.20 − 0.33	Hip. / van Leeuwen (2007a)	−3.15	E
CSS 1194	–	–	0.36	0.30 − 0.45	Hip. / van Leeuwen (2007a)	−2.34	*E*

adopt parametric treatments, where observations play a crucial role in fixing the (otherwise free) parameters (Wood, 2003; Olivier & Wood, 2003; Wood et al., 2004; Andersen et al., 2003).

Similar problems affect the estimates of the stellar luminosity. Observations are hampered by the difficulties of measuring the distances for single, often obscured objects like AGB stars. On the other hand, the luminosities derived from full stellar evolutionary models are affected by the uncertainties in the choice of the mixing parameters (in particular of the extension of convective overshoot) and of surface atomic and molecular opacities (Marigo et al., 2003). Models adopting large overshoot parameters (see e.g. Izzard et al., 2007) derive large values for the mass dredged-up after each thermal pulse, thus obtaining the surface enrichment in C and s-elements earlier and at a lower luminosity than models based on the Schwarzschild's criterion can do.

In a previous paper of this series, hereafter referred to as "Paper I" (Guandalini et al., 2006), we analyzed a sample of C stars reconstructing their SEDs up to far infrared, on the basis of space-borne infrared observations from the ISO and MSX missions. We found evidence for a relatively large average C-star luminosity, thus suggesting that the so-called "C-star luminosity problem" (Cohen et al., 1981) might not be real, being simply an effect of poor estimates of the luminosity, due to insufficient knowledge of the mid-infrared emission. We also reviewed the

Table 7. Sample C − First part.

IRAS name	Other name	Stephenson name	Coordinates ICRS	Spectral Type	Var. Type (GCVS)
04352+6602	T Cam	CSS 103	04 40 08.8768 +66 08 48.654	S4,7e−S8.5,8e	M
06571+5524	R Lyn	CSS 283	07 01 18.0093 +55 19 49.766	S2.5,5e−S6,8e:	M
07043+2246	R Gem	CSS 307	07 07 21.2744 +22 42 12.736	S2,9e−S8,9e(Tc)	M
07092+0735	WX CMi	CSS 316	07 11 57.45 +07 29 59.3	Se	M
12417+6121	S UMa	CSS 803	12 43 56.676 +61 05 35.51	S0,9e−S5,9e	M
15030−4116	GI Lup	CSS 872	15 06 16.31 −41 28 14.1	S7,8e	M
23554+5612	WY Cas	CSS 1345	23 58 01.30 +56 29 13.5	S6,5pe	M
00135+4644	X And	CSS 6	00 16 09.57 +47 00 44.8	S2,9e−S5,5e	M
00435+4758	U Cas	CSS 12	00 46 21.371 +48 14 38.72	S3,5e−S8,6e	M
06062+2830	GH Aur	CSS 191	06 09 27.71 +28 29 43.4	S	M
07197−1451	TT CMa	CSS 341	07 22 02.00 −14 56 56.7	S	M
07584−2051	EX Pup	CSS 443	08 00 38.31 −20 59 35.3	S2,4e	M
11179−6135	RY Car	CSS 742	11 20 11.39 −61 52 16.8	S7,8e	M
13226−6302	NZ Cen	CSS 820	13 26 02.52 −63 18 28.5	Se	M
14212+8403	R Cam	CSS 856	14 17 51.0439 +83 49 53.861	S2,8e−S8,7e	M
17478−2957	V762 Sgr	CSS 1001	17 51 04.04 −29 58 30.9	S6,4	M
17490−3502	V407 Sco	CSS 1004	17 52 25.53 −35 03 17.5	Se	M
19166+0318	ER Aql	CSS 1121	19 19 06.99 +03 24 05.2	S	M
23376+6304	V441 Cas	CSS 1338	23 39 58.92 +63 20 55.1	S	M
23489+6235	EO Cas	CSS 1342	23 51 27.30 +62 51 47.0	Se	M
00001+4826	IW Cas	CSS 1347	00 02 44.22 +48 42 50.9	S4.5,9e	M
−	−	CSS2 10	02 51 33.00 +57 50 34.5	S	M
10237−6135	AU Car	CSS 679	10 25 29.74 −61 50 59.1	MS	M
10349−6203	RX Car	CSS 690	10 36 45.82 −62 19 16.8	MS	M
02143+4404	W And	CSS 49	02 17 32.9606 +44 18 17.766	S6,1e−S9,2e/M4−M1	M
07149+0111	RR Mon	CSS 326	07 17 31.54 +01 05 41.5	S7,2e−S8,2e/M6−10	M
07545−4400	SU Pup	CSS 436	07 56 12.0813 −44 08 33.254	M/S4,2e	M
09338−5349	UU Vel	CSS 614	09 35 33.21 −54 03 25.9	M2e/S7,8e	M
17001−3651	RT Sco	CSS 954	17 03 32.56 −36 55 13.7	S7,2/M6e−M7e	M
20213+0047	V865 Aql	CSS 1211	20 23 54.6422 +00 56 44.794	M6−M7/S7,5e:	M
00445+3224	RW And	CSS 14	00 47 18.92 +32 41 08.6	M5e−M10e/S6,2e	M
07103−0258	AK Mon	CSS 319	07 12 49.91 −03 03 29.0	M5/S5,1	M
17521−2907	V745 Sgr	CSS 1007	17 55 19.00 −29 07 54.4	Se/M	M
20044+5750	S Cyg	CSS 1191	20 05 29.85 +57 59 09.1	S2.5,1e/M3.5−M7e	M
20369+3742	FF Cyg	CSS 1232	20 38 51.71 +37 53 23.2	S6,8e/M4e	M
03499+4730	FG Per	CSS 85	03 53 30.2 +47 39 04	M9	M
13163−6031	TT Cen	CSS 817	13 19 35.016 −60 46 46.26	CSe	M
18586−1249	ST Sgr	CSS 1096	19 01 29.20 −12 45 34.0	C4,3e−S9,5e	M
21540+4806	LX Cyg	CSS 1286	21 55 57.03 +48 20 52.6	SC3e−S5,5e:	M
18575−0139	VX Aql	CSS 1093	19 00 09.61 −01 34 56.8	C9,1p/M0ep	M
01097+6154	V418 Cas	CSS 23	01 12 59.89 +62 10 47.6	−	M

available mass loss rates and showed their correlation with infrared colors.

We want now to extend that analysis, considering those thermally-pulsing AGB stars where the enhancement of C (and s-elements) is more moderate than in C stars: it is the case of MS and S giants (Busso et al., 1992, 1995). In Sect. 2 we present the sample stars, and we discuss the choices made in selecting and organizing them in sub-samples, according to the quality of the available data. In Sect. 3 we present the IR colors and derive the bolometric corrections, based on a set of sources whose magnitude can be estimated safely through the integral of detailed SEDs. We also use these corrections for inferring the critical parameters (absolute Magnitudes or distances) of sources for which either i) we have incomplete IR coverage but reliable distance estimates; or ii) Period-Luminosity relations yield the Luminosity, and the distance needs to be inferred from the distance modulus. (For the sake of clarity, the adopted Period-Luminosity relations are discussed in Appendix A). Once the absolute Magnitudes are known, in Sect. 4 we can analyze HR diagrams and luminosity functions and on this base we also attempt a rough estimate of photometric parallaxes for Mira variables with no other available data on Luminosities. Then, in Sect. 5 some preliminary conclusions are derived, while we postpone to a forthcoming dedicated work the analysis of stellar winds.

2. The Sample of S Stars

We started from the extended lists by Stephenson (Stephenson, 1984, 1990), containing O-rich evolved red giants with known or suspected ”S star-like” chemical peculiarities. As mentioned, these last anomalies can be due either to in-situ dredge-up of newly produced elements (intrinsic-S stars) or to mass-transfer episodes in a binary system (extrinsic-S stars). From those catalogues we selected a total of 613 sources for which measurements in the near-IR are available (from 2MASS, see Cutri et al., 2003). Another required property for selection was the existence of mid-infrared photometry (although with varied detail and spectral coverage). The chosen sources fall into various categories, depending on the extension and quality of the information we could collect on their IR colors, distance, variability

Table 8. Sample C − Second part.

Source name	J [Jy]	H [Jy]	K [Jy]	[8.8] [Jy]	[9.8] [Jy]	[11.7] [Jy]	[12.5] [Jy]	D [Jy]	E [Jy]	Mid−IR Data Origin
T Cam	152	306	315	62.1	53.4	48.8	47.1	–	–	IRAS−LRS
R Lyn	51.7	77.7	91.1	29.9	29.9	29.2	28.5	–	–	IRAS−LRS
R Gem	155	226	174	24.1	–	–	21.4	16.3	7.5	MSX
WX CMi	8.9	13.8	17.3	8.3	–	–	9.2	6.3	4.1	MSX
S UMa	26.3	43.4	41.4	4.5	–	2.8	3.1	–	–	TIRCAM2
GI Lup	61.7	115	128	–	–	–	–	–	–	–
WY Cas	64.5	94.4	120	48.8	55.6	58.2	55.0	–	–	IRAS−LRS
X And	18.1	37.3	43.3	23.6	23.6	24.9	26.6	–	–	IRAS−LRS
U Cas	29.6	45.0	47.1	15.2	15.6	19.4	20.3	–	–	IRAS−LRS
GH Aur	4.4	7.8	10.2	1.5	–	–	1.8	–	–	MSX
TT CMa	29.6	50.1	54.3	12.3	–	–	14.1	10.8	7.7	MSX
EX Pup	3.9	5.9	5.8	0.54	–	–	–	–	–	MSX
RY Car	8.3	18.2	25.1	11.0	–	–	8.9	5.6	3.2	MSX
NZ Cen	8.3	15.7	17.2	9.1	–	–	9.3	6.3	5.2	MSX
R Cam	47.2	70.8	69.5	7.1	–	–	–	2.8	–	MSX
V762 Sgr	15.0	35.9	44.5	13.5	–	–	14.4	9.3	5.1	MSX
V407 Sco	9.8	18.1	19.4	6.1	–	–	5.6	3.8	–	MSX
ER Aql	34.4	61.5	62.3	10.1	–	–	6.9	4.7	–	MSX
V441 Cas	5.9	11.6	14.3	2.0	–	–	1.5	–	–	MSX
EO Cas	11.8	21.4	30.9	9.3	–	–	7.5	4.8	3.0	MSX
IW Cas	23.3	47.4	50.9	52.9	58.5	61.8	60.5	–	–	IRAS−LRS
CSS2 10	1.3	2.8	3.1	0.36	–	–	–	–	–	MSX
AU Car	5.9	9.0	10.3	2.1	–	–	–	–	–	MSX
RX Car	5.0	7.7	8.9	2.1	–	–	1.7	–	–	MSX
W And	368	643	591	185	198	163	143	–	–	IRAS−LRS
RR Mon	24.1	42.5	52.8	21.3	–	–	18.0	12.7	7.2	MSX
SU Pup	28.5	43.8	45.5	22.3	26.6	29.1	29.3	–	–	IRAS−LRS
UU Vel	23.5	46.9	51.6	13.6	–	–	11.5	7.5	4.1	MSX
RT Sco	285	460	512	162	–	–	163	108	67.4	MSX
V865 Aql	126	191	199	36.5	33.8	35.2	35.8	–	–	IRAS−LRS
RW And	95.9	132	131	48.8	52.8	53.0	50.1	–	–	IRAS−LRS
AK Mon	9.3	13.1	14.7	3.1	–	–	2.8	2.2	–	MSX
V745 Sgr	38.2	75.8	82.5	18.5	–	–	16.1	11.3	7.4	MSX
S Cyg	11.8	14.0	16.5	2.0	–	–	1.5	0.74	–	MSX
FF Cyg	37.8	65.8	82.0	8.5	–	–	6.4	4.9	–	MSX
FG Per	3.2	6.0	6.8	1.1	–	–	–	–	–	MSX
TT Cen	19.5	48.9	54.7	15.5	–	–	16.3	10.1	8.0	MSX
ST Sgr	97.7	148	149	61.6	63.2	61.1	56.4	–	–	IRAS−LRS
LX Cyg	14.2	28.0	44.9	10.2	–	–	9.4	5.1	–	MSX
VX Aql	13.5	33.6	37.7	9.3	–	–	10.6	6.8	3.5	MSX
V418 Cas	11.0	16.0	22.8	12.5	–	–	12.2	7.9	5.5	MSX

type, period, luminosity. As a result, we can organize the stars selected in the following four sub-samples:

- **Sub-sample** *A*. This contains 21 sources for which ISO-SWS measurements exist up to long wavelengths (40 – 45 μm), so that a detailed Spectral Energy Distribution (SED) can be obtained. The mid-IR SEDs can then be integrated together with near infrared photometric points, in order to infer a very reliable (apparent) bolometric magnitude, by means of the relations of fundamental photometry (Glass, 1999, see also Paper I). In this way we have a means for computing bolometric corrections and look for their correlations with available parameters. Much like for C stars (Paper I), these bolometric corrections are correlated to near-to-mid infrared color indexes. About 50% of the stars in sub-sample *A* have also astrometric estimates of the distance from the revised Hipparcos catalogue (van Leeuwen, 2007a,b); for some others we could infer a distance from the variability period. In all such cases, also the *absolute* Magnitudes can be obtained: the stars with these characteristics are therefore the fundamental bricks on which we build the rest of our work. In particular, bolometric corrections offer us the tools for deriving bolometric Magnitudes for AGB stars outside this main sub-sample *A*, whenever observations of at least one near-to-mid color index exist.
- **Sub-sample** *B*. Here we put all sources (21) for which a reliable estimate of the distance is available (e.g. from Hipparcos, especially after the recent revision by van Leeuwen, 2007a,b), but a detailed mid-infrared SED is not present. Although the stars of sub-sample *B* have only sparse mid-infrared photometry (from MSX, IRAS-LRS or ground-based measurements), thanks to the bolometric corrections discussed above absolute bolometric Magnitudes can be computed for all of them.
- **Sub-sample** *C*. This class contains 41 Mira-type stars, for which near-to-mid IR colors could be derived from either MSX or IRAS measurements. Their Mira variability, of known period, allows for the application of Period-Luminosity relations, yielding the absolute luminosities (see in particular Whitelock et al., 2008). Some comments on the procedure used in this case to homogenize Period-

Table 9. Sample C − Third part.

Source name	Var. Type (GCVS)	Period (GCVS)	Distance (kpc)	Ref. Distance	Bol. Magnitudes P−L Method	I. − E.
T Cam	M	373.2	0.50	P−L / this paper	−5.22	I
R Lyn	M	378.75	0.95	P−L / this paper	−5.19	I
R Gem	M	369.91	0.66	P−L / this paper	−5.23	I
WX CMi	M	420.1	2.35	P−L / this paper	−5.31	–
S UMa	M	225.87	0.96	P−L / this paper	−4.56	I
GI Lup	M	326.2	0.80	P−L / this paper	–	I
WY Cas	M	476.56	0.97	P−L / this paper	−5.50	I
X And	M	346.18	1.31	P−L / this paper	−5.03	I
U Cas	M	277.19	1.08	P−L / this paper	−4.74	I
GH Aur	M	349	2.64	P−L / this paper	−5.13	I
TT CMa	M	314	1.08	P−L / this paper	−4.95	I
EX Pup	M	289	3.02	P−L / this paper	−4.92	–
RY Car	M	424.3	1.95	P−L / this paper	−5.34	I
NZ Cen	M	382	2.22	P−L / this paper	−5.17	I
R Cam	M	270.22	0.84	P−L / this paper	−4.81	E
V762 Sgr	M	444	1.50	P−L / this paper	−5.42	I
V407 Sco	M	396	2.11	P−L / this paper	−5.26	I
ER Aql	M	337.6	1.04	P−L / this paper	−5.10	I
V441 Cas	M	175.6	1.40	P−L / this paper	−4.17	*E*
EO Cas	M	455	1.83	P−L / this paper	−5.47	I
IW Cas	M	396.38	1.34	P−L / this paper	−5.19	–
CSS2 10	M	250	3.78	P−L / this paper	−4.69	–
AU Car	M	332	2.54	P−L / this paper	−5.05	–
RX Car	M	332.8	2.75	P−L / this paper	−5.04	–
W And	M	395.93	0.38	P−L / this paper	−5.27	I
RR Mon	M	394.7	1.28	P−L / this paper	−5.24	I
SU Pup	M	339.8	1.26	P−L / this paper	−5.01	I
UU Vel	M	408.9	1.31	P−L / this paper	−5.32	I
RT Sco	M	449.04	0.45	P−L / this paper	−5.44	I
V865 Aql	M	364.8	0.62	P−L / this paper	−5.18	–
RW And	M	430.3	0.86	P−L / this paper	−5.36	–
AK Mon	M	328.6	2.12	P−L / this paper	−5.02	–
V745 Sgr	M	380.2	0.99	P−L / this paper	−5.23	–
S Cyg	M	322.93	1.94	P−L / this paper	−5.06	I
FF Cyg	M	323.82	0.87	P−L / this paper	−5.07	I
FG Per	M	340.3	3.16	P−L / this paper	−5.10	–
TT Cen	M	462	1.39	P−L / this paper	−5.48	–
ST Sgr	M	395.12	0.76	P−L / this paper	−5.24	I
LX Cyg	M	465.3	1.53	P−L / this paper	−5.51	I
VX Aql	M	604 Zijlstra et al. (2004)	1.99	P−L / this paper	−5.87	I
V418 Cas	M	480	2.24	P−L / this paper	−5.50	–

Luminosity relations are presented in Appendix A. By also applying the bolometric corrections computed from sub-sample *A* to their photometric data, the apparent bolometric magnitudes can be derived, so that an estimate for the distance can be inferred from the distance modulus.

- **Sub-sample** *D*. Here we collect all the remaining sources (~500). One or a few measurements at mid-infrared wavelengths exist also for this sub-sample; these data can be coupled to 2MASS photometry, giving near-to-mid infrared colors on which to apply the bolometric corrections. In this way, we can at least derive reliable bolometric (apparent) magnitudes. As the distance is in general not known from measurements (unlike for sub-sample *B*), and neither it can inferred from any known period (unlike for sub-sample *C*), a precise value for the absolute Magnitude cannot be given at this stage and will have to wait for estimates of the distance. However, we shall see that, at least for known Mira variables, fiducial intervals for the distance can be derived from the HR diagram and the luminosity functions, in the form of a rough photometric parallax.

The first three samples, together with the input data we shall analyze for them, and the resulting estimates for their fundamental parameters are included in this note as Tables 1 to 9. The tables of the last sample are placed in the ”online material” and are available electronically.

In general, we perform the same kind of analysis already presented in Paper I for C-rich AGB stars, computing the bolometric corrections and bolometric magnitudes, the absolute Magnitudes when possible, and expressing the color data in the photometric system described in Paper I and in Busso et al. (2007), hereafter Paper II. In order to adopt this photometric system, we need to perform a re-binning of space-borne spectroscopic data, by convolving them with the response of the filters. We then discuss luminosities and luminosity functions for understanding the evolutionary relations between S stars and C stars along the thermally-pulsing AGB.

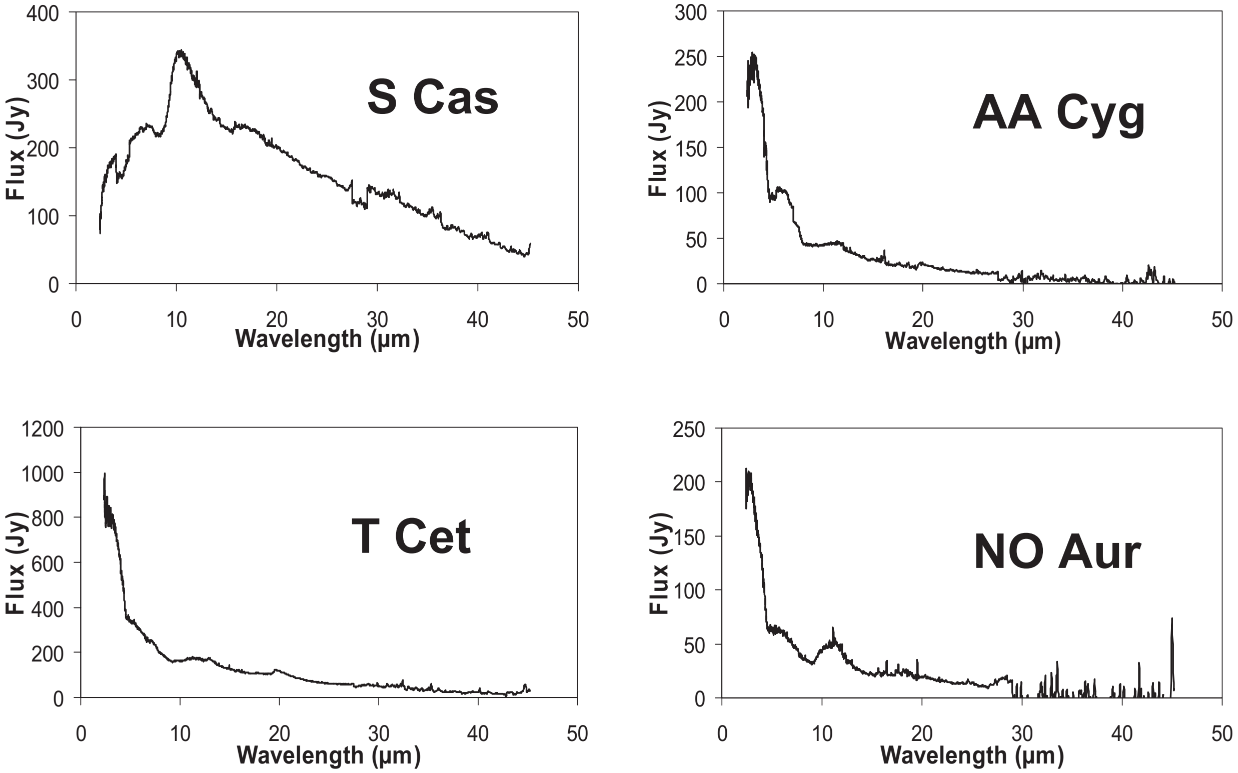

Fig. 1. Examples of ISO-SWS spectra of AGB Stars. Upper left: a S-type Mira Variable (S Cas). Upper right: a S-type Semiregular source (AA Cyg). Lower left and right: two MS stars.

3. Infrared Colors and Bolometric Corrections

We have made a preliminary control that the choice of near and mid IR wavelengths is sufficient for our scope. In fact, one might a priori believe that the inclusion of optical bands could increase the accuracy of bolometric corrections (despite the large uncertainties related to the photospheric variability). However, for all the stars of our samples for which we could find archived visual magnitudes, the optical-to-near-IR colors (e.g. V-J) are always in excess of 3mag. Most V-J colors lay in the range 4-7 and a few in the range 7-10mag, implying flux ratios f_J/f_V larger than at least a factor of 10 and more often a factor of 100. There would be therefore no significant change in the results by introducing optical photometric data. S stars are certainly bluer than C stars (only a couple of sources are dominated by mid-IR, as is instead common for C-rich Miras, like CW Leo); but even when the infrared excess by dust is minimal and the photospheres are optically bright, all AGB stars, including S stars, remain mainly IR objects. The bluest of our sources have maximum emission in the H band.

As discussed in the previous section, we then start from the sources of sub-sample *A* in order to derive the Bolometric Corrections, then proceed to the other stars in our selection. The relevant parameters we collect or derive can be divided into three categories, so we have three tables per each sub-sample. As mentioned before, we include here those referring to groups *A*, *B*, and *C*.

Table 1 presents the general characteristics of sub-sample *A*. This includes: i) the names of the sources (from IRAS, from the Stephenson's compilation (Stephenson, 1984, 1990) and, when available, from the variable star nomenclature); ii) the coordinates (with the equinox fixed at year 2000.0) as given by the ICRS on the SIMBAD database; iii) the spectral types; and iv) the variability type, according to the General Catalogue of Variable Stars (GCVS, Samus et al., 2004). Some of the stars we analyze have uncertain spectral classifications for various reasons. As this point is not among the main issues we want to address, in all these cases we indicate the alternative choices found in the literature, simply separating them by a slash (/). In some cases, our analysis will yield suggestions on the correct classification.

The ISO-SWS SEDs of a few sources of group *A* are shown in Fig. 1, organized according to their spectral classification (MS or S) and variability type (Mira, Semiregular or Irregular). The figure shows one of the most evident properties of AGB stars, present also in C- rich sources: the Mira-type variability is often associated with a remarkable IR excess and a SED peaked at longer wavelengths than for Semiregular or Irregular variables. As compared to C stars, however, the IR excess of S stars is in general much smaller, as we already mentioned. This is probably related to intrinsic properties of dust with O-based or C-based composition. A similar difference exists for molecules (e.g. gaseous component) of the two species, as seen from the photospheres, as we shall argue later.

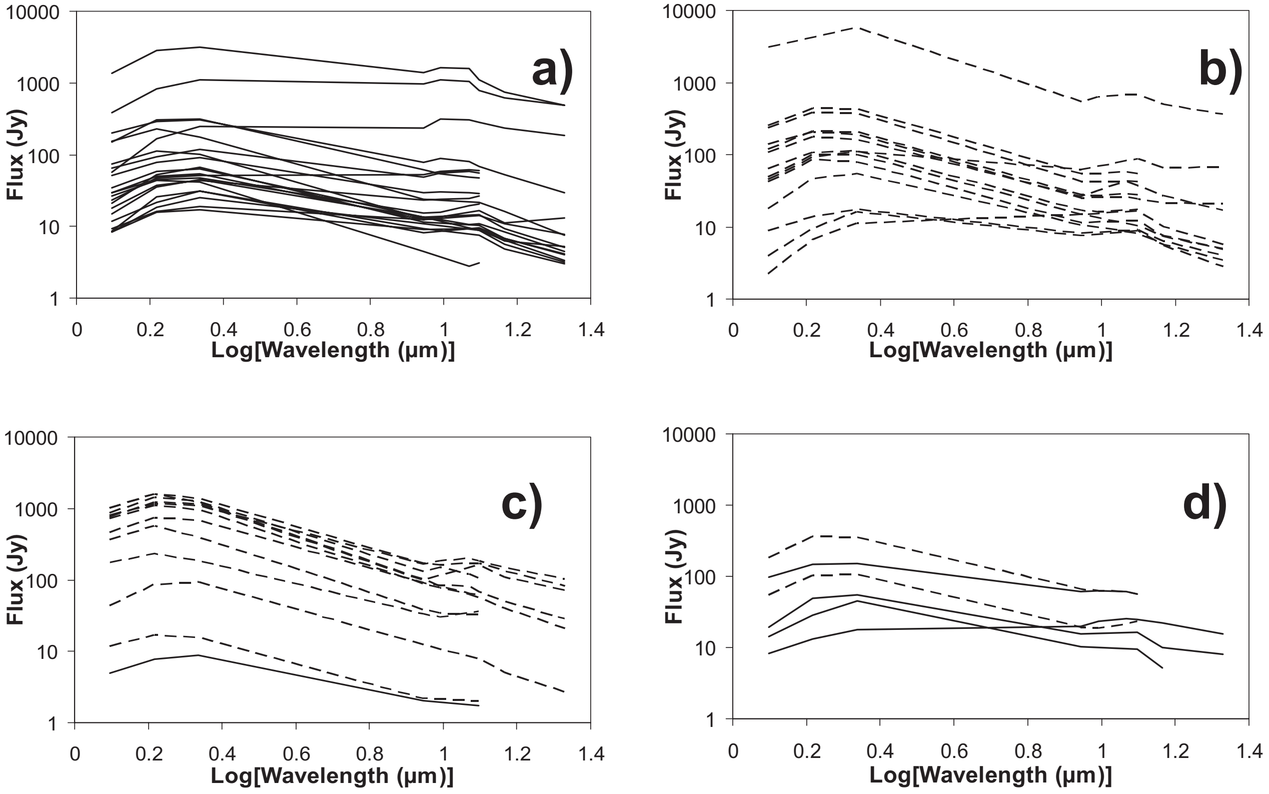

Fig. 2. Spectral energy distributions of sample stars after rebinning in the photometric system of Paper I. a) S Miras. b) S Semiregulars. c) MS sources. d) SC stars. Continuous lines refer to Miras, dashed ones to Semiregulars.

The above very detailed energy distributions are integrated to estimate the apparent bolometric magnitude, using the relation:

$$m_{bol} = -2.5 \int_0^\infty f_\nu d\nu + C \tag{1}$$

as discussed by Glass (1999), who also gives $C = -18.98$ in the case where the total flux is expressed in W m^{-2}. This relation also provides the zero-magnitude flux. From Equation 1 one obtains:

$$f_0 = \int_0^\infty f_\nu d\nu = 1.94 \times 10^{-7} \mathrm{Wm}^{-2} = 1.94 \times 10^{19} \mathrm{JyHz} \tag{2}$$

Following the procedure described in Papers I and II, we again operate a re-binning of the ISO spectra to derive estimates for the fluxes in a number of broader-band infrared filters (with 10% bandwidth), in the range between 8 and 14 μm (centered at 8.8, 9.8, 11.7 and 12.5 μm). (The fluxes in such filters are usually indicated as the equivalent wavelengths in normal brackets; the magnitudes use a similar notation but with squared brackets). These filters are of rather common use in ground-based infrared cameras; our choice is aimed at making the space-borne measurements more easily comparable with present and future photometric observations and to infer for these last suitable bolometric corrections. At long wavelengths ($\lambda > 14\,\mu$m) the re-binning is made using the response curve of the MSX filters D (14.6 μm) and E (21.3 μm). Zero-magnitude fluxes (in Jy) for our chosen photometric system are: 52.23 (8.8 μm), 42.07 (9.8 μm), 29.55 (11.7 μm), 25.88 (12.5 μm), 20.25 (14.6 μm), 8.91 (21.3 μm). For near-IR, 2MASS calibrations for the J, H and K$_s$ filters are given in Cohen et al. (2003).[Hereafter we shall adopt for the K ”short” K$_s$ filter the simple notation K].

Figure 2 gives some examples of the SEDs computed in the photometric system thus defined, for the various types of AGB stars discussed in this note. The same data are listed in Tables 2, 5 and 8, together with near-infrared fluxed obtained from the 2MASS catalogue.

As a consistency check, we repeated the calculations of Equation 1 using the apparent bolometric magnitudes previously derived from ISO spectra, and making the integral over the low-resolution SEDs of Fig. 2. By adopting the zero-magnitude fluxes by Bessell et al. (1998), we obtain for the integration constant an average value $C = -19.0$. The fact that this estimate be very close to the real C value given above certifies that the our re-binning is done properly, and does not alter in any significant way the integrals of Equation 1, hence the magnitudes of our stars.

Once the apparent bolometric magnitudes are known, for those sources for which a reliable estimate of the distance exists we can derive M_{bol}. This estimate can be obtained also for those Mira variables of sub-sample A for which an astrometric measurement of the distance is not available, but the variability period is known. Indeed, the Period-Luminosity relations of

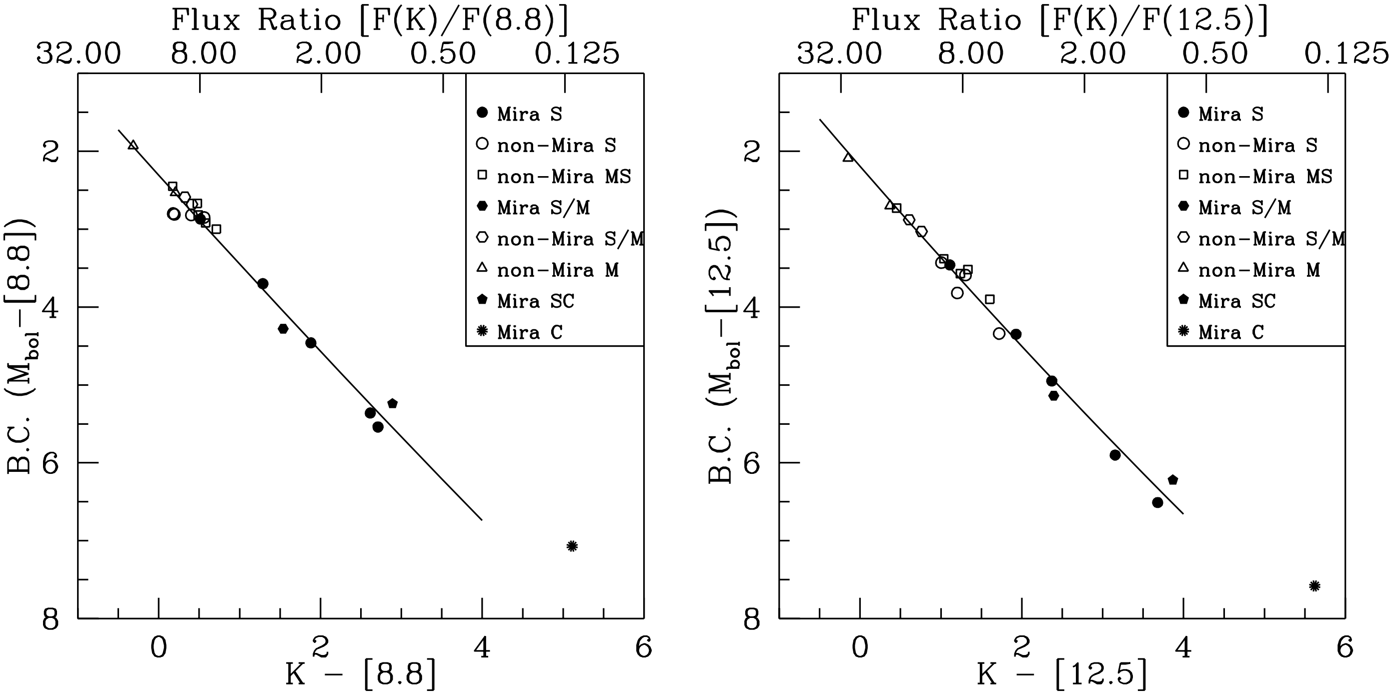

Fig. 3. Two examples of bolometric corrections, suitable for MS-S Stars with infrared photometry available. Correlation coefficients for the two relations are $R^2 = 0.98$ (left) and $R^2 = 0.99$ (right). Here and elsewhere ”K” is a compact notation for the 2MASS filter K_s (K-short).

Mira stars have become sufficiently reliable that we can use them to infer M_{bol} and then obtain the distance from the distance modulus (see Appendix A). The limit of this technique lays in the fact that, not having a proper description of the interstellar extinction, we are forced to exclude the extinction correction. The error introduced on infrared colors, however, is not large, and the related uncertainty remains within the (broad) observational errors of typical infrared photometry (see Paper I for a discussion).

Table 3 presents the absolute bolometric Magnitudes derived for sub-sample *A*, with the indication of the method used, i.e. Period-Luminosity relations (labeled ”this paper”) or distances in the literature (labeled after the reference adopted, either ”Hipparcos”, see van Leeuwen (2007a), or in a single case ”Groenewegen”, taken from Groenewegen et al. (2002)). The values adopted for either the period or the distance are also indicated.

We can then correlate the newly found bolometric Magnitudes with color indexes in the infrared, in order to infer bolometric corrections to be applied to the other groups of stars in our sample. In Fig. 3 we present two of the most significant such correlations. They are shown as corrections to a mid-infrared magnitude ([8.8] or [12.5]) as functions of near-to-mid infrared color indexes (K-[8.8] or K-[12.5] respectively). Least-square fits, shown in the panels of the figure, correspond to:

$$B.C. = -0.0118 \cdot (K - [8.8])^2 + 1.1552 \cdot (K - [8.8]) + 2.3061 \quad (3)$$

and to

$$B.C. = -0.0195 \cdot (K - [12.5])^2 + 1.1949 \cdot (K - [12.5]) + 2.1918 \quad (4)$$

with correlation coefficients of $R = 0.990$ and $R = 0.993$, respectively.

As shown in the figures, both relations are quite tight and offer a reliable way to estimate bolometric Magnitudes for stars for which we have only partial photometric coverage. In the two plots of Fig. 3, there is only one point which is significantly discrepant and does not follow the average correlation. Quite significantly, this point corresponds to *II Lup*, a star that, although listed in the Stephenson’s compilation of S stars, is instead a carbon-rich Mira variable and must therefore be excluded in discussing the photometric properties of O-rich AGB stars.

At this point we need to underline a relevant characteristic of the data displayed in Fig. 3. The corrections there used to infer the bolometric emission are applied to mid-infrared magnitudes, i.e. to data that, for our S stars with moderate IR excess, are essentially constant. This constancy of the mid-IR emission is important for estimating better bolometric corrections and is not shared by very red objects, e.g., by the carbon-rich Miras, where also the emission from the circumstellar envelope varies significantly in time (see Paper II). Anyhow, for our sample stars in Figure 3 we expect roughly constant magnitudes at 8.8 or 12.5 μm, while the K(short) estimates from 2MASS, being single-epoch measurements, are affected by the photospheric variability (that can be up to 1 - 1.5 mag in near-IR). Different stars were certainly (randomly) sampled by 2MASS in different epochs of their light curves, but despite this, all the data fit a single regression line quite well. This can be so only if, during a cycle, the representative points of our stars move along the regression line itself. One might wonder why. The variability of AGB stars is not necessarily related only to a transfer of energy from one wavelength range to another (due to the star becoming cooler and more extended or hotter and more compact). There might be actually a global variability of the bolometric magnitude itself, because we can see the addition, with different percent weight, of energy from finite-amplitude mechanical oscillations and shock waves affecting the envelope. The color dependence of these emissions is unknown to us, but we know experimentally that it does not extend to mid-IR for moderately red objects. If the chosen mid-IR magnitudes remain essentially constant, then bolometric corrections variable in time will be needed to compensate for the near-IR (and for the possible bolometric) variability. When the star is brighter it will require a larger correction, when it is dimmer the correction will be smaller, but as long as the regression line remains valid, the given formula for the B.C. should continue to hold. This would not be true if we had chosen, in the ordinate, a near-IR magnitude, still affected by the photospheric variability, having an unknown color dependence.

It remains however true the bolometric magnitudes given here, although possibly rather well estimated thanks to the use of mid-IR data, might be intrinsically variable. We have estimated how much the rather common variability by about 1 mag in K_s would affect the global flux, and this can reach up to 25% of the total. When estimating bolometric Magnitudes, throughout this paper, we apply both the corrections of Fig. 3 whenever possible, and then take the average of the absolute Magnitudes thus obtained (the values to be averaged are in any case very close to each other).

We then applied the above corrections to the IR colors of sub-sample *B*, thus deriving also for them an estimate of the bolometric Magnitude. The input data and the derived parameters for this sample are shown in Tables 4 to 6.

A somewhat inverse procedure is applied to the sources of sample *C*, where Luminosities can be inferred from Period-Luminosity relations. Here a comparison with the apparent bolometric magnitude, derived from bolometric corrections, yields the distance of the object. The recent updates in Period-Luminosity relations for AGB stars, which now allow for this possibility, are discussed in Appendix A.

The input data and the derived parameters for sample *C* are illustrated in Tables 7 to 9. The whole (more sparse) information we could compile for the bigger but so far incomplete sub-sample *D* is included instead in Tables 11 and 12, which we publish in electronic form due to their dimensions. For the content of Table 10 see next section.

4. HR Diagrams and Luminosity Functions

Using the IR fluxes collected in the previous section, and the information acquired on the absolute luminosities (see also Appendix A), we can now study the photometric properties of S stars and their relatives, with the aim of understanding how they are linked to the evolutionary status of the sources and to their chemical properties.

Figure 4 illustrates the J-K vs K-[8.8] color-color diagram of the sources in our sample. The variability types appear rather well discriminated from IR colors. With only one exception (an SC star believed to be of Semiregular variability, but that we suspect is instead a misclassified Mira), all Semiregular and Irregular variables lay in the lower-left part of diagram, and remain separated by Miras by a dividing gap (the dashed line is just an eye's guide to illustrate this). Similarly, only very few objects classified as Miras fall at the left of the guiding line, all of them with short periods, while the vast majority is, in both colors, redder than Semiregulars and Irregulars. This is not surprising, in view of the fact that Miras are more efficient mass-losers and, as we argue below, are on average more evolved. We actually interpret the emerging evidence (from both the present sample and those of Papers I and II) as a suggestion that efficient radiation pressure on dust grains, powering fast mass lost, starts when the star has reached the Mira-like variability at periods in excess of about 200 – 230 days. In any case, the use of IR colors for discriminating different sources is interesting because the separation of the types is quite good, to the point that the IR colors might be used for guessing the variability type. (For example, if one picks up an AGB star of unknown variability, with J-K and K-[8.8] colors near 2, then we can reliably assume that it must be a Mira star).

Figures 5 and 6 show two examples of the absolute H-R diagrams derived from our sample stars (the figures refer to both intrinsic and extrinsic sources). They are presented as a function of J-K and K-[8.8] colors, which can be considered as monitors either of the photosphere alone (J-K) or of the inner circumstellar environment (K-[8.8]). The link between fluxes in Jy and magnitudes in the various filters, hence to colors, is established by i) the distance correction (no extinction is assumed): and ii) the calibration of zero-magnitude fluxes given above.

The HR diagrams contain a large number of useful pieces of information on S Star morphology and physics. We identify here a few such issues.

- Absolute Magnitudes of Semiregular and Irregular variables stay on an almost vertical sequence, close to the region covered by AGB stellar models, albeit with remarkable scatter. Below this sequence, at the bottom of the plot, we find sources whose luminosities suggest that they are in an evolutionary stage preceding the thermally-pulsing AGB. These must necessarily be extrinsic S or MS stars; indeed, in most cases their extrinsic nature is already well established. For those sources (five) in this group for which no information on binarity is available, we suggest here, as a result of our luminosity calibration, that they are extrinsic and not yet on the TP-AGB (see the relative indication in bold and underlined in Tables 3, 6, 9). This suggestion will now need independent confirmations, which would also indirectly verify (or deny!) the validity of our bolometric corrections. If we are right, then extrinsic S stars should be the O-rich equivalent of the carbon rich R stars; Fig. 5 supports this guess in showing that lower-luminosity S stars are also warmer than the others.
- S-star infrared colors are different from those of C stars, being on average much bluer. Infrared excesses are less extreme, although mid-infrared (especially the [8.8] filter) remains the crucial wavelength range for understanding their physics: in particular we underline that, also for S stars, the best relations determining bolometric corrections are obtained by making use of mid-infrared colors.
- The un-reddened MS-S sources distributed along the vertical branch in Figs. 5 and 6 are more compatible with the evolutionary AGB tracks than for similarly-positioned C stars. Red-shifts of the track, requiring temperature corrections (and indicating inadequacy in molecular opacities of the envelope), although present, are largely reduced (by 0.5–1 mag.) as compared to C stars (see Paper II).
- Absolute Magnitudes of Mira variables are distributed over a relatively well defined distribution. They show a linear trend, indicating higher luminosities for redder colors and the correlation is clear, although the slope is small. In Fig. 6 we have added a least square curve based only on bona-fide, intrinsic S Miras. The relation is:

  $$M_{bol} = -0.2104 \cdot (K - [8.8]) - 4.9765 \qquad (5)$$

  with a correlation coefficient $R = 0.78$. Of course one expects different luminosities for sources of different colors (Period-Luminosity relations are such that the LPVs of longer period are also redder). It is however interesting to notice that, despite the infrared excesses increasingly separate the observed points from the AGB model tracks, we can

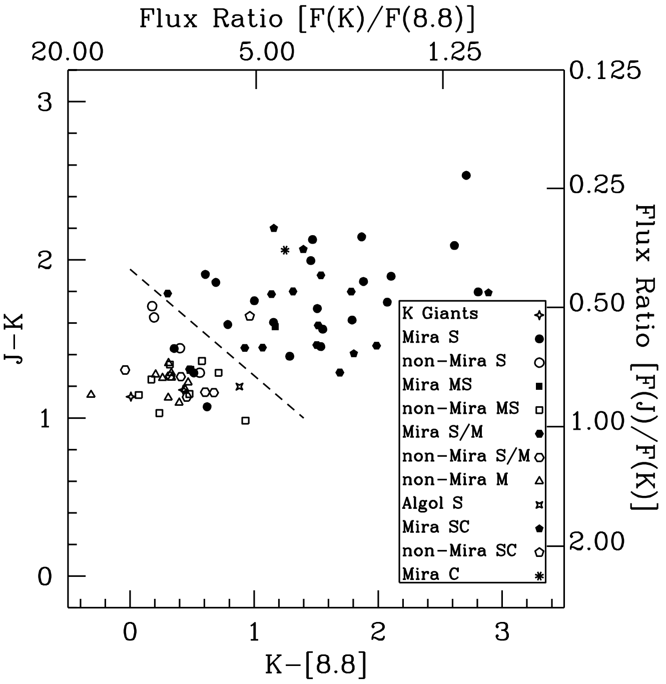

Fig. 4. A color-color diagram of the sources in samples A to C. All of them belong to the Stephenson's list, but some are misclassified: indeed, we find a few K and M giants, and a couple of C stars. Mira variables are redder than other sources in both colors and generally well separated from the rest by IR color criteria.

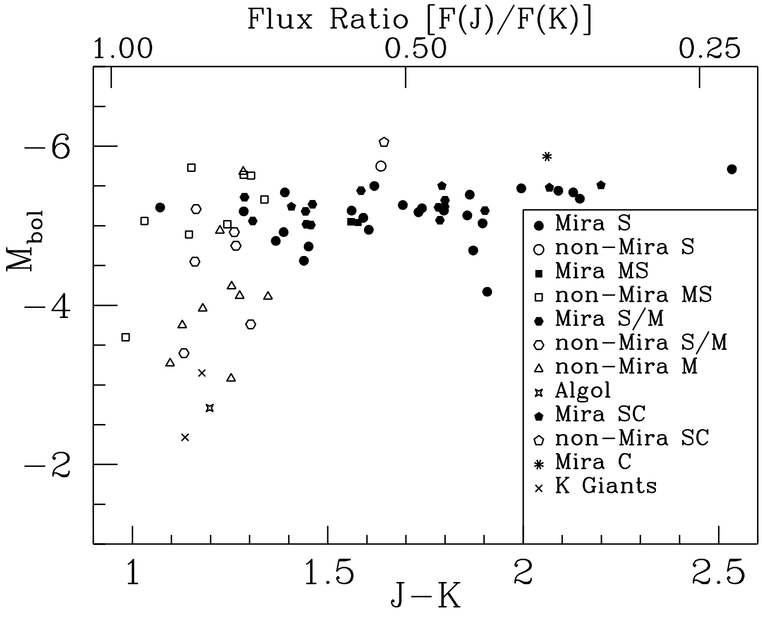

Fig. 5. An example of an absolute HR diagram, built using a near IR color index as abscissa.

nevertheless determine a systematic trend in the magnitude (now dominated by the circumstellar envelope). Moreover, it's remarkable that the correlation is sufficiently tight not to be confused by the observational errors.

If one computes a global average of the Magnitudes of Miras, this turns out to be −5.15 ± 0.4. Once stars have reached this luminosity range and are in the Mira variability stripe, further remarkable increases of luminosity seem to be no longer possible. This limiting range of luminosities (less than 1 mag. wide) is close to a similar one that can be inferred for C-rich Miras in the data of Paper I. Since the range is relatively small, Mira variables appear to have, on average, similar Magnitudes, independent of the chemical composition of the atmosphere.

– We can confirm for S stars what was already said for C-stars: the Mira variability type tends to occur primarily at the end of the evolution. It was argued in the past that Semiregulars might be AGB stars in the low-luminosity post-flash dip (Kerschbaum & Hron, 1996), so that a repeated transition between the two main variability types was expected. We cannot exclude this in general, but the high statistical relevance of Semiregular variables (almost as abundant as Miras in our global database, including sources of group *D*) cannot be explained by the post-flash phases, which, for advanced

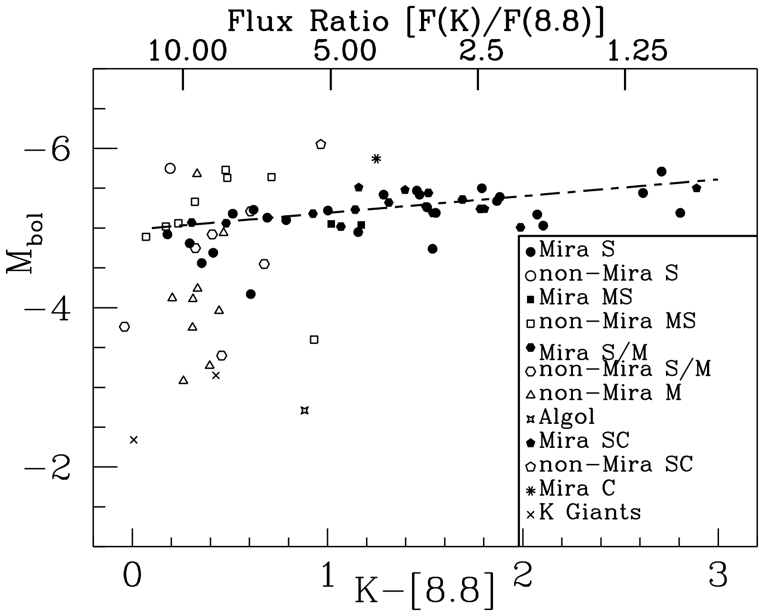

Fig. 6. An example of an absolute HR diagram, built using a near-to-mid IR color index as abscissa.

Table 10. Sample D − Distance Estimates.

Source name	Apparent bol. magnitudes	Distance (kpc)	Min. – Max. Distance (kpc)
NX Per	7.61	3.57	2.97 – 4.30
NU Pup	8.58	5.56	4.63 – 6.69
DK CMa	6.06	1.75	1.45 – 2.10
EW Pup	7.04	2.74	2.28 – 3.29
WY Pyx	5.01	1.08	0.90 – 1.29
V2434 Oph	4.95	1.05	0.87 – 1.26
V342 Ser	6.55	2.18	1.82 – 2.63
V471 Sct	5.85	1.59	1.32 – 1.91
V427 Sct	6.88	2.54	2.11 – 3.06
V1959 Cyg	6.47	2.11	1.76 – 2.54
PR Nor	4.51	0.85	0.71 – 1.03
PZ Vul	8.43	5.20	4.33 – 6.25
GY Lac	7.31	3.11	2.58 – 3.74
V928 Cas	8.22	4.73	3.93 – 5.69
V508 Aur	8.28	4.86	4.04 – 5.84
V1992 Cyg	7.90	4.07	3.38 – 4.89
V1850 Cyg	8.56	5.53	4.60 – 6.65
V1242 Cyg	8.12	4.50	3.74 – 5.41

thermal pulses, occupy at most 25% of the TP-AGB duration (see also Fig. 8).

– The limited spread of Mira Magnitudes and the sufficiently good correlation with IR colors offer a tool for obtaining a first-order approximation to the luminosity and distance of Mira stars for which we do not have information beyond the measured colors. Indeed, for them one can first derive the apparent bolometric magnitude from our bolometric corrections; then one can assume, as a reasonable guess, that bolometric absolute Magnitudes have an average of −5.15 ± 0.4 and a correlation with the K-[8.8] color like the one shown for Fig. 6. This allows a determination of the distance from the distance modulus. An example of the application of this procedure to Mira variables in sample *D* is shown in Table 10.

– Stars differently classified along the sequence MS, S, SC show a different behavior also for what concerns the variability. Albeit with some scatter, one can notice that the MS classification is in general (with two possible exceptions) accompanied by the Semiregular or Irregular variability types, while a much larger percentage (about 60%) of S stars shows the Mira-type variability. Concerning SC stars, of the 5 objects for which we have detailed information, 4 are of Mira type; from the color-color diagram of Fig. 4 we suspect this should be so also for the fifth member, for which we suggest that the previous classification as a Semiregular might be wrong. SC stars are in general red, cool and luminous, like most S Miras. They might be the final evolutionary status of stars whose mass is barely sufficient to dredge-up enough carbon to approach unity in the C/O ratio.

The luminosity properties illustrated by the HR diagrams, and in particular the narrow range over which the magnitudes of MS-S Miras are distributed, are illustrated by the histogram of Fig. 7, showing the luminosity function of our sources. The distribution has a very well defined peak: all MS, S, SC stars lay in

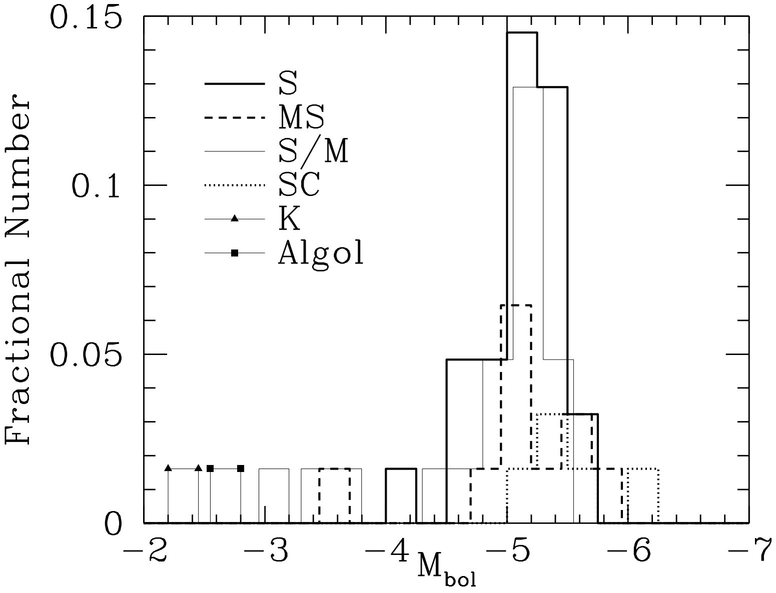

Fig. 7. The luminosity function of the stars in our samples *A* to *C*. Low luminosity sources are always extrinsic and the S stars define a very narrow distribution, characterized by a magnitude −5.15 ± 0.4.

the range −4 to −6 and Mira S stars occupy a thin slice across the magnitude values −4.8 to −5.5. All the data points significantly far from this peak refer to extrinsic sources not belonging to the TP-AGB phase. Many (most) sources of uncertain classification (so far indicated as S/M) fall in the fiducial interval of the 'best' S stars. We are pretty sure they are indeed S stars and probably Miras. In Tables 3, 6, 9 and 12 we indicate the possible classification deduced from Van Eck et al. (2000); Yang et al. (2006). In a few cases of discordant indications we prefer the physical analysis by Van Eck et al. (2000) and we show the other in parenthesis. For five sources in Tables 6 and 9, for which neither study offers a suggestion, we can infer that they are extrinsic from their low intrinsic Luminosity.

Like for C stars, and actually even more so, the Luminosities of Population I S stars are well defined inside a narrow range and are high enough that normal stellar models based on the Schwarzschild criterion for convection can adequately explain their formation. Once again, and as already noticed in Paper I, stellar models using large convective overshoot to favor dredge-up, and to obtain S-star and C-star chemical peculiarities at low luminosities (Izzard et al., 2007) appear to be unjustified, at least as far as the AGB evolutionary stages are concerned. Recently Bonačić Marinović et al. (2007) suggested that such models should be preferred for their capability of reproducing *s*-process abundances in stellar populations. One has however to mention that, from a theoretical point of view, the several free parameters still involved in any modelling probably make any conclusion provisional, and require observational verifications. Infrared observations, as presented here, do not confirm the need for large overshooting, at least for what concerns the ensuing stellar luminosities.

5. Conclusions

In this paper we have presented a reanalysis of the properties of MS-S-SC stars, based on a sample of about 600 sources, whose infrared fluxes from 1.25 to 21 μm were measured by the 2MASS, IRAS, ISO and MSX experiments. A 'best' group of 21 stars (for which detailed ISO-SWS spectra are available up to long wavelengths) allowed us to obtain the bolometric Magnitudes from an effective integral of the spectral energy distribution up to 45 μm. Correlations with near-to-mid IR colors then allowed us to infer bolometric corrections suitable to be applied to other groups of sources, with a less detailed coverage of the energy distribution. We can thus estimate with sufficient accuracy the apparent bolometric magnitudes of more than 500 sources. The whole analysis was performed in the photometric system suggested in Busso et al. (1996) and subsequently used in Paper I and Paper II.

Criteria for obtaining the distance have then been discussed, from the simple use of revised astrometric measurements to a reformulation of the known Period-Luminosity relations for O-rich Long Period variables. The results of our analysis suggest that Mira variables of the S type have on average magnitudes in the range −5.15 ± 0.4, showing a well-defined linear correlation with infrared colors, especially the K-[8.8] one. Low-mass AGB stars do not appear to proceed beyond the upper limit of the Mira luminosity range. Inside this range $P - L$ relations have become rather tight and accurate; they now form a very useful tool for determining intrinsic stellar parameters. From the $P-L$ relations and the $M_{bol} - (K - [8.8])$ relation of Equation 5 we now have tools to estimate the absolute Magnitudes, hence the distances, of Mira S variables for which either the period or the infrared colors have been determined.

From statistical considerations it is also argued that Mira variables should occupy mainly the final part of the AGB track, as the simple intermittency between low-luminosity post flash dips and high-luminosity H-shell-powered stages is not sufficient to explain the available numbers of Semiregulars and Miras.

Luminosity functions confirm that intrinsic S stars (especially if in the Mira class) are distributed over a narrow range around the above average magnitude, and that this last datum is very close to the one previously found for C-stars. This is so to the point that it appears unlikely that a single AGB star can follow the whole M-MS-S-SC-C sequence, by simply increasing gradually its content of carbon and heavy elements as time passes, new dredge-up episodes enrich the envelope and the luminosity increases. Most probably, small differences in the ini-

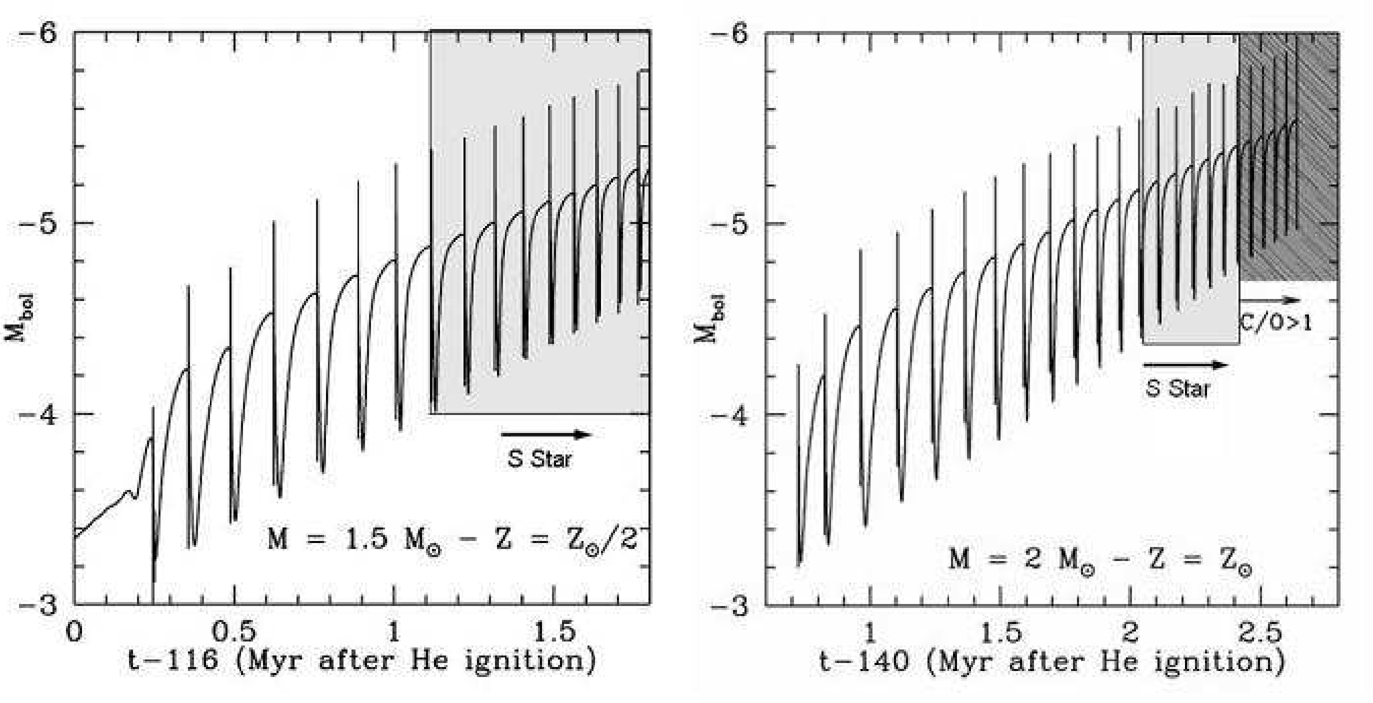

Fig. 8. The magnitude variations of two model stars of Population I, during the thermally pulsing AGB phase, as computed by the FRANEC code. The abscissa shows the time passed after the ignition of He-burning in the core, in Million years (once an offset is deduced, whose value is indicated). Most sources with features typical of S or C stars and magnitudes in the range -5.2 ± 0.4 should belong to the mass and metallicity range illustrated here, but only the star in the right panel does achieve the C/O > 1 condition.

tial mass and metallicity, almost indistinguishable once on the AGB, determine the final chemical fate of a star, which, for increasing initial mass, can end its life either as a MS-S giant, or a SC giant, or reaching effectively the C(N) stage. As an example of the effects of small mass (and metallicity) differences, Fig. 8 shows two AGB luminosity sequences obtained from the FRANEC code by Busso et al. (2003). The model star of the left panel does not reach the C-star phase, ending as an MS/S star. The evolutionary phases during which S-type chemical peculiarities are exhibited by the envelope are shaded in the plot. In the right panel we instead show the results of a model producing a real C-star: it has a slightly higher mass. Given the magnitudes we found in this paper for the sources of types MS and S, and those found in Paper I for C stars, most of the objects in our sample should belong to the mass and metallicity range covered by Fig. 8. If we broadly consider the typical magnitudes of S and C stars as being in the range -5.2 ± 0.4, then it is clear that this range includes both the S-star phase in the first panel of Fig. 8 and the S- and C-star phases in the right panel. It would be very difficult or impossible to distinguish between the two cases on the basis of their magnitudes, given the remaining uncertainties on distances and on possibly variable bolometric magnitudes.

The above results, and the typical initial mass implied for S and C stars (1.5 - 2 $M_\odot$) might appear rather peculiar, in view of the fact that about half of Planetary Nebulae are carbon rich. This cannot be explained by progenitors of around 2 $M_\odot$, at least according to the most common choices for the Initial Mass Function. However we must remember that the efficiency of dredge up strongly increases with decreasing metallicity. In halo stars one solar mass might be sufficient for forming a C star (also because the abundance of oxygen is very small). Hence the results presented here should be considered as valid only for galactic disc stars, at relatively high metallicities.

Acknowledgements. We are grateful to the anonymous referee for a very useful, careful and stimulating report, which greatly helped in the improvement of this work. We acknowledge support from the Italian Ministry of Research, under contract PRIN2006-022731, and from the Section of Perugia of the National Institute for Nuclear Physics (INFN). This study is also part of the preparatory work for the IRAIT Antarctic telescope, of the Piano Nazionale delle Ricerche in Antartide (PNRA). These studies on Antarctic Astronomy are profiting of the financial support and cultural possibilities offered by the European Coordinating Action ARENA (within the FP6 plan).
This research has made use of the SIMBAD database and the VizieR service (CDS, Strasbourg, France), and the IRSA (NASA/IPAC InfraRed Science Archive) database (USA), and the Astrogrid database (UK). In particular archived data from the experiments MSX, ISO-SWS and 2MASS were used. • The processing of the science data of the Midcourse Space eXperiment (MSX) was funded by the US Ballistic Missile Defense Organization with additional support from NASA Office of Space Science. • The Infrared Space Observatory (ISO) is an ESA project with instruments funded by ESA Member States (especially the PI countries: France, Germany, The Netherlands and UK). • 2MASS (Two Micron All Sky Survey) is a joint project of the Univ. of Massachusetts and the Infrared Processing and Analysis Center (IPAC) at California Institute of Technology, funded by NASA and the NSF (USA).

References

Alcock, C., Axelrod, T.S., Bennett, D.P., et al. 1992, Robotic telescopes in the 1990s; 103rd Annual Meeting of the Astronomical Society of the Pacific, Univ. of Wyoming, Laramie, 1991, p. 193
Allende Prieto, C., Lambert, D.L., & Asplund, M. 2002, ApJ, 573, L137
Anders, E., & Grevesse, N. 1989, Geochem. Cosmochem. Acta, 53, 197
Andersen, A.C., Höfner, S., & Gautschy-Loidl, R. 2003, A&A, 400, 981
Bedding, T.R., & Zijlstra, A.A. 1998, ApJ, 506, L47
Bessell, M.S., Castelli, F., & Plez, B. 1998, A&A, 333, 231
Bonačić Marinović, A., Izzard, R.G., Lugaro, M., & Pols, O.R. 2007, A&A, 469, 1013
Busso, M., Gallino, R., Lambert, D.L., Raiteri, C.M., & Smith, V.V. 1992, ApJ, 399, 218
Busso, M., Lambert, D.L., Beglio, L., et al. 1995, ApJ, 446, 775
Busso, M., Origlia, L., Marengo, M., et al. 1996, A&A, 311, 253
Busso, M., Gallino, R., & Wasserburg, G.J. 1999, ARA&A, 37, 239

Busso, M., Gallino, R., Lambert, D.L., Travaglio, C., & Smith, V.V. 2001, ApJ, 557, 802
Busso, M., Gallino, R., & Wasserburg, G.J. 2003, PASA, 20, 356
Busso, M., Guandalini, R., Persi, P., Corcione, L., & Ferrari-Toniolo, M. 2007, AJ, 133, 2310 (Paper II)
Carciofi, A.C., Bjorkman, J.E., & Magalhães, A.M. 2004, ApJ, 604, 238
Cioni, M.-R.L., Blommaert, J.A.D.L., Groenewegen, M.A.T., et al. 2003, A&A, 406, 51
Cohen, J.G., Persson, S.E., Elias, J.H., & Frogel, J.A. 1981, ApJ, 249, 481
Cohen, M., Wheaton, Wm.A., & Megeath, S.T. 2003, AJ, 126, 1090
Cutri, R.M., Skrutskie, M.F., van Dyk, S., et al. 2003, VizieR On-line Data Catalog: II/246, University of Massachusetts and Infrared Processing and Analysis Center, (IPAC/California Institute of Technology), 2003
Feast, M. 1999, IAUS, 191, 109
Feast, M. 2004, IAU Colloquium 193, Proceedings of the conference held 6-11 July, 2003 at Christchurch, New Zealand. Edited by D.W. Kurtz, & K.R. Pollard. ASP Conference Proceedings, Vol. 310. San Francisco: Astronomical Society of the Pacific, 2004., p.304
Feast, M.W., Glass, I.S., Whitelock, P.A., & Catchpole, R.M. 1989, MNRAS, 241, 375
Glass, I.S. 1999, The Handbook of Infrared Astronomy (Cambridge: England), Cambridge University Press
Groenewegen, M.A.T., Sevenster, M., Spoon, H.W.W., & Pérez, I. 2002, A&A, 390, 511
Guandalini, R., Busso, M., Ciprini, S., Silvestro, G., & Persi, P. 2006, A&A, 445, 1069 (Paper I)
Habing, H.J. 1996, A&ARv, 7, 97
Hughes, S.M.G, & Wood, P.R. 1990, AJ, 99, 784
Izzard, R.G., Jeffery, C.S., & Lattanzio, J.C. 2007, A&A, 470, 661
Kerschbaum, F., & Hron, J. 1996, A&A, 308, 489
Knapp, G.R., & Morris, M. 1985, ApJ, 292, 640
Le Bertre, T., Matsuura, M., Winters, J.M., et al. 2001, A&A, 376, 997
Le Bertre, T., Tanaka, M., Yamamura, I., & Murakami, H. 2003, A&A, 403, 943
Marigo, P., Girardi, L., & Chiosi, C. 2003, A&A, 403, 225
Merrill, S.P.W. 1952, ApJ, 116, 21
Olivier, E.A., & Wood, P.R. 2003, ApJ, 584, 1035
Olofsson, A.O.H., Olofsson, G., Hjalmarson, Å., et al. 2003, A&A, 402, 47
Omont, A., Gilmore, G.F., Alard, C., et al. 2003, A&A, 403, 975
Salpeter, E.E. 1974, ApJ, 193, 585
Samus, N.N., Durlevich, O.V., et al. 2004, VizieR On-line Data Catalog: II/250, Institute of Astronomy of Russian Academy of Science and Sternberg, State Astronomical Institute of the Moscow State University, 2004
Sandin, C., & Höfner, S. 2003a, A&A, 398, 253
Sandin, C., & Höfner, S. 2003b, A&A, 404, 789
Sedlmayr, E. 1994, Lecture Notes in Physics, 428, 163
Smith, V.V., & Lambert, D.L. 1986, ApJ, 311, 843
Smith, V.V., & Lambert, D.L. 1990, ApJS, 72, 387
Stephenson, C.B. 1984, A General Catalogue of Galactic S-Stars - ED.2. Publ. of the Warner & Swasey Observatory.
Stephenson, C.B. 1990, AJ, 100, 569
Tuchman, Y. 1999, IAUS, 191, 123
Uttenthaler, S., Hron, J., Lebzelter, T., et al. 2007, A&A, 463, 251
Van Eck, S., Jorissen, A., Udry, S., et al. 2000, A&AS, 145, 51
van Leeuwen, F. 2007a, Hipparcos: The new reduction of the raw data, Springer, Berlin
van Leeuwen, F. 2007b, A&A, 474, 653
Wachter, A., Schröder, K.-P., Winters, J.M., Arndt, T.U., Sedlmayr, E. 2002, A&A, 384, 452
Whitelock, P., & Feast, M. 2000, MNRAS, 319, 759
Whitelock, P., Menzies, J., Feast, M., et al. 1994, MNRAS, 267, 711
Whitelock, P.A., Feast, M.W., Marang, F., & Groenewegen, M.A.T. 2006, MNRAS, 369, 751
Whitelock, P.A., Feast, M.W., & van Leeuwen, F. 2008, MNRAS, Online Early, Vol. 393
Winters J.M., Le Bertre T., Jeong K.S., Nyman, L.-Å., & Epchtein, N. 2003, A&A, 409, 715
Wood, P.R. 2003, Mass-losing pulsating stars and their circumstellar matter. Workshop, May 13-16, 2002, Sendai, Japan. Ed: Y. Nakada, M. Honma, & M. Seki. Astrophysics and Space Science Library, Vol. 283, Dordrecht: Kluwer Academic Publishers, p.3
Wood, P.R., & Cohen, M. 2001, Post-AGB Objects as a Phase of Stellar Evolution, Proceedings of the Torun Workshop held July 5-7, 2000. Ed: R. Szczerba, & S.K. Górny. Astrophysics and Space Science Library Vol. 265. Publisher: Kluwer Academic Publishers, p.71
Wood, P.R., & Sebo, K.M. 1996, MNRAS, 282, 958
Wood, P.R., Alcock, C., Allsman, R.A., et al. 1999, IAUS, 191, 151
Wood, P.R., Olivier, E.A., & Kawaler, S.D. 2004, ApJ, 604, 800
Yang, X., Chen, P., Wang, J., & He, J. 2006, AJ, 132, 1468
Zijlstra, A.A., Bedding, T.R., Markwick, A.J., et al. 2004, MNRAS, 352, 325
Zinner, E. 2000, Meteoritics & Planetary Science 35, Supplement, p.A177

Appendix A: Period-Luminosity Relation

Mira stars have been alternatively suggested to be radially pulsating either in the fundamental mode, or in the first overtone (Tuchman, 1999; Feast, 1999). For Semiregular variables various overtones and the same fundamental mode are also possible. The discussion on these properties has gone on for three decades, although the large database made available by the MACHO project (Alcock et al., 1992) seems to favor the fundamental mode for Miras (Wood et al., 1999).

The non-unique pulsational properties of Semiregular variables imply that there is not a unique $P - L$ relation for them (Bedding & Zijlstra, 1998). Instead, such relations for O-rich and C-rich Miras have become increasingly accurate and statistically relevant, to the point of forming now an invaluable tool in the difficult task of determining the distances of Long Period Variables. Many studies in the past were dedicated to correlate $LogP$ with magnitudes obtained in the K filter (Feast et al., 1989; Hughes & Wood, 1990; Wood & Sebo, 1996). This method, however, meets the difficulty of the still remarkable light-curve amplitude at 2 μm. Relations directly connecting the period to the bolometric magnitude (Feast et al., 1989; Whitelock et al., 1994, 2006) are therefore precious, although obviously more difficult to obtain.

Different relations are expected (and found) for C-rich and O-rich objects (see in particular Whitelock & Feast, 2000; Whitelock et al., 2006). For our sample of S-stars, which have C/O ≤ 1, we can use the $M_{bol} - P$ relation suggested for O-rich Miras by Feast et al. (1989) and Whitelock et al. (1994).

Another formula, established for Magellanic Cloud O-rich Miras, but suitable also for the Galaxy in view of the universality of the slope (Feast, 2004), was presented recently by Whitelock et al. (2008). This last relation is based on the K-magnitude. It is difficult to establish criteria for choosing between the two, so that we decided to use both, and then take an average of the results. (We underline that both the original relations were derived for O-rich sources and should therefore apply also to S stars, where the ratio C/O does not reach unity). In particular, our procedure was the following one. i) We firstly derived apparent bolometric magnitudes from the bolometric corrections of Fig. 3, then we applied the relations by Whitelock et al. (1994) to obtain an estimate of the bolometric Magnitudes. Hence from the distance modulus we could infer a first value for the distance. ii) Separately, we applied the formula by Whitelock et al. (2008) to derive the absolute K magnitude, then by comparison with the 2MASS measurement we deduced a second estimate for the distance. The two distance values were then averaged to get a final choice. This choice for the stellar distance was then applied to our apparent bolometric magnitudes, thus deducing our best estimate for the absolute bolometric Magnitude.

Although certainly intricate, the above procedure should minimize the systematic errors of each individual method. The Magnitudes thus deduced are plotted as a function of the period in Fig.A.1, thus providing our choice for the *average* $P - L$ relation, descending primarily from the quoted works, but also from our averaging technique and from our estimate of the bolometric corrections. The derived Period-Magnitude relation can be expressed by a fitting spline with a high accuracy, as shown on the same graph. In the plot, we also included, as a comparison,

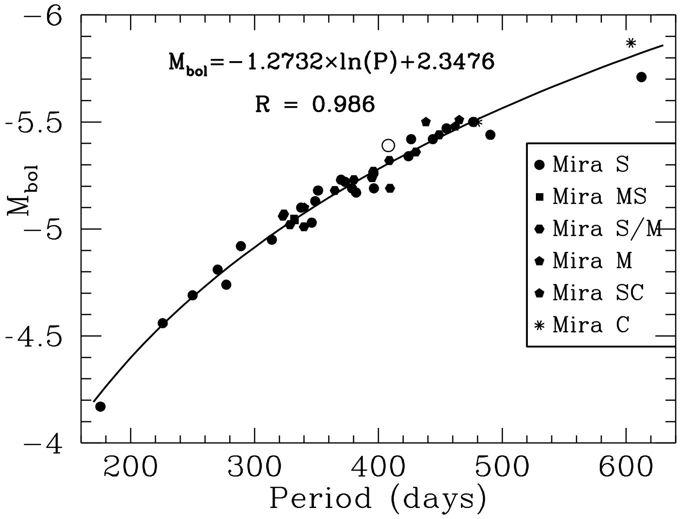

Fig. A.1. The average Period-Luminosity relation deduced for Miras (filled symbols). The open circle refers to χ Cyg, whose magnitude, deduced independently from its IR fluxes, its bolometric correction, and its Hipparcos distance, fits well in the general relation. The curve represents the written fitting relation, and R is its regression coefficient. See text for further explanations.

a point (the open circle) corresponding to the Mira star χ *Cyg*. For it we did not apply any $P-L$ relation: the magnitude was obtained from directly scaling our apparent bolometric magnitude with the known Hipparcos distance (van Leeuwen, 2007a). Although it's only a single point, its good accord with the trend defined by the other sources gives us a consistency check for the technique.

Online Material

Table 11. Sample D − First part.

IRAS name	Other name	Stephenson name	Coordinates ICRS	Spectral Type	Var. Type (GCVS)	Period (GCVS)
04199+4950	NX Per	CSS 91	04 23 39.35 +49 57 26.3	S	M	–
06312−4351	NU Pup	CSS 230	06 32 48.09 −43 54 13.6	S	M	–
06468−1342	DK CMa	CSS 264	06 49 06.38 −13 46 19.6	S:	M	–
07571−2350	EW Pup	CSS 440	07 59 16.04 −23 58 52.7	Se	M	–
08348−3617	WY Pyx	CSS 533	08 36 48.98 −36 27 36.5	S	M	–
17186−2914	V2434 Oph	CSS 975	17 21 46.79 −29 17 34.0	S	M	–
17589−1040	V342 Ser	CSS 1016	18 01 44.48 −10 40 25.2	S	M	–
18375−1010	V471 Sct	CSS 1064	18 40 18.8 −10 07 29	S	M	–
18404−0431	V427 Sct	CSS 1071	18 42 59.85 −04 28 19.4	S	M	–
21029+4917	V1959 Cyg	CSS 1259	21 04 35.42 +49 29 25.4	S	M	–
15437−5451	PR Nor	CSS 899	15 47 35.92 −55 00 40.2	–	M	–
–	PZ Vul	CSS 1154	19 44 08.73 +22 57 38.5	–	M	–
22457+5502	GY Lac	CSS 1307	22 47 46.19 +55 18 13.4	–	M	–
02080+6100	V928 Cas	CSS2 8	02 11 40.61 +61 14 26.3	–	M	–
05540+3222	V508 Aur	CSS2 20	05 57 14.8 +32 22 39	–	M	–
19444+3132	V1992 Cyg	CSS2 44	19 46 25.04 +31 40 08.1	–	M	–
–	V1850 Cyg	CSS2 60	20 47 56.33 +35 44 20.0	–	M	–
21229+4448	V1242 Cyg	CSS2 66	21 24 48.66 +45 00 55.0	–	M	–
14069−5905	V335 Cen	CSS 842	14 10 32.52 −59 19 38.1	S	SRA	256
16334−3107	ST Sco	CSS 931	16 36 36.22 −31 14 02.4	S4,7:(R5)	SRA	194.5
18241−1443	V385 Sct	CSS 1043	18 26 59.15 −14 41 48.3	Se	SRA	398
04543+4829	TV Aur	CSS 116	04 58 08.21 +48 33 37.1	S5,8:−S7,5	SRB	182
07183−0742	V685 Mon	CSS 338	07 20 47.63 −07 48 09.7	S	SRB	–
07399−1045	SU Mon	CSS 387	07 42 17.4600 −10 52 47.180	S3,6	SRB	–
10164−6044	V597 Car	CSS 674	10 18 10.32 −60 59 42.4	S	SRB	113
18300−1948	V2003 Sgr	CSS 1054	18 33 02.93 −19 46 26.1	S5,8	SRB	380
21075+4558	V575 Cyg	CSS 1263	21 09 19.24 +46 10 27.2	S	SRB	144
02228+3753	BI And	CSS 57	02 25 54.3270 +38 07 22.156	S8,8	SR	159.5
05429−0415	V1258 Ori	CSS 159	05 45 26.34 −04 14 33.7	S	SR	–
08102−3105	V536 Pup	CSS 476	08 12 12.7 −31 14 14	S	SR	–
10436−3459	Z Ant	CSS 704	10 45 58.898 −35 15 04.86	S5,4	SR	103.8
13240−5742	EE Cen	CSS 821	13 27 15.676 −57 58 14.48	S	SR	198
14215−6346	KQ Cen	CSS 850	14 25 25.44 −63 59 46.8	S7,6	SR	–
17594−2451	V4714 Sgr	CSS 1018	18 02 30.5 −24 51 27	S	SR	–
18138−1510	KL Ser	CSS 1032	18 16 45.56 −15 09 31.2	S	SR	490
22512+6100	V386 Cep	CSS 1314	22 53 12.37 +61 17 00.7	S	SR	–
23548+5808	V653 Cas	CSS 1344	23 57 21.31 +58 25 03.7	S:	SR	–
07141+0312	XY CMi	CSS 325	07 16 43.29 +03 06 58.1	S	L	–
00476+5956	OS Cas	CSS 16	00 50 38.48 +60 13 07.2	S	LB	–
01252+6056	PQ Cas	CSS 35	01 28 36.19 +61 12 07.7	S	LB	–
04094+4518	HX Per	CSS 88	04 13 01.11 +45 26 13.3	S	LB	–
–	DK Aur	CSS 120	05 06 30.15 +34 37 41.0	S	LB	–
06243+1806	CF Gem	CSS 220	06 27 15.33 +18 04 23.8	S	LB	–
06347+0057	CX Mon	CSS 237	06 37 18.48 +00 55 16.3	S6:/5+	LB	–
06419−0229	–	CSS 251	06 44 29.70 −02 32 31.1	S	LB	–
07117−1430	–	CSS 323	07 14 01.66 −14 36 00.7	S	LB	–
07226−0811	–	CSS 344	07 25 03.2990 −08 17 33.561	S	LB	–
07234−1035	KN Mon	CSS 348	07 25 50.84 −10 41 07.7	S	LB	–
07454−3026	KU Pup	CSS 407	07 47 27.79 −30 34 27.2	S6,8	LB	–
17188−4141	V635 Sco	CSS 974	17 22 22.9248 −41 44 41.377	S7,6:(Np)	LB	–
19008+1210	V915 Aql	CSS 1099	19 03 09.8933 +12 15 08.396	S5,2−S7,2	LB	–
19240+0841	V1318 Aql	CSS 1135	19 26 28.57 +08 47 10.6	S	LB	–
19311+2332	EP Vul	CSS 1141	19 33 17.838 +23 39 19.55	S6,5−S8,7	LB	–
19422+2347	–	CSS 1155	19 44 21.63 +23 53 48.3	S6	LB	–
20296+3223	AD Cyg	CSS 1224	20 31 36.5141 +32 33 52.354	S5,8(Nb)	LB	–
21345+4709	V633 Cyg	CSS 1279	21 36 26.88 +47 23 01.6	S	LB	–
00439+6339	–	CSS 13	00 46 54.59 +63 56 06.1	S	–	–
01263+6125	–	CSS 37	01 29 44.00 +61 41 41.7	S	–	–
01318+6001	–	CSS 38	01 35 09.71 +60 17 09.9	S	–	–
02048+6208	–	CSS 47	02 08 31.02 +62 22 44.5	S	–	–
02151+6234	–	CSS 50	02 18 52.44 +62 48 13.5	S	–	–
–	–	CSS 55	02 23 11.95 +63 51 58.1	S	–	–
02424+5955	–	CSS 64	02 46 23.19 +60 08 20.0	S	–	–
02478+5854	–	CSS 66	02 51 36.05 +59 07 11.7	S	–	–
03136+5930	–	CSS 71	03 17 36.46 +59 41 52.3	S	–	–

Table 11. continued.

IRAS name	Other name	Stephenson name	Coordinates ICRS	Spectral Type	Var. Type (GCVS)	Period (GCVS)
03361+5056	–	CSS 78	03 39 50.79 +51 06 30.6	S	–	–
05336+2900	–	CSS 146	05 36 52.06 +29 02 15.4	S	–	–
05350+3535	–	CSS 147	05 38 22.19 +35 37 29.2	S	–	–
05350+2809	–	CSS 148	05 38 17.62 +28 11 44.1	S	–	–
–	–	CSS 169	05 53 10.07 +29 13 27.9	S	–	–
06052+2807	–	CSS 188	06 08 26.23 +28 06 43.2	S	–	–
06208+2120	–	CSS 214	06 23 52.89 +21 18 30.1	S	–	–
06241+1555	–	CSS 219	06 27 04.3627 +15 53 42.154	S5.5,2	–	–
06337+0703	–	CSS 232	06 36 27.03 +07 00 33.3	S	–	–
–	–	CSS 250	06 44 42.71 +07 03 58.2	S	–	–
–	–	CSS 255	06 45 32.39 +06 47 06.4	S	–	–
06454+0632	–	CSS 259	06 48 08.67 +06 29 24.1	S	–	–
06462+0659	–	CSS 262	06 48 57.08 +06 56 33.2	S	–	–
07148−3014	–	CSS 328	07 16 45.86 −30 19 44.1	S	–	–
07165−1109	–	CSS 332	07 18 55.8304 −11 14 38.792	S3,1	–	–
07345−2333	–	CSS 371	07 36 44.05 −23 40 43.0	S	–	–
07405−2544	–	CSS 393	07 42 38.29 −25 51 15.4	S	–	–
07461−3705	–	CSS 408	07 47 58.968 −37 13 08.14	S	–	–
07475−1852	–	CSS 411	07 49 45.7504 −19 00 24.867	S	–	–
07496−2226	–	CSS 417	07 51 47.46 −22 33 58.6	S	–	–
07518−3156	–	CSS 427	07 53 46.23 −32 04 55.2	S	–	–
08403−3853	–	CSS 542	08 42 14.7168 −39 04 14.543	S	–	–
09146−5527	–	CSS 604	09 16 09.97 −55 39 48.1	S	–	–
–	–	CSS 610	09 22 16.31 −42 38 50.7	S	–	–
09518−5521	–	CSS 643	09 53 31.2 −55 35 35	S	–	–
09538−5205	–	CSS 645	09 55 41.4 −52 19 36	S	–	–
10038−6055	–	CSS 657	10 05 26.38 −61 10 15.3	S	–	–
–	–	CSS 703	10 44 16.4 −59 36 31	S	–	–
10513−5919	–	CSS 710	10 53 23.76 −59 35 12.3	S	–	–
11169−6111	–	CSS 738	11 19 03.60 −61 27 24.7	S	–	–
14372−6106	–	CSS 861	14 41 08.02 −61 18 54.2	S	–	–
14542−5858	–	CSS 868	14 58 05.11 −59 10 32.0	S	–	–
16219−4804	–	CSS 924	16 25 36.56 −48 11 06.0	S	–	–
16316−5026	–	CSS 929	16 35 31.03 −50 32 10.5	Se	–	–
16317−4933	–	CSS 930	16 35 32.3 −49 39 19	Se	–	–
16488−4407	–	CSS 942	16 52 24.5 −44 12 55	S	–	–
16490−4618	–	CSS 944	16 52 45.57 −46 23 54.4	S	–	–
16598−4117	–	CSS 952	17 03 21.5 −41 22 00	S	–	–
17483−2811	–	CSS 1003	17 51 29.70 −28 12 01.2	Se	–	–
17562−1133	–	CSS 1011	17 59 01.2 −11 33 29	S	–	–
–	–	CSS 1021	18 05 57.7 −25 40 23	S	–	–
18175−1408	–	CSS 1034	18 20 23.81 −14 06 46.2	Se	–	–
18198−1631	–	CSS 1035	18 22 42.51 −16 29 28.2	S:	–	–
–	–	CSS 1036	18 23 34.97 −17 05 10.2	S	–	–
19008+1154	–	CSS 1100	19 03 10.20 +11 59 00.9	S	–	–
19200+2228	–	CSS 1128	19 22 11.95 +22 34 39.5	S	–	–
19335+2213	–	CSS 1145	19 35 41.55 +22 20 08.3	S	–	–
–	–	CSS 1238	20 45 55.29 +36 32 18.6	S	–	–
–	–	CSS 1280	21 37 19.03 +47 59 59.1	S	–	–
–	–	CSS 1282	21 44 29.21 +50 57 16.8	S	–	–
–	–	CSS 1289	22 04 06.10 +59 52 45.2	S	–	–
22220+5645	–	CSS 1297	22 23 54.88 +57 00 16.5	S	–	–
23162+5816	–	CSS 1329	23 18 30.41 +58 33 11.1	S	–	–
20051+3531	–	CSS2 51	20 07 04.06 +35 40 11.0	S	–	–
06001+3138	BB Aur	CSS 181	06 03 25.0385 +31 38 40.898	M3−M4S	SRB	704
09564−5837	RR Car	CSS 649	09 58 04.819 −58 51 40.55	M6.5SII−III	SRB	–
22174+5054	YY Lac	CSS 1293	22 19 27.64 +51 09 43.8	M6S	SRB	140
22479+5923	CV Cep	CSS 1310	22 49 54.4498 +59 39 35.285	M4S	SR	60
06532−0527	EN Mon	CSS 277	06 55 40.14 −05 31 02.4	M2S	LB	–
07153−1407	DT CMa	CSS 329	07 17 40.99 −14 12 59.6	MS	LB	–
07277−1046	KP Mon	CSS 357	07 30 06.81 −10 53 20.9	M2S	LB	–
07495−2500	–	CSS 415	07 51 39.35 −25 07 59.6	MS	–	–
18375−0544	–	CSS 1066	18 40 13.55 −05 42 09.3	MS	–	–
12337−6124	BO Cru	CSS 799	12 36 38.89 −61 40 48.5	M0−M10/Se:	M	–
06331+1415	DY Gem	CSS 231	06 35 57.8124 +14 12 46.094	S8,5/M5	SRA	1145
20044+2417	DK Vul	CSS 1189	20 06 33.96 +24 26 00.0	S4,2/M6.5	SRA	370

Table 11. continued.

IRAS name	Other name	Stephenson name	Coordinates ICRS	Spectral Type	Var. Type (GCVS)	Period (GCVS)
20252+3623	V441 Cyg	CSS 1219	20 27 08.12 +36 33 06.5	M4/S4,6	SRA	375
00578+5620	V365 Cas	CSS 20	01 00 53.1576 +56 36 45.197	M5S/S7,2	SRB	136
17206−2826	V521 Oph	CSS 978	17 23 48.8966 −28 28 47.476	S5,4/M4	SRB	320
13477−6009	VX Cen	CSS 834	13 51 13.3401 −60 24 36.482	S8,5e/M4−8II−III	SR	307.8
19565+3707	V739 Cyg	CSS 1177	19 58 23.80 +37 15 51.9	S/M	SR	–
19133+0032	V354 Aql	CSS 1118	19 15 56.93 +00 37 32.2	M0−M7/S	L	–
05492+2549	BB Tau	CSS 165	05 52 18.620 +25 49 42.02	S4e/M0	LB	–
07360−1556	GG Pup	CSS 378	07 38 21.1128 −16 03 18.835	S5,6/M2	LB	–
10389−5149	HP Vel	CSS 696	10 41 02.7363 -52 05 08.834	S5,2/M4−5	LB	–
18171−2322	V3803 Sgr	CSS 1033	18 20 12.23 −23 20 49.9	S4,3/M7	LB	–
18284−0924	BP Sct	CSS 1052	18 31 09.78 −09 22 11.2	S4,9:/M3	LB	–
17081+6422	TV Dra	–	17 08 24.5042 +64 19 08.736	M8p/S	LB	–
–	–	CSS 1243	20 50 41.35 +39 49 41.4	S/M8−9III	–	–
04430−2356	EO Eri	CSS 109	04 45 08.45 −23 51 19.0	M8	M	–
19545−1122	V1407 Aql	CSS 1175	19 57 16.89 −11 14 16.7	M6se	M	–
06466−2022	KR CMa	CSS 265	06 48 50.5920 −20 25 32.239	M4III	SRB	–
20100−6225	V378 Pav	CSS 1195	20 14 25.7967 −62 16 45.128	M2IIs...	SRB	–
11246−6105	V771 Cen	CSS 752	11 26 59.6589 −61 22 09.557	M2Ib−II	SRC	–
01364+5927	V911 Cas	CSS 40	01 39 46.84 +59 42 29.3	M5	SR	–
20152+3124	V2012 Cyg	CSS 1201	20 17 11.0576 +31 33 18.096	M9	SR	–
23352+5834	V850 Cas	CSS 1337	23 37 39.74 +58 50 45.9	M7	SR	–
05208−0436	V535 Ori	CSS 134	05 23 20.6801 −04 34 14.430	M6	LB	–
06574−1606	GT CMa	CSS 289	06 59 44.73 −16 10 17.3	M9:	LB	–
–	EY Leo	CSS 706	10 50 30.7539 +10 19 48.874	M...	LB	–
02156+5928	–	CSS 53	02 19 16.76 +59 42 21.5	Ms	–	–
–	–	CSS 59	02 38 33.45 +61 54 31.1	Ms	–	–
03433+5254	–	CSS 81	03 47 06.76 +53 03 53.1	M3Iab:	–	–
04431+4234	–	CSS 108	04 46 40.226 +42 40 02.47	M0	–	–
–	–	CSS 136	05 25 29.98 +32 53 08.3	Ms	–	–
–	–	CSS 140	05 28 37.35 +34 02 28.1	Ms	–	–
05295+2900	–	CSS 143	05 32 44.19 +29 02 51.7	Ms	–	–
–	–	CSS 180	06 02 37.80 +29 07 05.8	Ms	–	–
06024+2220	–	CSS 185	06 05 27.89 +22 20 42.1	Ms	–	–
–	–	CSS 193	06 10 09.60 +23 33 00.9	Ms	–	–
06075+2339	–	CSS 195	06 10 34.60 +23 38 54.4	Ms	–	–
–	–	CSS 208	06 18 52.52 +21 12 16.1	Ms	–	–
06336+0200	–	CSS 233	06 36 12.1124 +01 57 29.192	M0	–	–
–	–	CSS 240	06 39 03.23 +02 34 00.2	Ms	–	–
06413+0148	–	CSS 249	06 43 56.34 +01 44 59.3	M4:s...	–	–
07169−1122	–	CSS 335	07 19 15.6794 −11 27 41.378	M3	–	–
07400−1943	–	CSS 388	07 42 16.109 −19 50 50.81	M	–	–
07595−3139	–	CSS 448	08 01 28.0152 −31 47 40.546	M5	–	–
11006−5600	–	CSS 720	11 02 47.8961 −56 16 21.588	M1/M2	–	–
11278−6053	–	CSS 755	11 30 10.3696 −61 09 56.330	M2/M3III:	–	–
14233−6003	–	CSS 853	14 27 03.5397 −60 17 28.299	M2III	–	–
16026−5436	–	CSS 909	16 06 33.82 −54 44 42.4	M3	–	–
17204−3258	–	CSS 977	17 23 44.025 −33 01 21.11	M4	–	–
17566−3019	–	CSS 1010	17 59 49.9284 −30 19 22.622	M2/M3III	–	–
19361−1658	–	CSS 1146	19 39 00.74 −16 51 56.6	M10III	–	–
19436+2028	–	CSS 1158	19 45 50.870 +20 36 07.63	M2	–	–
20055+3625	–	CSS 1192	20 07 26.5362 +36 34 03.952	M2	–	–
–	–	CSS 1283	21 46 42.9894 +28 02 56.928	M2	–	–
18076−1034	–	CSS2 25	18 10 24.80 −10 34 15.9	M8	–	–
19371+2855	–	CSS2 41	19 39 07.77 +29 02 38.6	M*	–	–
12135−5600	BH Cru	CSS 787	12 16 16.7913 −56 17 09.625	SC4.5/8−e−SC7/8−e	M	421
04599+1514	GP Ori	CSS 117	05 02 48.09 +15 19 12.2	C8,0J:/SCea	SRB	370
07228−2027	BX CMa	CSS 346	07 25 05.87 −20 33 45.3	S/C	SRB	117
07247−1137	FX CMa	CSS 350	07 27 03.9355 −11 43 14.448	S3,9/C1	SRB	40
06197+0327	FU Mon	CSS 212	06 22 23.8519 +03 25 27.886	C8,0J/Cse	SR	309.8
06390−0432	V372 Mon	CSS 244	06 41 26.13 −04 35 45.8	SC(N)	SR	–
13440−5306	AM Cen	CSS 830	13 47 17.6180 −53 21 25.921	SC	LB	–
20451+4552	CY Cyg	–	20 46 50.2459 +46 03 06.945	CS/M2p	LB	–
10045−5955	–	CSS 661	10 06 09.00 −60 10 37.0	Ce	SR	–
02176+6110	–	CSS2 9	02 21 20.28 +61 23 54.0	Cs...	–	–
10293−5912	–	CSS 683	10 31 10.74 −59 28 17.7	C	–	–
11487−6243	–	CSS 769	11 51 13.28 −63 00 08.6	C	–	–

Table 11. continued.

IRAS name	Other name	Stephenson name	Coordinates ICRS	Spectral Type	Var. Type (GCVS)	Period (GCVS)
20339+4112	–	CSS 1229	20 35 47.09 +41 22 44.7	WC+...	–	–
05016+4214	–	CSS 118	05 05 12.6146 +42 18 43.394	K5	–	–
07037−0346	–	CSS 306	07 06 12.20 −03 51 13.6	K	–	–
–	–	CSS 621	09 39 35.2886 −58 19 16.425	K	–	–
11456−5732	–	CSS 766	11 48 05.60 −57 49 37.7	K	–	–
20150+5400	V1190 Cyg	CSS 1203	20 16 20.42 +54 09 15.4	–	SRA	142
01186+6634	V899 Cas	CSS 29	01 22 04.06 +66 50 12.1	–	SR	–
06018+2746	V354 Gem	CSS 183	06 05 01.0 +27 45 55	–	SR	–
08065−2534	V527 Pup	CSS 468	08 08 39.6 −25 43 22	–	SR	–
18315−1535	V470 Sct	CSS 1058	18 34 29.7 −15 33 19	–	SR	–
22197+6028	V662 Cep	CSS 1296	22 21 29.2 +60 43 12	–	SR	–
03131+5541	V684 Per	CSS2 11	03 16 56.09 +55 52 33.1	–	SR	–
19356+1343	V1143 Aql	CSS2 40	19 38 00.83 +13 50 35.7	–	SR	168
–	V357 Sge	CSS2 42	19 41 38.29 +18 34 28.9	–	SR	–
–	V1738 Cyg	CSS2 70	21 56 28.58 +51 28 49.1	–	SR	–
–	MQ Aur	CSS 164	05 51 53.27 +31 51 20.0	–	LB	–
07470−3459	V481 Pup	CSS 410	07 48 53.3 −35 06 52	–	LB	–
–	V1925 Cyg	CSS 1250	20 54 04.9 +44 51 42	–	LB	–
00300+6342	–	CSS 10	00 32 55.95 +63 59 08.4	–	–	–
–	–	CSS 21	01 02 02.43 +59 15 07.0	–	–	–
01197+6143	–	CSS 30	01 23 01.88 +61 59 40.9	–	–	–
01201+6002	–	CSS 31	01 23 22.31 +60 18 14.7	–	–	–
01257+6701	–	CSS 34	01 29 18.15 +67 16 42.1	–	–	–
–	–	CSS 43	01 48 56.60 +63 52 23.9	–	–	–
–	–	CSS 51	02 19 24.19 +63 01 34.3	–	–	–
04323+4040	–	CSS 101	04 35 47.16 +40 46 06.3	–	–	–
04414+4616	–	CSS 105	04 45 11.58 +46 22 30.0	–	–	–
04467+3709	–	CSS 110	04 50 08.62 +37 14 38.6	–	–	–
04484+3958	–	CSS 111	04 51 54.14 +40 03 39.7	–	–	–
–	–	CSS 119	05 05 15.28 +42 17 42.3	–	–	–
05087+4649	–	CSS 124	05 12 30.80 +46 53 18.2	–	–	–
05223+2808	–	CSS 137	05 25 31.70 +28 11 18.8	–	–	–
05225+3221	–	CSS 138	05 25 45.60 +32 24 01.5	–	–	–
05289+4056	–	CSS 142	05 32 27.33 +40 58 43.8	–	–	–
–	–	CSS 157	05 44 23.0943 +32 10 24.404	–	–	–
05449−0423	–	CSS 162	05 47 28.26 −04 22 04.0	–	–	–
06105+0127	–	CSS 198	06 13 09.4126 +01 26 56.885	–	–	–
06109−0134	–	CSS 200	06 13 30.6 −01 35 53	–	–	–
06127+2501	–	CSS 203	06 15 49.23 +25 00 40.5	–	–	–
06116−6056	–	CSS 204	06 12 11.7079 −60 57 53.525	–	–	–
–	–	CSS 252	06 44 44.32 −01 14 06.3	–	–	–
–	–	CSS 258	06 46 26.56 +04 12 49.4	–	–	–
06471−0523	–	CSS 263	06 49 36.11 −05 27 13.3	–	–	–
06476+0216	–	CSS 267	06 50 17.77 +02 13 23.9	–	–	–
06484−1200	–	CSS 268	06 50 44.76 −12 04 22.8	–	–	–
06499−0509	–	CSS 269	06 52 26.62 −05 12 57.9	–	–	–
06503−1231	–	CSS 272	06 52 38.67 −12 34 46.2	–	–	–
06553−0645	–	CSS 282	06 57 48.95 −06 49 10.0	–	–	–
06573−0609	–	CSS 287	06 59 43.17 −06 13 33.5	–	–	–
06573−1412	–	CSS 288	06 59 38.7798 −14 16 35.697	–	–	–
06598+0001	–	CSS 295	07 02 24.30 −00 02 55.6	–	–	–
07012−0032	–	CSS 298	07 03 46.1294 −00 37 29.029	–	–	–
07010−1425	–	CSS 299	07 03 20.77 −14 29 58.5	–	–	–
07010−1943	–	CSS 300	07 03 12.0258 −19 47 45.986	–	–	–
07018−0236	–	CSS 301	07 04 18.58 −02 41 02.2	–	–	–
–	–	CSS 302	07 03 55.43 −19 06 28.5	–	–	–
07035−0048	–	CSS 305	07 06 06.49 −00 52 39.6	–	–	–
07045+0051	–	CSS 309	07 07 06.6383 +00 46 35.003	–	–	–
–	–	CSS 310	07 08 31.10 −01 57 16.1	–	–	–
07062+0314	–	CSS 311	07 08 49.62 +03 09 50.0	–	–	–
07076−0813	–	CSS 313	07 10 01.91 −08 18 44.7	–	–	–
07116−0834	–	CSS 322	07 14 00.56 −08 40 00.4	–	–	–
07180−1653	–	CSS 336	07 20 16.52 −16 59 09.4	–	–	–
07193−0752	–	CSS 340	07 21 44.53 −07 58 18.1	–	–	–
–	–	CSS 349	07 26 45.34 −18 31 33.4	–	–	–
07245−2014	–	CSS 351	07 26 44.97 −20 20 49.8	–	–	–

Table 11. continued.

IRAS name	Other name	Stephenson name	Coordinates ICRS	Spectral Type	Var. Type (GCVS)	Period (GCVS)
07250−2206	–	CSS 352	07 27 11.09 −22 12 35.7	–	–	–
07292−1109	–	CSS 360	07 31 36.93 −11 16 18.2	–	–	–
07313−2522	–	CSS 364	07 33 23.00 −25 28 47.4	–	–	–
–	–	CSS 366	07 34 31.86 −20 23 15.4	–	–	–
07325−1404	–	CSS 367	07 34 52.40 −14 10 53.3	–	–	–
07363−1218	–	CSS 379	07 38 39.34 −12 25 50.0	–	–	–
07391−2704	–	CSS 383	07 41 12.68 −27 11 14.6	–	–	–
07391−2756	–	CSS 384	07 41 11.15 −28 03 41.8	–	–	–
07395−2612	–	CSS 386	07 41 35.51 −26 19 35.2	–	–	–
07403−2625	–	CSS 389	07 42 23.10 −26 32 44.2	–	–	–
–	–	CSS 395	07 43 26.11 −29 18 28.5	–	–	–
07455−1712	–	CSS 404	07 47 50.89 −17 20 22.4	–	–	–
–	–	CSS 406	07 47 57.18 −18 39 02.2	–	–	–
–	–	CSS 409	07 48 27.83 −35 12 13.3	–	–	–
–	–	CSS 432	07 54 24.84 −36 33 15.5	–	–	–
07538−1930	–	CSS 433	07 56 01.972 −19 38 32.13	–	–	–
–	–	CSS 437	07 57 25.19 −23 25 40.3	–	–	–
07559−2929	–	CSS 438	07 57 57.65 −29 37 32.1	–	–	–
07562−2849	–	CSS 439	07 58 17.94 −28 57 53.8	–	–	–
07583−3452	–	CSS 444	08 00 15.12 −35 00 55.0	–	–	–
–	–	CSS 450	08 01 40.24 −38 03 23.4	–	–	–
–	–	CSS 463	08 06 25.76 −38 06 52.8	–	–	–
08059−3545	–	CSS 466	08 07 49.79 −35 53 59.6	–	–	–
–	–	CSS 467	08 08 25.93 −27 32 23.9	–	–	–
08066−3333	–	CSS 469	08 08 32.84 −33 42 22.7	–	–	–
08074−3040	–	CSS 470	08 09 25.38 −30 49 24.9	–	–	–
–	–	CSS 473	08 11 34.00 −26 07 52.5	–	–	–
08098−2809	–	CSS 474	08 11 55.36 −28 18 30.8	–	–	–
–	–	CSS 479	08 14 30.90 −30 42 23.1	–	–	–
08133−2934	–	CSS 480	08 15 22.78 −29 43 46.9	–	–	–
08145−2956	–	CSS 486	08 16 34.9650 −30 05 40.923	–	–	–
08164−2946	–	CSS 489	08 18 29.06 −29 56 17.4	–	–	–
08166−3239	–	CSS 490	08 18 35.8606 −32 48 31.316	–	–	–
08198−4000	–	CSS 497	08 21 38.29 −40 10 08.2	–	–	–
08199−3707	–	CSS 498	08 21 50.79 −37 16 59.1	–	–	–
08229−3200	–	CSS 504	08 24 53.85 −32 10 05.9	–	–	–
08234−3536	–	CSS 506	08 25 21.95 −35 46 18.7	–	–	–
08233−3843	–	CSS 507	08 25 13.67 −38 52 57.4	–	–	–
–	–	CSS 509	08 26 19.75 −30 38 14.8	–	–	–
08274−3519	–	CSS 515	08 29 24.36 −35 29 55.6	–	–	–
08308−3840	–	CSS 526	08 32 44.02 −38 50 19.9	–	–	–
08319−4037	–	CSS 527	08 33 43.26 −40 47 36.8	–	–	–
08318−4703	–	CSS 528	08 33 27.87 −47 14 15.1	–	–	–
08330−5237	–	CSS 531	08 34 29.13 −52 47 22.7	–	–	–
08389−4145	–	CSS 539	08 40 47.28 −41 56 36.0	–	–	–
08388−5116	–	CSS 540	08 40 23.85 −51 26 46.4	–	–	–
08390−4914	–	CSS 541	08 40 36.51 −49 24 58.0	–	–	–
–	–	CSS 547	08 45 28.7679 −48 24 32.310	–	–	–
08454−3959	–	CSS 548	08 47 17.13 −40 10 53.7	–	–	–
08457−4548	–	CSS 550	08 47 28.72 −45 59 19.6	–	–	–
08466−3814	–	CSS 553	08 48 35.51 −38 25 53.3	–	–	–
08490−5026	–	CSS 559	08 50 35.68 −50 37 23.8	–	–	–
–	–	CSS 567	08 55 41.78 −46 34 03.2	–	–	–
08559−4716	–	CSS 569	08 57 40.87 −47 27 53.7	–	–	–
–	–	CSS 580	09 03 36.58 −40 31 22.7	–	–	–
09017−4838	–	CSS 581	09 03 23.33 −48 50 56.6	–	–	–
–	–	CSS 583	09 04 42.02 −43 22 38.5	–	–	–
09049−4038	–	CSS 584	09 06 53.67 −40 50 40.7	–	–	–
–	–	CSS 592	09 08 51.6 −41 57 20	–	–	–
–	–	CSS 596	09 10 56.7 −53 34 45	–	–	–
09100−5336	–	CSS 598	09 11 32.19 −53 48 45.2	–	–	–
–	–	CSS 601	09 16 32.93 −42 11 15.2	–	–	–
–	–	CSS 606	09 19 36.8 −38 03 10	–	–	–
09182−4956	–	CSS 608	09 19 56.96 −50 09 47.1	–	–	–
09199−5615	–	CSS 609	09 21 27.64 −56 28 11.7	–	–	–
09370−5533	–	CSS 619	09 38 40.18 −55 47 27.6	–	–	–

Table 11. continued.

IRAS name	Other name	Stephenson name	Coordinates ICRS	Spectral Type	Var. Type (GCVS)	Period (GCVS)
09400−4642	–	CSS 625	09 41 57.34 −46 56 30.1	–	–	–
09452−4650	–	CSS 633	09 47 06.04 −47 04 51.7	–	–	–
09459−4715	–	CSS 635	09 47 48.86 −47 29 03.7	–	–	–
09560−5545	–	CSS 648	09 57 48.46 −56 00 01.8	–	–	–
09572−4943	–	CSS 650	09 59 10.24 −49 58 19.9	–	–	–
09598−5430	–	CSS 651	10 01 39.18 −54 44 53.2	–	–	–
–	–	CSS 660	10 06 35.82 −51 51 36.4	–	–	–
10053−6042	–	CSS 664	10 06 56.74 −60 57 10.1	–	–	–
10125−5055	–	CSS 665	10 14 27.43 −51 10 20.5	–	–	–
10138−6046	–	CSS 668	10 15 26.12 −61 01 07.4	–	–	–
10155−5439	–	CSS 672	10 17 22.4402 −54 54 11.910	–	–	–
–	–	CSS 676	10 21 26.13 −52 01 58.9	–	–	–
–	–	CSS 678	10 25 46.50 −54 30 40.9	–	–	–
–	–	CSS 681	10 26 43.95 −61 47 33.2	–	–	–
10256−5158	–	CSS 682	10 27 40.53 −52 13 11.5	–	–	–
10296−5625	–	CSS 684	10 31 34.43 −56 41 08.6	–	–	–
10308−6707	–	CSS 687	10 32 22.33 −67 23 16.2	–	–	–
–	–	CSS 691	10 37 56.10 −55 05 53.3	–	–	–
10358−6028	–	CSS 692	10 37 42.72 −60 44 09.2	–	–	–
10359−6018	–	CSS 693	10 37 50.4892 −60 34 21.314	–	–	–
–	–	CSS 698	10 42 51.40 −62 16 55.3	–	–	–
10418−5624	–	CSS 699	10 43 52.86 −56 40 12.1	–	–	–
10422−5448	–	CSS 702	10 44 19.25 −55 04 36.4	–	–	–
–	–	CSS 707	10 50 55.17 +04 29 58.5	–	–	–
10548−6008	–	CSS 713	10 56 54.37 −60 25 08.6	–	–	–
–	–	CSS 715	10 57 29.02 −60 42 53.2	–	–	–
10561−6050	–	CSS 716	10 58 07.04 −61 06 36.6	–	–	–
10590−6210	–	CSS 718	11 01 01.13 −62 26 32.6	–	–	–
10599−5615	–	CSS 719	11 02 05.37 −56 31 33.7	–	–	–
11039−6228	–	CSS 723	11 06 01.03 −62 45 12.3	–	–	–
–	–	CSS 725	11 06 31.8 −61 58 26	–	–	–
–	–	CSS 727	11 09 01.61 −58 44 52.1	–	–	–
11078−5957	–	CSS 728	11 09 56.58 −60 14 14.0	–	–	–
11103−6141	–	CSS 732	11 12 28.45 −61 57 42.2	–	–	–
–	–	CSS 733	11 13 09.16 −60 09 06.0	–	–	–
11180−5559	–	CSS 741	11 20 17.97 −56 15 57.6	–	–	–
11182−5958	–	CSS 743	11 20 27.44 −60 14 50.7	–	–	–
–	–	CSS 747	11 25 03.75 −57 27 35.4	–	–	–
–	–	CSS 748	11 25 22.77 −61 25 07.2	–	–	–
11232−6059	–	CSS 749	11 25 27.11 −61 15 33.0	–	–	–
11244−5740	–	CSS 750	11 26 47.99 −57 57 06.4	–	–	–
11247−5727	–	CSS 751	11 26 58.59 −57 43 17.6	–	–	–
–	–	CSS 754	11 29 16.99 −61 10 44.4	–	–	–
–	–	CSS 758	11 34 27.35 −59 06 31.6	–	–	–
–	–	CSS 759	11 36 12.59 −59 20 09.0	–	–	–
–	–	CSS 760	11 38 04.37 −59 37 19.7	–	–	–
11362−6333	–	CSS 761	11 38 37.45 −63 50 31.5	–	–	–
11396−5749	–	CSS 762	11 42 04.71 −58 06 12.6	–	–	–
11421−6514	–	CSS 763	11 44 30.34 −65 31 44.8	–	–	–
11430−5832	–	CSS 765	11 45 27.32 −58 49 28.2	–	–	–
–	–	CSS 767	11 49 10.75 −58 12 42.3	–	–	–
11506−6245	–	CSS 771	11 53 09.97 −63 02 17.0	–	–	–
11526−5922	–	CSS 773	11 55 09.53 −59 39 14.8	–	–	–
11556−6308	–	CSS 776	11 58 10.93 −63 24 46.8	–	–	–
11590−6113	–	CSS 779	12 01 34.57 −61 30 24.9	–	–	–
12032−6414	–	CSS 781	12 05 50.87 −64 30 58.7	–	–	–
12137−6429	–	CSS 789	12 16 28.69 −64 46 24.2	–	–	–
12354−5851	–	CSS 800	12 38 18.44 −59 08 22.9	–	–	–
12448−6207	–	CSS 805	12 47 51.0 −62 23 49	–	–	–
12455−6148	–	CSS 806	12 48 33.93 −62 04 52.0	–	–	–
12581−6638	–	CSS 810	13 01 24.25 −66 54 30.9	–	–	–
12598−6042	–	CSS 811	13 02 57.05 −60 58 15.4	–	–	–
13277−5954	–	CSS 823	13 31 05.26 −60 09 48.4	–	–	–
13352−6121	–	CSS 825	13 38 38.33 −61 37 02.9	–	–	–
–	–	CSS 838	14 00 45.88 −61 35 22.4	–	–	–
–	–	CSS 840	14 05 20.36 −61 20 39.0	–	–	–

Table 11. continued.

IRAS name	Other name	Stephenson name	Coordinates ICRS	Spectral Type	Var. Type (GCVS)	Period (GCVS)
14134−5959	–	CSS 846	14 17 02.32 −60 13 43.4	–	–	–
14199−6104	–	CSS 847	14 23 38.67 −61 17 59.4	–	–	–
–	–	CSS 849	14 24 38.25 −57 31 21.9	–	–	–
–	–	CSS 852	14 26 14.53 −60 14 56.3	–	–	–
14427−5656	–	CSS 862	14 46 26.02 −57 08 54.7	–	–	–
14549−6313	–	CSS 869	14 59 03.64 −63 25 07.1	–	–	–
14556−5455	–	CSS 870	14 59 21.40 −55 07 35.8	–	–	–
15003−5829	–	CSS 871	15 04 13.89 −58 40 48.3	–	–	–
15078−5435	–	CSS 878	15 11 33.59 −54 46 36.3	–	–	–
–	–	CSS 879	15 12 40.29 −52 47 53.2	–	–	–
15133−6107	–	CSS 881	15 17 28.70 −61 18 45.1	–	–	–
15217−5827	–	CSS 888	15 25 40.14 −58 38 06.0	–	–	–
15240−5657	–	CSS 890	15 27 58.6 −57 08 13	–	–	–
15280−5555	–	CSS 891	15 31 59.1 −56 05 57	–	–	–
–	–	CSS 893	15 32 48.5 −56 18 26	–	–	–
15347−5555	–	CSS 897	15 38 38.95 −56 05 06.1	–	–	–
15496−5550	–	CSS 901	15 53 37.90 −55 58 54.1	–	–	–
15530−5201	–	CSS 905	15 56 46.9 −52 09 53	–	–	–
–	–	CSS 906	15 56 49.55 −48 43 32.2	–	–	–
16094−4600	–	CSS 915	16 13 06.21 −46 07 48.6	–	–	–
16147−4808	–	CSS 917	16 18 28.07 −48 15 55.2	–	–	–
16149−5022	–	CSS 918	16 18 44.10 −50 29 25.0	–	–	–
16156−5030	–	CSS 919	16 19 28.37 −50 37 50.7	–	–	–
16205−5449	–	CSS 921	16 24 31.29 −54 56 51.2	–	–	–
16208−4658	–	CSS 922	16 24 31.6 −47 05 23	–	–	–
16220−4940	–	CSS 925	16 25 52.26 −49 47 19.2	–	–	–
–	–	CSS 933	16 39 36.69 −46 37 14.4	–	–	–
16361−4626	–	CSS 934	16 39 49.61 −46 31 59.0	–	–	–
16445−4321	–	CSS 939	16 48 08.62 −43 26 55.3	–	–	–
16522−4320	–	CSS 946	16 55 48.55 −43 24 49.7	–	–	–
–	–	CSS 950	17 02 35.71 −49 01 19.0	–	–	–
16591−4143	–	CSS 951	17 02 37.8 −41 47 16	–	–	–
–	–	CSS 953	17 03 08.84 −36 43 27.3	–	–	–
17034−4049	–	CSS 956	17 06 57.91 −40 53 52.3	–	–	–
17035−4051	–	CSS 957	17 07 01.4 −40 55 35	–	–	–
17072−4129	–	CSS 960	17 10 47.7 −41 33 02	–	–	–
–	–	CSS 962	17 13 47.394 −32 23 29.77	–	–	–
17162−2844	–	CSS 969	17 19 23.876 -28 47 27.47	–	–	–
17180−3655	–	CSS 973	17 21 26.9 −36 58 04	–	–	–
17212−3714	–	CSS 979	17 24 41.04 −37 16 57.0	–	–	–
17217−4200	–	CSS 982	17 25 18.5406 −42 03 26.037	–	–	–
17243−2429	–	CSS 987	17 27 22.84 −24 32 01.0	–	–	–
17546−1327	–	CSS 1008	17 57 30.05 −13 27 35.8	–	–	–
17563−1438	–	CSS 1012	17 59 13.558 −14 38 17.16	–	–	–
18027−2555	–	CSS 1020	18 05 52.80 −25 55 19.8	–	–	–
–	–	CSS 1039	18 25 56.42 −22 55 37.7	–	–	–
18269−1111	–	CSS 1047	18 29 41.21 −11 09 55.8	–	–	–
18276−1524	–	CSS 1050	18 30 29.08 −15 22 37.2	–	–	–
18299−0931	–	CSS 1055	18 32 44.5 −09 29 11	–	–	–
18339−0424	–	CSS 1061	18 36 34.6 −04 22 20	–	–	–
18382−1350	–	CSS 1068	18 41 08.07 −13 47 56.2	–	–	–
18449−0713	–	CSS 1077	18 47 41.73 −07 10 22.2	–	–	–
–	–	CSS 1082	18 52 40.49 −01 23 58.6	–	–	–
19057+0425	–	CSS 1104	19 08 16.67 +04 29 51.8	–	–	–
19060+0225	–	CSS 1105	19 08 33.42 +02 30 08.8	–	–	–
19098+1049	–	CSS 1109	19 12 12.41 +10 54 39.1	Y.S.O. ?	–	–
–	–	CSS 1134	19 26 14.01 +13 57 10.0	–	–	–
19359+1934	–	CSS 1147	19 38 08.47 +19 40 54.1	–	–	–
19358+3040	–	CSS 1149	19 37 46.88 +30 47 38.1	–	–	–
19408+2007	–	CSS 1153	19 43 05.14 +20 14 32.1	–	–	–
19434+2150	–	CSS 1156	19 45 37.64 +21 57 51.0	–	–	–
19463+2837	–	CSS 1161	19 48 21.87 +28 45 28.0	–	–	–
19495+2559	–	CSS 1166	19 51 33.97 +26 07 23.0	–	–	–
–	–	CSS 1171	19 54 07.56 +32 00 06.3	–	–	–
19537+2730	–	CSS 1174	19 55 46.65 +27 38 10.1	–	–	–
20151+3758	–	CSS 1202	20 16 58.065 +38 07 25.81	–	–	–

Table 11. continued.

IRAS name	Other name	Stephenson name	Coordinates ICRS	Spectral Type	Var. Type (GCVS)	Period (GCVS)
20201+2837	–	CSS 1208	20 22 11.27 +28 47 34.6	–	–	–
20199+4335	–	CSS 1210	20 21 37.26 +43 45 35.3	–	–	–
S20490+456	–	CSS 1245	20 50 45.59 +45 46 14.8	–	–	–
20576+4732	V1542 Cyg	CSS 1255	20 59 23.25 +47 44 42.8	–	IS:	–
21205+5158	–	CSS 1270	21 22 09.45 +52 11 59.0	–	–	–
21281+5103	–	CSS 1274	21 29 52.4768 +51 16 21.114	–	–	–
–	–	CSS 1278	21 36 26.78 +46 35 57.6	–	–	–
21371+5153	–	CSS 1281	21 38 54.47 +52 06 37.7	–	–	–
–	–	CSS 1287	21 59 17.7565 +24 40 56.895	–	–	–
–	–	CSS 1299	22 31 58.41 +02 01 20.7	–	–	–
23115+6050	–	CSS 1323	23 13 42.48 +61 06 54.2	–	–	–
23119+6157	–	CSS 1325	23 14 03.04 +62 14 20.6	–	–	–
23172+5745	–	CSS 1330	23 19 26.69 +58 02 24.3	–	–	–
–	–	CSS 1331	23 19 46.77 +62 55 41.5	–	–	–
–	–	CSS 1333	23 27 13.95 +56 33 07.5	–	–	–
–	–	CSS2 1	00 21 22.87 +63 36 55.5	–	–	–
00248+6439	–	CSS2 2	00 27 40.63 +64 56 40.7	–	–	–
–	–	CSS2 3	00 50 57.53 +62 36 15.7	–	–	–
–	–	CSS2 5	01 26 31.42 +67 02 53.5	–	–	–
–	–	CSS2 6	01 59 45.17 +66 00 48.1	–	–	–
01561+6627	–	CSS2 7	01 59 59.52 +66 41 57.3	–	–	–
04055+5258	–	CSS2 13	04 09 21.96 +53 06 25.9	–	–	–
–	–	CSS2 14	04 15 24.99 +53 42 46.6	–	–	–
04118+4851	–	CSS2 15	04 15 33.17 +48 58 47.8	–	–	–
04147+5030	–	CSS2 16	04 18 28.20 +50 37 47.0	–	–	–
–	–	CSS2 17	04 49 18.29 +45 46 23.1	–	–	–
–	–	CSS2 18	05 37 17.66 +35 30 21.3	–	–	–
–	–	CSS2 21	07 27 41.27 −21 31 14.5	–	–	–
17547−2615	–	CSS2 22	17 57 54.35 −26 15 19.4	–	–	–
–	–	CSS2 23	17 58 29.52 −19 02 22.8	–	–	–
18046−0756	–	CSS2 24	18 07 20.13 −07 55 50.5	–	–	–
18281−0513	–	CSS2 26	18 30 47.80 −05 11 21.7	–	–	–
–	–	CSS2 27	18 48 49.6694 −01 04 35.094	–	–	–
18471+0137	–	CSS2 28	18 49 42.8 +01 41 03	–	–	–
18529−0132	–	CSS2 29	18 55 31.01 −01 28 46.2	–	–	–
19046+0444	–	CSS2 30	19 07 08.48 +04 49 31.6	–	–	–
–	–	CSS2 31	19 11 22.87 +14 48 16.3	–	–	–
19104+0619	–	CSS2 32	19 12 51.61 +06 24 14.7	–	–	–
19188+2026	–	CSS2 33	19 21 00.95 +20 32 08.6	–	–	–
–	–	CSS2 34	19 24 01.16 +15 54 43.2	–	–	–
19270+2239	–	CSS2 35	19 29 12.40 +22 44 53.2	–	–	–
19294+1358	–	CSS2 36	19 31 43.58 +14 05 22.7	–	–	–
19298+1751	–	CSS2 37	19 32 05.18 +17 57 40.7	–	–	–
19301+1404	–	CSS2 38	19 32 31.43 +14 11 47.4	–	–	–
19323+1917	–	CSS2 39	19 34 32.60 +19 24 02.7	–	–	–
19408+2038	–	CSS2 43	19 43 04.47 +20 45 23.4	–	–	–
19497+3052	–	CSS2 45	19 51 47.67 +31 00 41.8	–	–	–
19500+3015	–	CSS2 46	19 52 02.63 +30 22 42.5	–	–	–
–	–	CSS2 48	19 59 46.26 +26 08 25.3	–	–	–
19596+3350	–	CSS2 49	20 01 35.61 +33 59 02.7	–	–	–
20021+3118	–	CSS2 50	20 04 06.00 +31 27 10.7	–	–	–
–	–	CSS2 52	20 13 41.68 +37 42 46.7	–	–	–
20173+3334	–	CSS2 53	20 19 17.28 +33 44 26.7	–	–	–
20223+3059	–	CSS2 54	20 24 22.41 +31 09 26.0	–	–	–
20246+3423	–	CSS2 55	20 26 32.38 +34 33 35.1	–	–	–
20250+3342	–	CSS2 56	20 26 58.08 +33 52 14.8	–	–	–
20255+3758	–	CSS2 57	20 27 23.53 +38 08 29.8	–	–	–
–	–	CSS2 58	20 37 43.86 +43 34 41.7	–	–	–
–	–	CSS2 59	20 42 54.49 +41 04 53.3	–	–	–
20502+4833	–	CSS2 61	20 51 54.01 +48 44 50.0	–	–	–
20531+4710	–	CSS2 62	20 54 49.95 +47 22 03.7	–	–	–
20536+4723	–	CSS2 63	20 55 20.61 +47 35 13.2	–	–	–
S20596+421	–	CSS2 64	21 01 33.38 +42 27 46.2	–	–	–
–	–	CSS2 65	21 19 49.08 +43 04 56.6	–	–	–
21314+4816	–	CSS2 67	21 33 13.19 +48 29 55.6	–	–	–
21336+5343	–	CSS2 68	21 35 15.88 +53 57 04.2	–	–	–

Table 11. continued.

IRAS name	Other name	Stephenson name	Coordinates ICRS	Spectral Type	Var. Type (GCVS)	Period (GCVS)
–	–	CSS2 71	22 11 34.11 +52 51 00.5	–	–	–
23113+5639	–	CSS2 73	23 13 34.22 +56 55 25.0	–	–	–
–	–	CSS2 74	23 31 50.70 +64 16 24.0	–	–	–

Table 12. Sample D − Second part.

Source name	J [Jy]	H [Jy]	K [Jy]	[8.8] [Jy]	[9.8] [Jy]	[11.7] [Jy]	[12.5] [Jy]	D [Jy]	E [Jy]	Mid−IR Data Origin	Apparent bol. magnitudes	I. − E.
NX Per	1.9	4.5	5.8	1.1	–	–	1.3	0.96	–	MSX	7.61	–
NU Pup	1.5	2.2	2.4	0.47	–	–	–	–	–	MSX	8.58	I
DK CMa	14.1	21.7	22.7	3.1	–	–	–	–	–	MSX	6.06	I
EW Pup	5.6	8.5	9.1	1.1	–	–	–	–	–	MSX	7.04	–
WY Pyx	34.8	58.0	62.8	13.6	–	–	8.8	6.4	3.4	MSX	5.01	I
V2434 Oph	21.2	53.1	65.9	11.4	–	–	10.3	6.9	4.0	MSX	4.95	I
V342 Ser	4.9	10.6	14.5	1.9	–	–	–	–	–	MSX	6.55	I
V471 Sct	8.6	25.6	30.8	8.1	–	–	9.6	6.8	4.1	MSX	5.85	–
V427 Sct	3.9	8.8	11.8	2.9	–	–	3.1	2.2	–	MSX	6.88	–
V1959 Cyg	9.3	16.2	19.1	12.5	–	–	16.8	11.1	13.1	MSX	6.47	–
PR Nor	42.5	89.9	94.3	12.9	–	–	9.3	6.0	2.7	MSX	4.51	I
PZ Vul	0.56	1.8	2.5	0.32	–	–	–	–	–	MSX	8.43	–
GY Lac	3.9	6.8	7.1	0.92	–	–	–	–	–	MSX	7.31	–
V928 Cas	0.91	2.4	3.4	0.83	–	–	–	–	–	MSX	8.22	–
V508 Aur	1.3	2.3	2.7	0.23	–	–	–	–	–	MSX	8.28	–
V1992 Cyg	1.6	3.8	4.7	1.4	–	–	1.4	–	–	MSX	7.90	–
V1850 Cyg	1.2	2.2	2.3	0.31	–	–	–	–	–	MSX	8.56	–
V1242 Cyg	1.6	3.1	3.2	0.29	–	–	–	–	–	MSX	8.12	–
V335 Cen	23.2	44.1	42.4	4.3	–	–	3.6	2.2	–	MSX	5.34	I
ST Sco	255	442	427	55.6	54.8	57.7	55.2	–	–	IRAS−LRS	2.88	I
V385 Sct	18.1	47.5	54.9	10.8	–	–	8.3	5.7	3.4	MSX	5.15	I
TV Aur	65.4	108	110	8.5	–	–	5.3	4.8	–	MSX	4.23	I
V685 Mon	13.9	20.2	18.6	2.1	–	–	–	–	–	MSX	6.25	I
SU Mon	120	213	209	28.0	27.1	28.4	28.2	–	–	IRAS−LRS	3.66	I
V597 Car	14.7	23.1	20.8	3.3	–	–	2.3	1.5	–	MSX	6.17	I
V2003 Sgr	40.3	80.2	78.5	8.0	–	–	7.2	5.0	–	MSX	4.68	I
V575 Cyg	7.7	13.9	14.2	1.7	–	–	1.4	1.1	–	MSX	6.55	–
BI And	63.6	109	114	17.1	16.3	17.2	17.4	–	–	IRAS−LRS	4.34	I
V1258 Ori	49.1	101	100	15.1	–	–	10.4	7.4	4.9	MSX	4.45	I
V536 Pup	2.8	4.8	4.9	0.51	–	–	–	–	–	MSX	7.69	I
Z Ant	107	178	163	26.8	32.1	43.0	42.1	–	–	IRAS−LRS	4.00	I
EE Cen	42.9	85.8	80.0	11.5	–	–	12.2	7.6	5.0	MSX	4.72	–
KQ Cen	35.5	66.8	66.4	7.2	–	–	4.7	3.0	–	MSX	4.84	I
V4714 Sgr	2.2	6.6	11.2	14.9	–	–	16.5	10.0	5.7	MSX	7.10	–
KL Ser	4.0	9.5	16.4	7.7	–	–	8.9	5.5	2.8	MSX	6.60	–
V386 Cep	45.9	93.2	110	61.9	–	–	88.6	66.1	67.0	MSX	4.56	I
V653 Cas	6.0	11.2	11.9	1.4	–	–	–	–	–	MSX	6.73	–
XY CMi	4.0	5.7	5.4	0.89	–	–	–	–	–	MSX	7.65	I
OS Cas	7.5	12.3	13.4	1.4	–	–	–	–	–	MSX	6.60	E
PQ Cas	3.3	5.9	5.7	0.69	–	–	–	–	–	MSX	7.55	–
HX Per	3.9	7.6	7.8	0.77	–	–	–	–	–	MSX	7.17	I
DK Aur	1.1	2.3	2.4	0.44	–	–	–	–	–	MSX	8.55	–
CF Gem	4.2	7.4	7.5	0.87	–	–	–	–	–	MSX	7.24	–
CX Mon	25.9	56.4	58.5	6.7	–	–	5.4	2.9	–	MSX	5.01	I
CSS 251	2.1	3.9	3.7	0.32	–	–	–	–	–	MSX	7.98	E
CSS 323	18.7	42.1	39.1	5.4	–	–	3.1	2.5	–	MSX	5.44	I
CSS 344	9.2	12.7	12.7	1.1	–	–	–	–	–	MSX	6.63	E
KN Mon	8.2	12.7	13.4	1.3	–	–	–	–	–	MSX	6.59	E
KU Pup	11.8	18.5	18.8	2.3	–	–	2.0	1.1	–	MSX	6.26	I
V635 Sco	148	247	221	19.8	–	–	11.9	7.9	3.8	MSX	3.49	I (E)
V915 Aql	63.8	103	97.3	15.4	–	–	9.9	6.7	2.9	MSX	4.49	I
V1318 Aql	2.6	5.8	7.3	2.4	–	–	3.1	2.1	–	MSX	7.45	I
EP Vul	137	268	263	38.6	–	–	29.6	19.1	11.6	MSX	3.41	I
CSS 1155	1.3	4.4	5.9	0.93	–	–	–	–	–	MSX	7.55	–
AD Cyg	55.0	103	101	11.7	–	–	7.5	4.7	2.8	MSX	4.40	I
V633 Cyg	12.1	20.4	20.6	2.1	–	–	1.8	1.2	–	MSX	6.12	E
CSS 13	9.3	19.7	23.7	3.0	–	–	2.0	1.4	–	MSX	5.98	I
CSS 37	4.1	7.3	7.3	0.72	–	–	–	–	–	MSX	7.25	–
CSS 38	2.9	5.1	5.2	0.52	–	–	–	–	–	MSX	7.61	–
CSS 47	3.4	6.0	5.5	0.49	–	–	–	–	–	MSX	7.55	E
CSS 50	4.3	8.1	8.3	0.91	–	–	–	–	–	MSX	7.12	–
CSS 55	0.81	1.5	1.5	0.15	–	–	–	–	–	MSX	8.93	–
CSS 64	1.2	2.3	2.3	0.24	–	–	–	–	–	MSX	8.52	E
CSS 66	1.9	3.9	4.0	0.50	–	–	–	–	–	MSX	7.93	–
CSS 71	0.98	2.3	2.6	0.41	–	–	–	–	–	MSX	8.43	–

Table 12. continued.

Source name	J [Jy]	H [Jy]	K [Jy]	[8.8] [Jy]	[9.8] [Jy]	[11.7] [Jy]	[12.5] [Jy]	D [Jy]	E [Jy]	Mid−IR Data Origin	Apparent bol. magnitudes	I. – E.
CSS 78	17.0	28.5	31.4	2.8	–	–	1.6	–	–	MSX	5.61	E
CSS 146	2.6	5.4	6.2	0.70	–	–	–	–	–	MSX	7.45	–
CSS 147	10.6	22.1	24.8	5.1	–	–	4.9	2.6	–	MSX	6.04	I
CSS 148	3.6	6.1	5.8	0.61	–	–	–	–	–	MSX	7.50	–
CSS 169	1.1	1.8	1.6	0.14	–	–	–	–	–	MSX	8.86	–
CSS 188	2.8	4.5	4.1	0.19	–	–	–	–	–	MSX	7.74	E
CSS 214	6.1	9.6	9.3	0.54	–	–	–	–	–	MSX	6.90	–
CSS 219	24.8	38.2	35.6	2.8	–	–	1.8	1.0	–	MSX	5.46	E
CSS 232	2.5	4.6	4.6	0.47	–	–	–	–	–	MSX	7.76	–
CSS 250	1.5	2.6	2.6	0.29	–	–	–	–	–	MSX	8.39	–
CSS 255	1.8	3.0	3.0	0.28	–	–	–	–	–	MSX	8.22	–
CSS 259	2.9	4.8	4.8	0.65	–	–	–	–	–	MSX	7.75	–
CSS 262	8.4	12.0	12.5	1.2	–	–	–	–	–	MSX	6.66	–
CSS 328	3.6	5.3	4.5	–	–	–	–	–	–	–	–	I (E)
CSS 332	21.6	42.8	36.7	4.1	–	–	2.8	1.5	–	MSX	5.49	–
CSS 371	2.9	5.2	5.5	0.61	–	–	–	–	–	MSX	7.58	–
CSS 393	3.4	4.8	4.9	0.50	–	–	–	–	–	MSX	7.69	I
CSS 408	60.0	102	93.0	18.2	21.5	25.0	26.3	–	–	IRAS−LRS	4.62	I
CSS 411	19.7	33.3	26.5	2.7	–	–	–	–	–	MSX	5.85	I
CSS 417	4.6	7.7	7.9	0.79	–	–	–	–	–	MSX	7.16	–
CSS 427	3.0	6.2	6.9	0.94	–	–	–	–	–	MSX	7.35	I
CSS 542	83.2	157	151	17.8	–	–	13.1	8.6	5.2	MSX	3.97	I
CSS 604	2.3	4.1	4.3	0.29	–	–	–	–	–	MSX	7.75	E
CSS 610	7.4	11.7	13.9	1.4	–	–	–	0.63	–	MSX	6.55	–
CSS 643	2.0	4.5	5.4	0.66	–	–	–	–	–	MSX	7.60	–
CSS 645	2.0	4.3	4.7	0.52	–	–	–	–	–	MSX	7.75	–
CSS 657	2.3	4.2	4.8	1.2	–	–	–	–	–	MSX	7.84	I
CSS 703	7.1	16.4	23.7	3.9	–	–	4.3	5.1	22.0	MSX	6.06	I
CSS 710	5.9	12.2	–	2.3	–	–	2.1	1.2	–	MSX	–	I
CSS 738	4.8	11.1	15.9	17.8	–	–	28.6	19.5	22.2	MSX	6.72	–
CSS 861	11.7	23.5	30.8	20.3	–	–	21.2	13.8	7.6	MSX	5.94	I
CSS 868	5.6	18.2	28.7	15.5	–	–	23.3	15.4	14.1	MSX	6.02	–
CSS 924	12.0	34.7	39.0	10.0	–	–	13.6	8.6	7.3	MSX	5.60	I
CSS 929	41.9	124	173	87.0	–	–	90.4	57.8	37.0	MSX	4.05	I
CSS 930	4.4	8.5	11.1	4.6	–	–	5.0	3.3	–	MSX	7.01	I
CSS 942	11.6	52.7	81.3	48.1	–	–	46.6	30.1	22.3	MSX	4.88	–
CSS 944	18.4	57.1	75.4	71.2	–	–	126	88.4	70.8	MSX	5.02	–
CSS 952	9.4	40.0	64.6	85.4	–	–	153	109	83.6	MSX	5.21	–
CSS 1003	3.3	7.6	10.2	4.2	–	–	4.6	2.7	–	MSX	7.10	I
CSS 1011	6.0	14.2	19.0	6.0	–	–	6.0	4.2	–	MSX	6.38	–
CSS 1021	6.8	10.6	11.4	1.2	–	–	–	–	–	MSX	6.78	I
CSS 1034	17.8	74.3	99.8	31.6	–	–	37.0	26.4	23.6	MSX	4.60	–
CSS 1035	6.3	13.6	17.8	2.4	–	–	1.6	1.3	–	MSX	6.31	I
CSS 1036	4.9	8.0	7.4	0.69	–	–	–	–	–	MSX	7.22	–
CSS 1100	10.5	16.6	22.4	2.5	–	–	2.2	1.1	–	MSX	6.05	I
CSS 1128	5.4	12.4	15.3	3.9	–	–	3.4	2.3	–	MSX	6.59	I
CSS 1145	19.5	50.1	61.0	7.8	–	–	4.8	2.9	–	MSX	4.95	–
CSS 1238	1.6	2.6	2.4	0.27	–	–	–	–	–	MSX	8.45	–
CSS 1280	0.81	1.4	1.4	0.12	–	–	–	–	–	MSX	9.05	–
CSS 1282	1.2	2.3	2.4	0.23	–	–	–	–	–	MSX	8.45	–
CSS 1289	1.5	2.6	2.5	0.24	–	–	–	–	–	MSX	8.39	–
CSS 1297	13.6	21.2	21.6	3.0	–	–	3.0	1.9	–	MSX	6.14	–
CSS 1329	14.0	32.0	35.1	5.5	–	–	4.1	2.8	–	MSX	5.60	–
CSS2 51	3.3	6.3	6.8	1.1	–	–	1.2	–	–	MSX	7.42	–
BB Aur	18.8	30.7	31.0	0.77	–	–	–	–	–	MSX	5.42	I
RR Car	768	1223	1154	99.7	–	–	161	110	72.4	MSX	1.78	I
YY Lac	11.8	17.1	15.6	2.2	–	–	2.0	–	–	MSX	6.49	I
CV Cep	43.2	85.9	94.6	12.5	–	–	8.0	5.1	2.7	MSX	4.49	I
EN Mon	2.8	4.4	4.2	0.37	–	–	–	–	–	MSX	7.82	E
DT CMa	8.3	13.0	12.8	1.3	–	–	–	–	–	MSX	6.63	E
KP Mon	2.3	3.7	3.3	0.33	–	–	–	–	–	MSX	8.09	–
CSS 415	4.6	7.5	7.3	0.74	–	–	–	–	–	MSX	7.25	–
CSS 1066	3.4	11.3	23.4	109	–	–	123	89.0	88.5	MSX	6.36	–
BO Cru	8.0	18.3	24.5	7.4	–	–	10.6	6.6	3.8	MSX	6.13	–
DY Gem	85.4	156	143	21.3	–	–	18.9	12.7	7.8	MSX	4.09	–
DK Vul	79.3	135	138	18.6	–	–	16.5	11.2	7.4	MSX	4.10	–

Table 12. continued.

Source name	J [Jy]	H [Jy]	K [Jy]	[8.8] [Jy]	[9.8] [Jy]	[11.7] [Jy]	[12.5] [Jy]	D [Jy]	E [Jy]	Mid−IR Data Origin	Apparent bol. magnitudes	I. − E.
V441 Cyg	71.7	136	130	16.2	–	–	11.3	7.2	3.4	MSX	4.14	I
V365 Cas	178	280	262	30.8	32.2	34.0	33.3	–	–	IRAS−LRS	3.40	I
V521 Oph	266	442	424	51.7	–	–	31.9	22.2	12.2	MSX	2.84	I
VX Cen	273	429	419	59.7	–	–	40.8	26.1	13.0	MSX	2.89	I
V739 Cyg	0.79	1.4	1.6	0.31	–	–	–	–	–	MSX	9.04	–
V354 Aql	20.0	38.5	35.6	3.3	–	–	–	–	–	MSX	5.52	I
BB Tau	16.3	33.9	39.1	4.7	–	–	3.2	1.5	–	MSX	5.43	I
GG Pup	39.8	73.4	66.9	6.5	–	–	4.6	2.9	–	MSX	4.82	–
HP Vel	79.4	126	117	19.8	20.9	–	–	–	–	IRAS−LRS	4.32	I
V3803 Sgr	20.9	38.9	36.7	4.2	–	–	3.7	2.2	–	MSX	5.52	–
BP Sct	33.2	82.6	94.1	11.5	–	–	8.0	5.2	2.8	MSX	4.49	I
TV Dra	266	386	352	68.4	65.0	63.9	63.8	–	–	IRAS−LRS	3.15	–
CSS 1243	29.2	58.4	80.4	17.6	–	–	19.6	15.5	9.9	MSX	4.78	–
EO Eri	35.8	59.1	63.2	19.3	22.9	25.6	26.1	–	–	IRAS−LRS	5.09	–
V1407 Aql	6.7	8.4	9.3	17.6	25.3	27.2	27.5	–	–	IRAS−LRS	7.33	I
KR CMa	75.7	120	109	10.3	–	–	6.3	3.6	–	MSX	4.27	E
V378 Pav	128	188	157	19.8	20.8	23.2	24.3	–	–	IRAS−LRS	3.99	I (E)
V771 Cen	124	171	154	22.2	–	–	17.3	12.9	10.3	MSX	3.99	–
V911 Cas	8.1	12.3	11.7	2.1	–	–	1.7	–	–	MSX	6.82	I
V2012 Cyg	24.5	41.0	41.8	3.8	–	–	2.2	1.5	–	MSX	5.30	E
V850 Cas	5.3	10.8	15.3	9.7	–	–	9.4	6.9	6.8	MSX	6.70	–
V535 Ori	43.9	77.7	75.9	16.8	–	–	17.8	12.3	10.3	MSX	4.84	I
GT CMa	8.2	12.8	12.9	2.0	–	–	–	–	–	MSX	6.70	I
EY Leo	17.7	31.8	27.6	2.6	–	–	1.2	1.3	–	MSX	5.73	–
CSS 53	3.6	6.3	6.1	0.63	–	–	–	–	–	MSX	7.45	–
CSS 59	1.1	1.9	1.8	0.18	–	–	–	–	–	MSX	8.80	–
CSS 81	29.4	55.7	62.9	4.8	–	–	2.8	1.8	–	MSX	4.82	E
CSS 108	12.3	20.4	18.9	1.9	–	–	1.5	–	–	MSX	6.21	I
CSS 136	2.3	4.1	3.9	0.39	–	–	–	–	–	MSX	7.93	–
CSS 140	4.2	7.3	–	0.96	–	–	–	–	–	MSX	–	–
CSS 143	2.1	4.0	4.0	0.47	–	–	–	–	–	MSX	7.91	–
CSS 180	1.7	2.9	2.7	0.28	–	–	–	–	–	MSX	8.32	–
CSS 185	7.7	13.0	13.6	1.5	–	–	–	–	–	MSX	6.59	–
CSS 193	1.8	3.0	2.7	0.28	–	–	–	–	–	MSX	8.34	–
CSS 195	3.5	5.7	5.1	0.50	–	–	–	–	–	MSX	7.63	–
CSS 208	2.1	3.5	3.3	0.32	–	–	–	–	–	MSX	8.11	–
CSS 233	9.9	13.0	13.1	1.2	–	–	–	–	–	MSX	6.59	E
CSS 240	1.5	2.9	2.9	0.27	–	–	–	–	–	MSX	8.22	–
CSS 249	3.3	5.4	5.3	0.55	–	–	–	–	–	MSX	7.60	–
CSS 335	36.2	60.7	54.4	5.9	–	–	3.2	2.0	–	MSX	5.04	E
CSS 388	16.0	32.7	28.9	3.9	–	–	3.0	2.0	–	MSX	5.79	I
CSS 448	38.2	66.1	57.9	6.9	–	–	4.7	2.8	–	MSX	5.01	I
CSS 720	11.3	13.3	13.1	1.2	–	–	–	–	–	MSX	6.59	E
CSS 755	14.5	22.3	18.4	1.8	–	–	1.3	0.76	–	MSX	6.23	–
CSS 853	36.2	58.5	48.2	3.9	–	–	2.6	1.7	0.88	MSX	5.14	E
CSS 909	6.0	13.1	17.5	4.6	–	–	3.9	2.3	–	MSX	6.44	I
CSS 977	20.9	43.0	35.9	4.1	–	–	2.7	1.6	–	MSX	5.52	I
CSS 1010	27.1	44.8	37.0	3.9	–	–	2.2	1.5	0.80	MSX	5.46	E
CSS 1146	29.3	51.9	60.5	65.0	112	94.7	78.6	–	–	IRAS−LRS	5.26	–
CSS 1158	11.7	18.4	17.1	2.1	–	–	1.6	0.97	–	MSX	6.35	–
CSS 1192	58.2	78.5	80.3	5.9	–	–	3.2	2.2	–	MSX	4.54	E
CSS 1283	11.6	19.8	21.3	1.9	–	–	1.1	0.84	–	MSX	6.03	–
CSS2 25	59.7	128	155	101	187	145	116	–	–	IRAS−LRS	4.19	–
CSS2 41	6.1	14.7	17.8	30.0	–	–	34.2	23.4	24.8	MSX	6.61	–
BH Cru	83.9	139	147	29.9	26.8	28.2	28.8	–	–	IRAS−LRS	4.11	I
GP Ori	55.2	103	105	19.4	18.7	21.4	23.1	–	–	IRAS−LRS	4.47	I
BX CMa	13.6	23.4	23.5	2.5	–	–	–	–	–	MSX	5.99	–
FX CMa	19.0	35.4	31.6	3.8	–	–	2.5	1.3	–	MSX	5.67	I
FU Mon	69.9	148	143	13.3	–	–	7.8	3.8	–	MSX	3.97	I
V372 Mon	19.5	45.0	41.7	3.4	–	–	–	1.8	–	MSX	5.32	–
AM Cen	82.4	158	156	24.6	23.5	23.9	23.3	–	–	IRAS−LRS	4.01	I
CY Cyg	45.8	80.4	82.2	16.6	–	–	15.7	7.9	4.3	MSX	4.73	–
CSS 661	5.1	8.8	9.9	3.0	–	–	3.6	1.8	–	MSX	7.10	I
CSS2 9	4.5	11.7	13.9	1.7	–	–	–	–	–	MSX	6.58	–
CSS 683	1.8	4.0	5.3	1.6	–	–	1.5	1.2	–	MSX	7.77	I
CSS 769	3.7	8.1	10.3	1.8	–	–	2.3	1.2	–	MSX	6.99	I

Table 12. continued.

Source name	J [Jy]	H [Jy]	K [Jy]	[8.8] [Jy]	[9.8] [Jy]	[11.7] [Jy]	[12.5] [Jy]	D [Jy]	E [Jy]	Mid−IR Data Origin	Apparent bol. magnitudes	I. − E.
CSS 1229	2.4	3.3	4.2	1.1	–	–	1.0	0.98	–	MSX	7.98	–
CSS 118	10.9	13.0	12.0	1.1	–	–	–	–	–	MSX	6.70	E
CSS 306	12.1	17.6	15.7	1.6	–	–	1.3	–	–	MSX	6.42	–
CSS 621	4.3	5.9	4.9	0.25	–	–	–	–	–	MSX	7.58	–
CSS 766	19.8	38.8	33.6	2.5	–	–	2.2	1.6	–	MSX	5.54	I
V1190 Cyg	13.6	16.0	19.5	2.3	–	–	1.7	1.1	–	MSX	6.19	I
V899 Cas	18.8	44.7	54.6	6.1	–	–	4.1	2.1	–	MSX	5.06	I
V354 Gem	5.6	8.6	8.1	0.76	–	–	–	–	–	MSX	7.12	–
V527 Pup	5.8	8.0	7.9	0.48	–	–	–	–	–	MSX	7.08	–
V470 Sct	11.8	18.2	21.5	2.6	–	–	2.4	1.1	–	MSX	6.11	–
V662 Cep	9.3	21.4	21.1	3.9	–	–	2.9	1.9	–	MSX	6.18	–
V684 Per	0.99	2.7	4.0	3.5	–	–	5.2	3.2	–	MSX	8.21	–
V1143 Aql	0.56	1.4	2.0	0.44	–	–	–	–	–	MSX	8.76	–
V357 Sge	2.5	4.6	5.1	1.2	–	–	–	–	–	MSX	7.77	–
V1738 Cyg	1.6	2.7	2.8	0.18	–	–	–	–	–	MSX	8.22	–
MQ Aur	2.2	3.6	3.3	0.33	–	–	–	–	–	MSX	8.11	–
V481 Pup	8.5	13.0	15.5	1.1	–	–	–	–	–	MSX	6.38	–
V1925 Cyg	4.5	10.1	13.1	1.5	–	–	1.1	0.67	–	MSX	6.62	–
CSS 10	4.5	8.5	8.2	0.79	–	–	–	–	–	MSX	7.11	E
CSS 21	1.3	2.0	1.7	0.18	–	–	–	–	–	MSX	8.81	–
CSS 30	6.9	18.1	25.5	4.5	–	–	3.2	1.9	–	MSX	5.97	–
CSS 31	3.8	7.3	7.8	1.2	–	–	–	–	–	MSX	7.24	–
CSS 34	3.6	6.3	5.5	0.56	–	–	–	–	–	MSX	7.55	–
CSS 43	2.7	4.2	3.6	0.31	–	–	–	–	–	MSX	7.98	–
CSS 51	1.1	2.0	1.9	0.15	–	–	–	–	–	MSX	8.70	–
CSS 101	3.3	5.3	5.0	0.36	–	–	–	–	–	MSX	7.60	E
CSS 105	4.3	6.5	5.6	0.47	–	–	–	–	–	MSX	7.50	E
CSS 110	5.2	8.9	8.6	0.59	–	–	–	–	–	MSX	7.01	–
CSS 111	6.3	9.3	8.7	0.82	–	–	–	–	–	MSX	7.04	–
CSS 119	3.5	5.4	5.2	0.59	–	–	–	–	–	MSX	7.63	–
CSS 124	4.6	7.7	6.8	0.64	–	–	–	–	–	MSX	7.31	–
CSS 137	3.4	6.1	5.9	0.54	–	–	–	–	–	MSX	7.47	–
CSS 138	2.4	4.1	3.6	0.33	–	–	–	–	–	MSX	7.99	E
CSS 142	3.6	6.4	6.1	0.45	–	–	–	–	–	MSX	7.39	–
CSS 157	3.1	4.6	4.2	0.37	–	–	–	–	–	MSX	7.82	–
CSS 162	8.0	11.9	12.6	1.2	–	–	–	–	–	MSX	6.65	E
CSS 198	4.7	7.0	6.1	0.44	–	–	–	–	–	MSX	7.39	E
CSS 200	5.4	8.5	8.4	1.2	–	–	–	–	–	MSX	7.15	–
CSS 203	3.6	6.7	–	0.93	–	–	–	–	–	MSX	–	–
CSS 204	4.8	6.3	5.5	0.41	–	–	–	–	–	MSX	7.51	E
CSS 252	1.5	2.3	2.1	0.22	–	–	–	–	–	MSX	8.61	–
CSS 258	1.6	2.3	2.0	0.17	–	–	–	–	–	MSX	8.63	–
CSS 263	11.0	18.4	19.8	2.6	–	–	2.6	–	–	MSX	6.22	–
CSS 267	2.2	4.2	4.3	0.45	–	–	–	–	–	MSX	7.83	–
CSS 268	2.7	4.5	4.5	0.42	–	–	–	–	–	MSX	7.77	–
CSS 269	5.6	8.8	8.6	0.82	–	–	–	–	–	MSX	7.06	–
CSS 272	5.8	9.7	9.5	0.81	–	–	–	–	–	MSX	6.94	–
CSS 282	2.6	5.2	5.4	0.57	–	–	–	–	–	MSX	7.58	–
CSS 287	3.1	4.8	4.5	0.42	–	–	–	–	–	MSX	7.76	–
CSS 288	13.9	20.2	19.6	1.5	–	–	–	–	–	MSX	6.13	E
CSS 295	5.0	9.0	8.7	1.4	–	–	–	–	–	MSX	7.13	I
CSS 298	3.0	4.9	4.6	0.43	–	–	–	–	–	MSX	7.74	–
CSS 299	3.5	6.2	5.7	0.56	–	–	–	–	–	MSX	7.51	–
CSS 300	5.2	7.3	6.5	0.49	–	–	–	–	–	MSX	7.32	E
CSS 301	2.3	4.2	4.1	0.44	–	–	–	–	–	MSX	7.88	E
CSS 302	3.0	4.3	3.7	0.25	–	–	–	–	–	MSX	7.91	–
CSS 305	5.1	7.9	7.5	0.68	–	–	–	–	–	MSX	7.21	E
CSS 309	2.6	4.1	4.0	0.39	–	–	–	–	–	MSX	7.88	–
CSS 310	2.4	3.5	3.0	0.29	–	–	–	–	–	MSX	8.21	–
CSS 311	5.6	7.7	6.9	0.56	–	–	–	–	–	MSX	7.27	E
CSS 313	2.8	4.2	4.1	0.37	–	–	–	–	–	MSX	7.86	E
CSS 322	4.2	6.3	5.8	0.48	–	–	–	–	–	MSX	7.47	–
CSS 336	11.2	16.4	17.2	2.4	–	–	1.8	1.2	–	MSX	6.36	–
CSS 340	2.0	3.5	3.3	0.39	–	–	–	–	–	MSX	8.14	–
CSS 349	1.8	3.0	2.7	0.25	–	–	–	–	–	MSX	8.32	–
CSS 351	2.8	4.6	4.7	0.49	–	–	–	–	–	MSX	7.72	–

Table 12. continued.

Source name	J [Jy]	H [Jy]	K [Jy]	[8.8] [Jy]	[9.8] [Jy]	[11.7] [Jy]	[12.5] [Jy]	D [Jy]	E [Jy]	Mid−IR Data Origin	Apparent bol. magnitudes	I. − E.
CSS 352	3.3	5.4	5.4	0.60	–	–	–	–	–	MSX	7.60	–
CSS 360	5.5	9.2	9.0	0.79	–	–	–	–	–	MSX	7.00	I
CSS 364	1.7	3.4	3.5	0.43	–	–	–	–	–	MSX	8.06	–
CSS 366	0.92	1.7	1.8	0.19	–	–	–	–	–	MSX	8.79	–
CSS 367	3.3	5.5	5.4	0.78	–	–	–	–	–	MSX	7.64	–
CSS 379	2.9	4.7	4.6	0.48	–	–	–	–	–	MSX	7.76	E
CSS 383	3.0	5.1	5.0	0.79	–	–	–	–	–	MSX	7.73	I
CSS 384	3.9	6.1	5.6	0.54	–	–	–	–	–	MSX	7.52	–
CSS 386	1.9	3.3	3.2	0.34	–	–	–	–	–	MSX	8.15	–
CSS 389	7.4	11.3	11.1	1.2	–	–	–	–	–	MSX	6.79	E
CSS 395	1.7	2.9	2.9	0.32	–	–	–	–	–	MSX	8.26	–
CSS 404	7.8	12.1	11.1	1.2	–	–	–	–	–	MSX	6.81	–
CSS 406	1.8	2.9	2.6	0.27	–	–	–	–	–	MSX	8.39	–
CSS 409	1.7	3.2	3.1	0.20	–	–	–	–	–	MSX	8.10	–
CSS 432	1.7	3.0	2.8	0.21	–	–	–	–	–	MSX	8.24	–
CSS 433	5.3	7.7	6.7	0.58	–	–	–	–	–	MSX	7.31	–
CSS 437	1.3	2.0	1.9	0.20	–	–	–	–	–	MSX	8.73	–
CSS 438	1.5	3.5	4.7	1.1	–	–	1.3	0.83	–	MSX	7.89	I
CSS 439	4.0	5.9	5.1	0.37	–	–	–	–	–	MSX	7.57	–
CSS 444	2.5	4.4	4.3	0.48	–	–	–	–	–	MSX	7.84	E
CSS 450	1.6	2.7	2.4	0.21	–	–	–	–	–	MSX	8.41	–
CSS 463	1.2	2.0	2.0	0.20	–	–	–	–	–	MSX	8.65	–
CSS 466	2.5	4.5	5.8	2.3	–	–	2.1	1.7	–	MSX	7.70	I
CSS 467	1.7	2.8	2.5	0.21	–	–	–	–	–	MSX	8.36	–
CSS 469	2.3	3.7	3.7	0.36	–	–	–	–	–	MSX	7.97	–
CSS 470	5.2	8.0	7.7	0.82	–	–	–	–	–	MSX	7.19	I
CSS 473	1.9	2.9	2.7	0.24	–	–	–	–	–	MSX	8.30	–
CSS 474	28.9	52.6	54.1	7.9	–	–	5.3	3.4	–	MSX	5.11	I
CSS 479	1.5	2.5	2.4	0.26	–	–	–	–	–	MSX	8.49	–
CSS 480	7.1	10.6	9.7	1.3	–	–	–	–	–	MSX	6.99	–
CSS 486	12.7	16.9	16.3	1.6	–	–	–	–	–	MSX	6.37	E
CSS 489	4.8	7.0	6.4	0.62	–	–	–	–	–	MSX	7.38	I
CSS 490	7.2	10.0	8.9	0.76	–	–	–	–	–	MSX	7.01	I
CSS 497	1.7	4.0	4.5	0.50	–	–	–	–	–	MSX	7.80	–
CSS 498	3.4	5.3	4.8	0.43	–	–	–	–	–	MSX	7.69	E
CSS 504	2.3	3.9	4.1	0.56	–	–	–	–	–	MSX	7.93	–
CSS 506	11.0	17.4	15.1	1.9	–	–	–	–	–	MSX	6.50	I
CSS 507	1.5	3.3	3.7	0.45	–	–	–	–	–	MSX	8.02	–
CSS 509	2.0	3.1	2.7	0.20	–	–	–	–	–	MSX	8.29	–
CSS 515	0.60	1.4	1.8	0.61	–	–	–	–	–	MSX	8.97	I
CSS 526	11.0	21.5	24.7	4.1	–	–	2.9	1.6	–	MSX	5.99	I
CSS 527	11.0	16.7	17.7	3.8	–	–	3.7	2.6	0.97	MSX	6.41	–
CSS 528	4.1	6.5	6.4	0.67	–	–	–	–	–	MSX	7.40	E
CSS 531	2.6	4.6	4.8	0.54	–	–	–	–	–	MSX	7.73	–
CSS 539	5.4	12.9	17.8	2.6	–	–	1.7	1.0	–	MSX	6.32	I
CSS 540	29.2	63.3	61.6	6.7	–	–	3.7	2.4	–	MSX	4.90	I
CSS 541	3.3	5.6	5.2	0.43	–	–	–	–	–	MSX	7.59	E
CSS 547	4.0	6.2	5.4	0.43	–	–	–	–	–	MSX	7.54	–
CSS 548	5.2	14.2	19.0	2.9	–	–	2.1	1.4	–	MSX	6.26	–
CSS 550	7.3	19.1	16.2	2.0	–	–	–	0.98	–	MSX	6.42	I
CSS 553	5.7	9.7	10.0	1.5	–	–	–	–	–	MSX	6.97	–
CSS 559	14.0	22.3	19.3	2.1	–	–	1.6	0.92	–	MSX	6.20	I
CSS 567	2.4	4.7	4.8	0.44	–	–	–	–	–	MSX	7.70	E
CSS 569	4.3	16.3	22.2	3.8	–	–	3.1	2.0	1.2	MSX	6.12	I
CSS 580	1.7	2.7	2.5	0.20	–	–	–	–	–	MSX	8.38	E
CSS 581	6.9	10.9	10.7	0.99	–	–	–	–	–	MSX	6.82	E
CSS 583	2.5	5.7	6.3	0.82	–	–	–	–	–	MSX	7.45	–
CSS 584	4.2	8.1	8.5	0.79	–	–	–	–	–	MSX	7.08	I
CSS 592	7.1	10.9	9.9	0.85	–	–	–	–	–	MSX	6.89	E
CSS 596	1.8	3.1	3.0	0.34	–	–	–	–	–	MSX	8.24	–
CSS 598	3.1	5.2	5.1	0.47	–	–	–	–	–	MSX	7.63	E
CSS 601	7.7	11.1	11.2	1.0	–	–	0.62	–	–	MSX	6.73	–
CSS 606	0.37	0.61	0.63	0.07	–	–	–	–	–	MSX	9.92	–
CSS 608	1.7	4.6	6.6	3.5	–	–	3.1	1.8	–	MSX	7.59	–
CSS 609	17.5	32.8	29.5	2.2	–	–	2.2	2.0	–	MSX	5.69	–
CSS 619	2.7	4.3	4.3	0.45	–	–	–	–	–	MSX	7.84	–

Table 12. continued.

Source name	J [Jy]	H [Jy]	K [Jy]	[8.8] [Jy]	[9.8] [Jy]	[11.7] [Jy]	[12.5] [Jy]	D [Jy]	E [Jy]	Mid−IR Data Origin	Apparent bol. magnitudes	I. – E.
CSS 625	10.9	18.3	17.0	1.9	–	–	–	–	–	MSX	6.34	E (I)
CSS 633	3.8	5.5	6.1	1.9	–	–	–	–	–	MSX	7.62	I
CSS 635	2.7	4.8	4.6	0.46	–	–	–	–	–	MSX	7.74	–
CSS 648	4.6	13.0	19.2	6.1	–	–	6.7	5.3	6.3	MSX	6.38	I
CSS 650	4.7	7.2	6.8	0.34	–	–	–	–	–	MSX	7.21	I
CSS 651	1.5	3.3	4.1	0.45	–	–	–	–	–	MSX	7.90	–
CSS 660	1.7	2.6	2.3	0.18	–	–	–	–	–	MSX	8.43	E
CSS 664	14.1	24.2	23.4	2.9	–	–	–	1.8	–	MSX	6.02	I
CSS 665	3.1	5.1	4.9	0.35	–	–	–	–	–	MSX	7.61	E
CSS 668	13.2	26.5	21.9	2.6	–	–	1.4	–	–	MSX	6.04	I
CSS 672	7.0	9.6	8.8	0.82	–	–	–	–	–	MSX	7.04	E
CSS 676	1.6	2.2	1.9	0.16	–	–	–	–	–	MSX	8.66	–
CSS 678	0.86	1.3	1.2	0.13	–	–	–	–	–	MSX	9.26	–
CSS 681	2.0	3.1	2.9	0.31	–	–	–	–	–	MSX	8.24	–
CSS 682	5.9	9.0	9.0	0.94	–	–	–	–	–	MSX	7.03	I
CSS 684	11.0	21.8	20.9	3.4	–	–	2.2	1.4	–	MSX	6.16	I
CSS 687	33.8	69.6	69.7	14.2	15.8	19.6	21.3	–	–	IRAS−LRS	4.94	I
CSS 691	1.4	2.2	1.9	0.16	–	–	–	–	–	MSX	8.69	–
CSS 692	3.3	5.7	5.5	0.56	–	–	–	–	–	MSX	7.57	I
CSS 693	17.8	23.5	20.2	3.7	–	–	3.5	2.3	–	MSX	6.24	I
CSS 698	1.7	2.4	2.1	0.16	–	–	–	–	–	MSX	8.56	–
CSS 699	8.3	12.2	11.7	1.3	–	–	–	–	–	MSX	6.75	I (E)
CSS 702	23.0	46.3	46.3	4.6	–	–	3.4	2.9	–	MSX	5.23	I
CSS 707	11.5	15.6	15.9	1.4	–	–	1.1	–	–	MSX	6.36	–
CSS 713	3.2	6.2	6.8	0.72	–	–	–	–	–	MSX	7.34	–
CSS 715	3.4	5.1	4.5	0.42	–	–	–	–	–	MSX	7.76	I
CSS 716	4.4	11.0	13.5	8.9	–	–	15.8	10.1	11.2	MSX	6.86	–
CSS 718	5.0	7.5	7.4	0.76	–	–	–	–	–	MSX	7.24	I
CSS 719	4.4	7.8	7.8	0.86	–	–	–	–	–	MSX	7.18	I
CSS 723	2.4	3.8	4.3	0.70	–	–	–	–	–	MSX	7.91	–
CSS 725	2.4	3.6	3.2	0.26	–	–	–	–	–	MSX	8.10	E
CSS 727	1.1	1.6	1.5	0.14	–	–	–	–	–	MSX	8.97	–
CSS 728	6.4	12.0	12.4	1.5	–	–	1.1	–	–	MSX	6.69	I
CSS 732	4.7	9.2	12.5	2.3	–	–	2.0	1.4	–	MSX	6.77	–
CSS 733	2.4	3.9	3.5	0.31	–	–	–	–	–	MSX	8.01	–
CSS 741	3.3	5.0	4.4	0.36	–	–	–	–	–	MSX	7.76	I
CSS 743	2.9	4.4	4.1	0.47	–	–	–	–	–	MSX	7.88	I
CSS 747	2.4	3.4	3.2	0.28	–	–	–	–	–	MSX	8.14	–
CSS 748	3.8	5.5	4.9	0.41	–	–	–	–	–	MSX	7.66	–
CSS 749	4.2	7.5	8.6	1.0	–	–	–	–	–	MSX	7.10	I
CSS 750	5.6	8.1	7.7	0.70	–	–	–	–	–	MSX	7.18	–
CSS 751	3.4	5.3	4.7	0.41	–	–	–	–	–	MSX	7.70	E
CSS 754	3.1	4.8	4.2	0.36	–	–	–	–	–	MSX	7.83	–
CSS 758	2.5	4.0	3.6	0.32	–	–	–	–	–	MSX	7.99	–
CSS 759	3.1	4.9	4.6	0.39	–	–	–	–	–	MSX	7.72	–
CSS 760	1.5	2.4	2.2	0.19	–	–	–	–	–	MSX	8.53	–
CSS 761	5.8	9.7	9.7	0.97	–	–	–	–	–	MSX	6.94	–
CSS 762	3.0	4.5	4.1	0.31	–	–	–	–	–	MSX	7.82	I
CSS 763	4.1	6.8	7.0	0.86	–	–	–	–	–	MSX	7.32	–
CSS 765	2.7	4.4	4.0	0.35	–	–	–	–	–	MSX	7.89	E
CSS 767	3.9	5.9	5.3	0.28	–	–	–	–	–	MSX	7.49	–
CSS 771	1.8	4.6	5.8	1.1	–	–	–	–	–	MSX	7.60	I
CSS 773	1.5	4.2	6.1	3.4	–	–	4.6	3.2	–	MSX	7.69	I
CSS 776	2.8	7.8	10.5	5.1	–	–	7.2	4.3	5.0	MSX	7.10	–
CSS 779	2.1	6.6	8.9	3.3	–	–	3.6	2.8	–	MSX	7.23	–
CSS 781	3.9	10.1	15.7	13.9	–	–	12.9	8.6	4.5	MSX	6.70	I
CSS 789	1.6	2.7	3.5	1.6	–	–	1.7	1.1	–	MSX	8.28	–
CSS 800	11.5	22.4	25.6	5.9	–	–	5.3	3.3	–	MSX	6.01	–
CSS 805	3.3	8.0	9.5	1.2	–	–	–	–	–	MSX	7.00	I
CSS 806	2.2	5.2	6.4	0.68	–	–	–	–	–	MSX	7.40	–
CSS 810	8.5	13.3	12.4	1.4	–	–	–	–	–	MSX	6.69	I
CSS 811	8.4	13.5	14.2	1.5	–	–	–	–	–	MSX	6.53	I
CSS 823	4.8	9.1	9.7	1.1	–	–	–	–	–	MSX	6.97	–
CSS 825	4.6	11.0	11.8	2.1	–	–	1.6	–	–	MSX	6.80	–
CSS 838	3.3	5.6	5.4	0.53	–	–	–	–	–	MSX	7.58	–
CSS 840	11.7	19.0	17.4	2.0	–	–	1.6	0.80	–	MSX	6.32	–

Table 12. continued.

Source name	J [Jy]	H [Jy]	K [Jy]	[8.8] [Jy]	[9.8] [Jy]	[11.7] [Jy]	[12.5] [Jy]	D [Jy]	E [Jy]	Mid−IR Data Origin	Apparent bol. magnitudes	I. – E.
CSS 846	8.2	14.2	15.7	1.7	–	–	1.3	0.98	–	MSX	6.42	I
CSS 847	7.3	20.8	26.7	4.9	–	–	5.2	3.7	3.1	MSX	5.95	–
CSS 849	1.8	2.7	2.4	0.22	–	–	–	–	–	MSX	8.42	–
CSS 852	3.4	9.0	11.7	1.7	–	–	1.5	–	–	MSX	6.80	–
CSS 862	3.5	8.2	10.6	1.3	–	–	–	–	–	MSX	6.87	–
CSS 869	16.3	30.5	29.6	5.0	–	–	4.5	3.0	–	MSX	5.81	I
CSS 870	5.5	12.5	21.5	3.4	–	–	3.2	2.3	–	MSX	6.16	I
CSS 871	5.3	15.6	18.5	4.9	–	–	7.1	4.6	2.8	MSX	6.42	–
CSS 878	3.4	8.9	11.6	1.6	–	–	1.4	0.97	–	MSX	6.80	I
CSS 879	3.3	5.0	4.4	0.34	–	–	–	–	–	MSX	7.77	–
CSS 881	3.8	8.1	8.8	1.1	–	–	–	–	–	MSX	7.08	–
CSS 888	5.6	11.1	16.0	2.0	–	–	1.8	0.95	–	MSX	6.43	I
CSS 890	4.0	12.5	16.6	4.5	–	–	4.8	3.1	2.4	MSX	6.52	–
CSS 891	2.3	8.1	12.0	1.8	–	–	1.6	1.3	–	MSX	6.78	–
CSS 893	–	0.06	0.24	0.84	–	–	1.1	0.92	–	MSX	11.31	–
CSS 897	10.0	38.2	52.1	41.7	–	–	66.6	48.5	46.4	MSX	5.40	–
CSS 901	2.7	6.3	7.5	0.92	–	–	–	–	–	MSX	7.25	I
CSS 905	13.5	58.0	80.2	53.7	–	–	82.8	57.9	51.1	MSX	4.92	–
CSS 906	2.7	4.2	3.7	0.32	–	–	–	–	–	MSX	7.95	–
CSS 915	10.4	23.4	25.3	4.2	–	–	2.6	2.1	–	MSX	5.95	I
CSS 917	6.6	14.0	19.7	2.1	–	–	1.7	–	–	MSX	6.18	–
CSS 918	3.1	7.7	10.2	2.1	–	–	1.8	1.8	3.7	MSX	6.99	–
CSS 919	4.2	6.7	7.7	1.5	–	–	1.1	0.89	–	MSX	7.29	–
CSS 921	6.8	11.0	10.2	0.97	–	–	–	–	–	MSX	6.88	–
CSS 922	5.7	10.1	12.7	3.0	–	–	2.7	1.4	–	MSX	6.78	I
CSS 925	4.4	11.8	14.9	2.5	–	–	2.5	1.7	–	MSX	6.57	I
CSS 933	3.7	7.9	8.8	1.1	–	–	0.74	0.80	–	MSX	7.06	–
CSS 934	6.0	15.0	18.2	6.1	–	–	8.4	5.7	5.4	MSX	6.46	–
CSS 939	11.3	36.8	40.1	6.4	–	–	4.6	3.1	–	MSX	5.46	I
CSS 946	4.8	13.4	22.0	4.4	–	–	4.7	2.8	–	MSX	6.17	–
CSS 950	3.0	4.8	4.6	0.40	–	–	–	–	–	MSX	7.73	–
CSS 951	6.1	22.3	28.7	4.7	–	–	4.0	3.0	–	MSX	5.84	–
CSS 953	3.8	6.0	5.8	0.56	–	–	–	–	–	MSX	7.48	–
CSS 956	14.8	38.4	49.2	27.6	–	–	43.6	29.4	27.4	MSX	5.44	–
CSS 957	11.4	35.2	49.6	35.4	–	–	50.4	34.7	35.5	MSX	5.45	–
CSS 960	7.7	13.6	16.6	2.3	–	–	2.0	1.3	–	MSX	6.41	–
CSS 962	7.6	11.4	10.3	0.92	–	–	–	–	–	MSX	6.85	E
CSS 969	3.7	5.6	4.8	0.42	–	–	–	–	–	MSX	7.67	–
CSS 973	0.002	0.05	0.30	2.2	–	–	4.2	4.0	4.6	MSX	11.09	–
CSS 979	5.8	12.5	14.5	2.4	–	–	1.4	0.98	–	MSX	6.55	I
CSS 982	12.1	21.8	18.5	1.7	–	–	–	–	–	MSX	6.23	–
CSS 987	1.7	3.6	4.5	1.5	–	–	–	–	–	MSX	7.94	I
CSS 1008	1.9	3.5	3.7	0.44	–	–	–	–	–	MSX	8.03	I
CSS 1012	7.7	11.6	11.2	1.1	–	–	–	–	–	MSX	6.78	–
CSS 1020	12.9	33.1	34.7	4.7	–	–	2.8	1.5	–	MSX	5.57	I
CSS 1039	0.94	1.5	1.4	0.15	–	–	–	–	–	MSX	9.07	–
CSS 1047	27.5	69.1	77.5	11.7	–	–	12.0	8.7	4.9	MSX	4.76	–
CSS 1050	9.8	14.3	13.0	1.7	–	–	–	–	–	MSX	6.67	–
CSS 1055	8.0	25.7	36.0	20.9	–	–	35.0	22.6	16.2	MSX	5.78	–
CSS 1061	4.4	11.3	–	1.8	–	–	1.7	1.1	–	MSX	–	–
CSS 1068	7.9	14.3	15.5	3.4	–	–	3.0	1.7	–	MSX	6.55	–
CSS 1077	5.3	8.0	7.5	0.79	–	–	–	–	–	MSX	7.22	–
CSS 1082	0.79	1.4	1.3	0.10	–	–	–	–	–	MSX	9.06	–
CSS 1104	10.3	22.8	25.2	10.5	–	–	11.4	6.9	4.2	MSX	6.12	–
CSS 1105	6.4	10.3	10.0	0.93	–	–	–	–	–	MSX	6.90	–
CSS 1109	7.8	20.9	26.3	3.4	–	–	2.6	1.6	0.64	MSX	5.89	I
CSS 1134	0.64	1.5	1.8	0.21	–	–	–	–	–	MSX	8.76	–
CSS 1147	6.1	10.9	10.8	1.1	–	–	–	–	–	MSX	6.83	–
CSS 1149	2.0	3.1	2.8	0.40	–	–	–	–	–	MSX	8.35	I
CSS 1153	7.1	13.5	15.3	1.8	–	–	1.6	1.1	–	MSX	6.47	–
CSS 1156	1.6	4.1	5.4	0.77	–	–	–	–	–	MSX	7.62	–
CSS 1161	5.1	9.6	9.7	1.0	–	–	–	–	–	MSX	6.95	–
CSS 1166	5.4	12.2	14.2	1.9	–	–	1.7	0.84	–	MSX	6.58	–
CSS 1171	2.1	2.8	2.3	0.19	–	–	–	–	–	MSX	8.49	–
CSS 1174	11.9	24.5	32.0	4.0	–	–	2.7	2.0	–	MSX	5.66	–
CSS 1202	5.3	11.4	12.3	1.4	–	–	–	–	–	MSX	6.71	–

Table 12. continued.

Source name	J [Jy]	H [Jy]	K [Jy]	[8.8] [Jy]	[9.8] [Jy]	[11.7] [Jy]	[12.5] [Jy]	D [Jy]	E [Jy]	Mid−IR Data Origin	Apparent bol. magnitudes	I. – E.
CSS 1208	12.1	21.9	21.2	3.5	–	–	1.9	1.3	–	MSX	6.13	I
CSS 1210	4.0	7.1	6.9	0.67	–	–	–	–	–	MSX	7.31	–
CSS 1245	1.5	3.6	4.3	0.56	–	–	–	–	–	MSX	7.87	–
V1542 Cyg	15.8	30.8	35.5	4.0	–	–	3.1	1.9	–	MSX	5.54	I
CSS 1270	4.6	10.3	–	1.7	–	–	–	–	–	MSX	–	–
CSS 1274	4.1	6.0	5.2	0.45	–	–	–	–	–	MSX	7.59	I
CSS 1278	2.7	4.0	3.4	0.28	–	–	–	–	–	MSX	8.04	–
CSS 1281	4.2	6.7	6.1	0.52	–	–	–	–	–	MSX	7.41	I
CSS 1287	8.9	–	10.2	0.81	–	–	–	–	–	MSX	6.85	–
CSS 1299	4.2	6.1	5.5	0.49	–	–	–	–	–	MSX	7.54	–
CSS 1323	11.3	30.5	38.6	6.2	–	–	4.4	2.7	–	MSX	5.50	–
CSS 1325	11.4	23.6	24.5	3.3	–	–	2.2	1.6	–	MSX	5.96	–
CSS 1330	7.0	11.4	11.4	1.1	–	–	–	–	–	MSX	6.75	E
CSS 1331	2.3	3.7	3.3	0.29	–	–	–	–	–	MSX	8.11	–
CSS 1333	2.4	3.6	3.1	0.28	–	–	–	–	–	MSX	8.16	–
CSS2 1	0.68	1.6	1.8	0.22	–	–	–	–	–	MSX	8.77	–
CSS2 2	1.2	3.7	5.6	2.2	–	–	2.2	1.9	–	MSX	7.75	–
CSS2 3	0.83	1.8	2.0	0.23	–	–	–	–	–	MSX	8.66	–
CSS2 5	1.4	2.9	2.9	0.30	–	–	–	–	–	MSX	8.25	–
CSS2 6	1.4	3.1	3.4	0.41	–	–	–	–	–	MSX	8.12	–
CSS2 7	1.6	3.5	3.6	0.48	–	–	–	–	–	MSX	8.07	–
CSS2 13	1.5	2.6	2.7	0.41	–	–	–	–	–	MSX	8.38	–
CSS2 14	0.76	1.5	1.5	0.18	–	–	–	–	–	MSX	8.97	–
CSS2 15	2.2	5.1	5.8	0.63	–	–	–	–	–	MSX	7.51	–
CSS2 16	1.7	4.1	4.7	0.71	–	–	–	0.76	–	MSX	7.79	–
CSS2 17	1.1	2.5	2.9	0.32	–	–	–	–	–	MSX	8.26	–
CSS2 18	1.1	2.6	2.9	0.36	–	–	–	–	–	MSX	8.27	–
CSS2 21	0.93	1.9	2.1	0.29	–	–	–	–	–	MSX	8.67	–
CSS2 22	0.70	3.0	5.8	3.9	–	–	4.3	2.8	–	MSX	7.76	–
CSS2 23	0.96	2.4	2.8	0.40	–	–	–	–	–	MSX	8.34	–
CSS2 24	7.4	14.4	19.3	11.9	–	–	12.9	8.2	6.1	MSX	6.44	–
CSS2 26	4.2	9.2	13.5	3.9	–	–	5.0	3.1	–	MSX	6.76	–
CSS2 27	2.6	6.4	7.9	1.0	–	–	–	–	–	MSX	7.21	–
CSS2 28	3.1	9.8	16.2	4.9	–	–	5.5	3.3	–	MSX	6.56	–
CSS2 29	0.48	1.6	2.3	2.2	–	–	3.0	1.9	–	MSX	8.78	–
CSS2 30	1.2	3.4	5.5	7.3	–	–	8.3	5.6	3.9	MSX	7.88	–
CSS2 31	1.9	3.8	4.0	0.47	–	–	–	–	–	MSX	7.91	–
CSS2 32	4.1	10.9	16.9	3.9	–	–	4.2	2.6	–	MSX	6.48	–
CSS2 33	1.7	4.8	6.4	0.99	–	–	–	–	–	MSX	7.46	–
CSS2 34	0.99	2.9	4.1	1.2	–	–	1.5	–	–	MSX	8.05	–
CSS2 35	1.1	3.9	5.8	0.88	–	–	–	–	–	MSX	7.56	–
CSS2 36	2.1	4.4	5.0	0.77	–	–	–	–	–	MSX	7.72	–
CSS2 37	1.9	5.2	6.7	0.81	–	–	–	–	–	MSX	7.37	–
CSS2 38	1.8	4.1	4.8	0.57	–	–	–	–	–	MSX	7.72	–
CSS2 39	2.0	6.3	8.8	1.8	–	–	2.0	1.4	–	MSX	7.17	–
CSS2 43	2.0	4.8	6.9	1.9	–	–	1.9	0.86	–	MSX	7.48	–
CSS2 45	4.2	7.8	8.2	1.1	–	–	–	–	–	MSX	7.16	–
CSS2 46	1.8	3.8	4.3	0.50	–	–	–	–	–	MSX	7.86	–
CSS2 48	1.4	3.4	4.0	0.51	–	–	–	–	–	MSX	7.95	–
CSS2 49	1.9	4.5	–	1.0	–	–	–	–	–	MSX	–	–
CSS2 50	2.3	5.0	6.0	0.81	–	–	–	–	–	MSX	7.51	–
CSS2 52	0.89	3.0	4.2	0.65	–	–	–	–	–	MSX	7.90	–
CSS2 53	2.9	8.4	11.6	1.8	–	–	1.2	1.0	–	MSX	6.79	–
CSS2 54	2.4	4.5	5.4	0.76	–	–	–	–	–	MSX	7.62	–
CSS2 55	2.8	7.8	10.4	1.4	–	–	–	–	–	MSX	6.91	–
CSS2 56	2.0	5.3	6.8	0.88	–	–	–	–	–	MSX	7.37	–
CSS2 57	1.7	4.8	6.4	0.80	–	–	–	–	–	MSX	7.43	–
CSS2 58	1.5	5.8	9.8	3.1	–	–	3.0	2.2	–	MSX	7.10	–
CSS2 59	1.4	4.9	6.8	1.1	–	–	1.2	–	–	MSX	7.43	–
CSS2 61	1.3	3.7	4.8	0.73	–	–	–	–	–	MSX	7.76	–
CSS2 62	2.3	6.6	8.9	2.2	–	–	2.1	1.1	1.5	MSX	7.18	–
CSS2 63	2.8	6.3	7.7	0.88	–	–	–	–	–	MSX	7.21	–
CSS2 64	1.1	2.5	2.9	1.3	–	–	1.2	0.68	–	MSX	8.47	–
CSS2 65	1.2	2.2	2.4	0.30	–	–	–	–	–	MSX	8.48	–
CSS2 67	2.8	5.9	6.2	0.79	–	–	–	–	–	MSX	7.46	–
CSS2 68	2.1	4.8	5.4	0.60	–	–	–	–	–	MSX	7.59	–

Table 12. continued.

Source name	J [Jy]	H [Jy]	K [Jy]	[8.8] [Jy]	[9.8] [Jy]	[11.7] [Jy]	[12.5] [Jy]	D [Jy]	E [Jy]	Mid−IR Data Origin	Apparent bol. magnitudes	I. − E.
CSS2 71	1.2	2.3	2.7	0.31	–	–	–	–	–	MSX	8.37	–
CSS2 73	0.77	2.0	2.8	0.58	–	–	–	–	–	MSX	8.40	–
CSS2 74	0.35	1.0	1.3	0.15	–	–	–	–	–	MSX	9.18	–